

**ANALYTICAL STUDY ON IDENTIFICATION OF ENERGY EFFICIENT  
LIQUID DESICCANT AT OPTIMUM OPERATING PARAMETERS FOR  
LIQUID DESICCANT AIR CONDITIONING SYSTEM**

*A Thesis submitted in the partial fulfillment of the requirements for  
the award of the degree of*

**DOCTOR OF PHILOSOPHY**

**by**

**Y. SIVA KUMAR REDDY**

(ROLL NO: 716014)



**DEPARTMENT OF MECHANICAL ENGINEERING**

**NATIONAL INSTITUTE OF TECHNOLOGY**

**WARANGAL (T.S) INDIA 506 004**

**MAY - 2020**

**ANALYTICAL STUDY ON IDENTIFICATION OF ENERGY EFFICIENT  
LIQUID DESICCANT AT OPTIMUM OPERATING PARAMETERS FOR  
LIQUID DESICCANT AIR CONDITIONING SYSTEM**

*A Thesis submitted in the partial fulfillment of the requirements for  
the award of the degree of*

**DOCTOR OF PHILOSOPHY**

by

**Y. SIVA KUMAR REDDY**

(ROLL NO: 716014)

Under the supervision of

**Dr. KARTHIK BALASUBRAMANIAN**

&

**Dr. V.P. CHANDRAMOHAN**



**DEPARTMENT OF MECHANICAL ENGINEERING**

**NATIONAL INSTITUTE OF TECHNOLOGY**

**WARANGAL (T.S) INDIA 506 004**

**May 2020**

## **THESIS APPROVAL FOR Ph.D.**

This thesis entitled “**Analytical study on identification of energy efficient liquid desiccant at optimum operating parameters for liquid desiccant air conditioning system**” by **Mr. Y. Siva Kumar Reddy** is approved for the degree of Doctor of Philosophy.

### **Examiners**

---

---

---

### **Supervisor(s)**

**Dr. Karthik Balasubramanian**  
**(Supervisor)**

Assistant Professor, Mechanical Engineering Department, NIT Warangal

**Dr. V.P. Chandramohan**  
**(Co-Supervisor)**

Associate Professor, Mechanical Engineering Department, NIT Warangal

### **Chairman**

**Prof. R N Rao**

Head, Mechanical Engineering Department, NIT Warangal

*Dedicated*

*to*

- ❖ My beloved **Parents & Family**
- ❖ All my **Teachers and friends** who inspired and encouraged me



**NATIONAL INSTITUTE OF TECHNOLOGY  
WARANGAL (T.S) INDIA 506 004**

---

---

**DECLARATION**

I, hereby declare that the matter embodied in this thesis titled “**Analytical study on identification of energy efficient liquid desiccant at optimum operating parameters for liquid desiccant air conditioning system**” is the result of research carried out by me under the supervision of **Dr. Karthik Balasubramanian** and **Dr. V.P. Chandramohan**, Department of Mechanical Engineering, National Institute of Technology, Warangal, Telangana. This work or any part of this work has not been submitted to any other University or Institute for the award of any other degree or diploma.

Date: 14/05/2020  
Place: Warangal

**(Y. Siva Kumar Reddy)**  
Research Scholar,  
Roll No.716014



**NATIONAL INSTITUTE OF TECHNOLOGY  
WARANGAL (T.S) INDIA 506 004**

**CERTIFICATE**

This is to certify that the thesis entitled “**Analytical study on identification of energy efficient liquid desiccant at optimum operating parameters for liquid desiccant air conditioning system**” submitted by **Mr. Y. Siva Kumar Reddy (Roll No. 716014)** for the award of Doctor of Philosophy in the Department of Mechanical Engineering, National Institute of Technology Warangal, is a bonafide research work carried out by him under our guidance and supervision. The results embodied in this thesis have not been submitted to any other Universities or Institutes for the award of any degree or diploma.

Place: Warangal.

Date: 14/05/2020

**Dr. Karthik Balasubramanian**

Assistant Professor  
Department of Mechanical Engineering  
NIT Warangal- India.

**Dr. V.P. Chandramohan**

Associate Professor  
Department of Mechanical Engineering  
NIT Warangal - India.

## ACKNOWLEDGEMENTS

I would like to express my sincere gratitude and it gives me an immense pleasure to acknowledge the people who were the part of this research work in plenty ways. It would not have been possible without close association with many people. I take this opportunity to extend my sincere gratitude and appreciation to all those who made this research work possible. First and foremost, I would like to express my sincere gratitude to my research supervisor **Dr. Karthik Balasubramanian** for introducing me to this exciting field of desiccant air conditioning system and for his dedicated help, advice, inspiration, encouragement and continuous support, throughout my research work. His enthusiasm, integral view on research and mission for providing high-quality work, has made a deep impression on me. I indebted to him for his persistence in molding me as a researcher with his methodical supervision that enabled me to complete the research work in the present form. I will never forget his association and encouragement and whole hearted support during my entire tenure of research. During our course of interaction, I have learnt many things, like how to explore new possibilities and how to approach a problem by systematic thinking. He inspired me how to live the each moment of life happily. I owe him with lots of gratitude for showing me this way of research.

I would like to express special words of thanks to my research co-supervisor **Dr. V.P. Chandramohan** for his continuous support, guidance, cooperation and encouragement. His constant motivation and support have always kept me going ahead. I owe a lot of gratitude to him for always being there for me in spite of his busy schedule and I feel privileged to be associated with him.

Thanks are also due to **Prof. C. S. P. Rao, Prof. P. Bangaru Babu and Prof. N Selvaraj** former Head, Mechanical Engineering Department, National Institute of Technology, Warangal, for their timely suggestions, support and for providing necessary departmental facilities and services during successful completion of research work.

I wish to express my sincere and whole hearted thanks and gratitude to my DSC Members **Dr. K Kiran Kumar**, Associate Professor, **Prof. S Srinivasa Rao**, Mechanical Engineering

Department, and **Dr. P V Suresh**, Associate Professor, Chemical Engineering Department for their kind help, encouragement and valuable suggestions for successful completion of research work.

I would like to acknowledge with gratitude to **Prof. R N Rao**, Head, Department of Mechanical Engineering for providing the necessary facilities to carry out the research.

My heartfelt thanks to fellow-scholars for their consistent help, moral support and encouragement. My special thanks to **Ranjith Kumar V, Siva Prasad K, Chandra shekhar S, Manoj D, Shashi, Deepak, Sangamesh** and many others for always standing by my side and sharing a great relationship as compassionate friends. I will always cherish the warmth shown by them.

In this auspicious moment, I owe my deepest regards to my family members for their eternal support and understanding of my goals and aspirations. My heartfelt regards goes to my parents, Sri Y Siva Narayana Reddy, and Smt. Y Swarna Latha. My wife Chandrika, share a perpetual role with her infallible affection, love and support, it has always been my strength. Her patience and sacrifice will remain my inspiration throughout my life. Without her support, I would not have been able to complete what I have done and become who I am. My special regards to my sister Smt. K Vasavi, and brother-in-law Sri K Madhusudan and many other friends for their patience and understanding during the entire period of the research work. I also must thank all my hostel mates for making my stay at NIT Warangal become more memorable.

As always it is impossible to mention everybody who had an impact to this work, however, there are those whose spiritual support is even more important. I feel a deep sense of gratitude to each and every one who directly or indirectly extended their support to fulfill my research.

Finally, I am thankful to library staff and administrative staff of NITW for their cooperation.

NIT Warangal

(Y. Siva Kumar Reddy)

May 2020

## **Abstract**

In recent times, liquid desiccant air conditioning has become an inquisitive phenomenon among researchers being one of the best alternatives for conventional vapor compression refrigeration system (VCRS) in hot and humid climates, for large scale applications, because of its energy efficient and eco-friendly nature. It is revealed that membrane based liquid desiccant air conditioning system (LDAS) considered as energy efficient technology for air dehumidification which independently handles the air latent load and required sensible cooling of air will be taken care by other systems like VCRS or Indirect evaporative cooling system.

Several researchers investigated the effect of desiccant material with different operating parameters on the different system configuration types considering the dehumidification rate and energy exchanger effectiveness as performance parameters. However, identification of the potential liquid desiccant at optimum operating parameters for a given air conditioning application has not been addressed in open literature which is essential in attaining the energy savings. This research gap is fulfilled in this study considering the solution heater load, solution cooler load and chiller load as primary performance indices.

In this study, dehumidifier and regenerators are considered as counter-flow type liquid air membrane energy exchangers (LAMEE) which comprises of series of alternate solution and air channels separated by membrane which is impermeable to liquid but not water vapor. As the solution and air output parameters at each channel outlet in full scale LAMEE will be same, control volume which covers half width air channel, membrane and half width solution channel of full scale LAMEE has been chosen to investigate the heat and mass transfer processes at each given solution inlet condition.

Considering dehumidifier air inlet condition and dehumidification rates are fixed, initially effect of different solution operating parameters of a given solution on the performance indices were studied to identify the suitable liquid desiccant operating parameters. LiCl solution is considered

as liquid desiccant and its operating parameters considered are, solution concentration,  $C_s=0.25, 0.3, 0.35$  and  $0.40$  and heat capacity ratios,  $C_r^*=2.5, 3, 4$  and  $5$ . The results indicate that system chiller load ( $Q_{chiller}$ ) decreases with increase in solution concentration ( $C_s$ ) as well as with decrease in heat capacity ratio ( $C_r^*$ ). This implies  $Q_{chiller}$  is  $0.29\text{kW}$  to achieve  $0.61\text{kW}$  cooling load at  $C_s =0.40$  and  $C_r^*=2.5$ . Solution heat addition rate ( $Q_{add}$ ) per kW cooling capacity ( $Q_{cc}$ ) at this solution condition is found as  $0.85\text{kW}$ . Therefore it can be observed that, any given solution with maximum safe concentration (just below saturation concentration) requires lesser chiller load ( $Q_{chiller}$ ). In addition to this, as  $Q_{chiller}$  is found to decrease with heat capacity ratio, optimum heat capacity ratio needs to be determined for any given solution.

As ambient condition changes frequently, it is required to precisely control the desiccant solution operating parameters to suit the required conditioned space load. Initially, optimum liquid desiccant heat capacity ratio (mass flow rate) were found for the liquid desiccant air conditioning system (LDAS) at peak ambient condition. Later, effect of two control strategies which are dehumidifier solution inlet temperature (DSIT) control strategy and dehumidifier solution inlet mass flow rate (DSIM) control strategy on the performance indices were studied at different ambient conditions. It is seen that required chiller load is nearly same at both control strategies but little drop (3-14.5% variation) is observed at DSIT strategy at low ambient conditions. However, considerable drop in solution pumping power due to the significant reduction in solution mass flow rate and its pressure drop at DSIM strategy suggests that it is found as energy efficient control strategy.

Lastly, considering the commonly used potential solutions  $\text{LiCl}$ ,  $\text{CaCl}_2$ ,  $\text{LiBr}$  and  $\text{KCOOH}$  solutions at their maximum safe concentrations ( $0.40, 0.35, 0.55$  and  $0.75$  which are just below their saturation concentrations), performance indices were analyzed at different heat capacity ratios ( $C_r^*=4.0, 3.0, 2.5, 2.0$  and  $1.5$ ). At their corresponding optimum  $C_r^*$ ,  $Q_{add}$  is observed to be low for  $\text{CaCl}_2$  whereas high for  $\text{LiBr}$  compared to other solutions that are considered. Solution pumping power and  $Q_{chiller}$  are observed to be lesser for *LiBr* solution. At their corresponding design (optimum) parameters, even though  $\text{LiBr}$  solution investment cost is found to be 30%

higher than LiCl solution, its operating cost (pumping power) is nearly 26%-40% lesser than the LiCl solution which suggests that LiBr solution at  $C_r^*=2.5$  is efficient solution among four. Later, at observed optimum heat capacity ratio for each solution, same considered performance indices were estimated at different ambient conditions by adopting a DSIM control strategy to suit the required conditioned load, which frequently varies according to changes in ambient conditions. Even though ambient condition varies, performance parameters for all solutions follow the same trends as they followed at the fixed peak ambient condition. The analysis done in this study therefore suggests that the LiBr solution is an appropriate solution to achieve energy savings due to its low chiller load requirement and its low operating cost. The drawback of the LiBr solution is high investment cost and requires little high  $Q_{add}$  than LiCl solution. The  $\text{CaCl}_2$  solution requires lesser  $Q_{add}$  but its operating cost and  $Q_{chiller}$  are very high. The LiCl solution followed by the KCOOH solution are next to the LiBr solution in attaining energy savings.

The methodology followed in this study is beneficial for LDAS designers in choosing the suitable liquid desiccant at its corresponding operating parameters to design an energy efficient LDAS for any given air conditioning application.

# CONTENTS

<b>Abstract</b>	<b>i</b>
<b>Contents</b>	<b>iv</b>
<b>List of tables</b>	<b>viii</b>
<b>List of figures</b>	<b>ix</b>
<b>Nomenclature</b>	<b>xiv</b>
<b>Chapter 1: Introduction</b>	<b>1-4</b>
1.1. Background	1
1.2. Objectives	3
1.3. Scope	3
1.4. Thesis structure	3
<b>Chapter 2: Literature survey</b>	<b>5-26</b>
2.1. Fundamental understanding of different desiccant materials, liquid desiccant air conditioning system, different system configurations	5
2.1.1. Solid desiccant material and its function in dehumidification system	6
2.1.2. Liquid desiccant material and its function in dehumidification system	8
2.1.3. Dehumidifier/regenerator (energy exchanger)	9
2.1.3.1. Direct solution-air contact based energy exchangers	9
2.1.3.2. Indirect solution-air contact based energy exchangers	13
2.2. Effect of desiccant solution and air operating parameters on performance of dehumidifier/regenerator	16
2.3. Effect of desiccant material on performance of dehumidifier/regenerator	21
2.4. Research gap and motivation	23
2.5. Objectives of thesis	25
<b>Chapter 3: System description and solution procedure</b>	<b>27-45</b>

3.1. System description and control volume modelling	27
3.2. Solution procedure	30
3.3. Assumptions	32
3.4. Governing equations for air and solution	33
3.5. Performance indices	41
3.6. Boundary conditions	43
3.7. Validation of analytical model	44

#### **Chapter 4: Identification of optimum desiccant solution parameters**

<b>for a given liquid desiccant</b>	<b>45-64</b>
4.1. Methodology	45
4.2. Results and discussions	49
4.2.1. Variation in dehumidifier parameters and dehumidifier related performance Indices	51
4.2.1.1. Variation in required dehumidifier solution inlet temperature ( $T_{d,s,i}$ )	51
4.2.1.2. Variation in dehumidifier solution outlet temperature ( $T_{d,s,o}$ )	51
4.2.1.3. Variation in dehumidifier air outlet temperature ( $T_{d,a,o}$ )	52
4.2.1.4. Variation in air cooling capacity achieved in the dehumidifier ( $Q_{cc}$ )	53
4.2.1.5. Variation in required air sensible cooling after dehumidification ( $Q_{sen2}$ )	54
4.2.2. Variation in regenerator parameters and regenerator related performance indices	57
4.2.2.1. Variation in required regenerator solution inlet temperature ( $T_{r,s,i}$ )	57
4.2.2.2. Variation in regenerator air outlet temperature ( $T_{r,a,o}$ )	57
4.2.2.3. Variation in regenerator solution outlet temperature ( $T_{r,s,o}$ )	58
4.2.3. Variation in solution pressure drop in dehumidifier and regenerator channels ( $\Delta P_{r,s}$ and $\Delta P_{d,s}$ )	59
4.2.4. Variation in required solution heat addition rate ( $Q_{add}$ )	60

4.2.5. Variation in required solution heat removal rate ( $Q_{rem}$ )	61
4.2.6. Variation in chiller load ( $Q_{chiller}$ )	62
4.3. Major observations	63
<b>Chapter 5: Choosing the energy efficient liquid desiccant control strategy for system control performance</b>	<b>65-83</b>
5.1. Methodology	65
5.2. Results and discussions	66
5.2.1. Methodology to choose design solution parameters	66
5.2.2. Solution control strategies to suit the conditioned space load at different ambient conditions	69
5.2.2.1. Variation in dehumidifier solution inlet temperature ( $T_{d,s,i}$ ) and its mass flow rate ( $m_{d,s,i}$ )	71
5.2.2.2. Variation in air cooling capacity ( $Q_{cc}$ )	72
5.2.2.3. Variation in required dehumidified air sensible cooling ( $Q_{sen2}$ )	74
5.2.2.4. Variation in regenerator solution inlet temperature ( $T_{r,s,i}$ )	75
5.2.2.5. Variation in regenerator solution and air outlet temperatures ( $T_{r,s,o}$ and $T_{r,a,o}$ )	76
5.2.2.6. Variation in chiller load ( $Q_{chiller}$ )	78
5.2.2.7. Variation in solution heat addition rate ( $Q_{add}$ )	79
5.2.2.8. Variation in pressure drops in dehumidifier and regenerator solution channels ( $\Delta P_{r,s}$ and $\Delta P_{r,s}$ )	79
5.2.3. Impact of design solution parameters on performance at both control Strategies	80
5.3. Major observations	81

<b>Chapter 6: Identification of the energy efficient liquid desiccant among potential liquid desiccants at optimum operating parameters</b>	<b>83-100</b>
6.1. Methodology	83
6.2. Results and discussions	88
6.2.1. Variation in air cooling capacity ( $Q_{cc}$ ) and required dehumidified air sensible cooling ( $Q_{sen2}$ )	90
6.2.2. Variation in the required solution heat addition rate ( $Q_{add}$ )	92
6.2.3. Variation in chiller load ( $Q_{chiller}$ )	93
6.2.4. Variation in solution pressure drop ( $\Delta p_{d,s}$ and $\Delta p_{r,s}$ ) and its pumping power ( $P_{d,s}$ and $P_{r,s}$ )	94
6.2.5. Solution and air conditions at different ambient conditions	97
6.2.6. Variation in solution heat addition rate ( $Q_{add}$ ), chiller load ( $Q_{chiller}$ ) and solution pumping power ( $P_{d,s}$ & $P_{r,s}$ ) at different ambient conditions	98
6.3. Major observations	98
<b>Chapter 7: Conclusions and Recommendations for future work</b>	<b>101-103</b>
7.1. Conclusions	101
7.2. Recommendations for future work	103
<b>List of research articles published in Journals</b>	<b>104</b>
<b>References</b>	<b>105-112</b>

## List of Tables

<b>Table</b>	<b>Title</b>	<b>Page</b>
3.1	Specifications of LAMEE control volume	30
3.2	Air ambient parameters (Mumbai summer peak condition) and other required parameters	31
3.3	Ambient test conditions considered in the experiment	44
4.1	Different combinations of solution parameters (16 nos)	48
5.1	Dehumidifier and regenerator parameters at different heat capacity ratios ( $C_r^*$ )	67

## List of Figures

<b>Figure</b>	<b>Title</b>	<b>Page</b>
1.1	Schematic figure of rotary desiccant wheel	7
1.2	Conceptual schematics for (a) adiabatic and (b) isothermal packed beds	11
1.3	Conceptual schematics for (a) adiabatic and (b) isothermal spray towers	11
1.4	Falling film type energy exchanger schematic for (a) crossflow (b) parallel and (c) counter flow arrangements	12
1.5	A conceptual representation for moisture transfer between air and liquid streams through a semi permeable hydrophobic membrane	13
1.6	Flat plate LAMEE configuration	14
1.7	Hollow fiber LAMEE configuration	15
3.1	Schematic diagram of LDAS	28
3.2	Sectional plan views of (a) Full scale LAMEE and (b) Control volume	29
3.3	Comparison of $\varepsilon_{sen,d}$ and $\varepsilon_{lat,d}$ obtained from current analytical model with existing experimental and numerical results at different ambient conditions (F1-F4)	45

4.1	LiCl solution psychrometric chart	49
4.2	Psychrometric chart indicates dehumidifier air and solution conditions at (a) $C_r^*=2.5$ , (b) $C_r^*=3.0$ , (c) $C_r^*=4.0$ & (d) $C_r^*=5.0$ and different concentrations	50
4.3	Heat capacity ratio ( $C_r^*$ ) vs. air total cooling (sensible + latent cooling) achieved in the dehumidifier ( $Q_{cc}$ ) at different concentrations	53
4.4	Heat capacity ratio ( $C_r^*$ ) Vs. required air sensible cooling after dehumidification ( $Q_{sen2}$ ) at different concentrations	54
4.5	Psychrometric chart indicates regenerator air and solution conditions at (a) $C_r^*=2.5$ , (b) $C_r^*=3.0$ , (c) $C_r^*=4.0$ & (d) $C_r^*=5.0$ and different concentrations	55
4.6	Heat capacity ratio ( $C_r^*$ ) vs. Solution pressure drop in the dehumidifier ( $\Delta P_{d,s}$ ) and in regenerators ( $\Delta P_{r,s}$ ) at different concentrations	57
4.7	Heat capacity ratio ( $C_r^*$ ) Vs. heat addition rate ( $Q_{add}$ ) required for solution sensible heating at different concentrations	58
4.8	Heat capacity ratio ( $C_r^*$ ) Vs. heat removal rate ( $Q_{rem}$ ) required for solution sensible cooling at different concentrations	60
4.9	Heat capacity ratio ( $C_r^*$ ) vs. required chiller load ( $Q_{chiller}$ ) at different concentrations	66

5.1	Variation in (a) solution heat removal rate ( $Q_{rem}$ ), (b) Required dehumidified air sensible cooling ( $Q_{sen2}$ ), (c) Chiller load ( $Q_{chiller}$ ) and (d) Solution heat addition rate ( $Q_{add}$ ) with heat capacity ratio ( $C_r^*$ )	68
5.2	Psychrometric chart indicates dehumidifier air and solution conditions at different ambient conditions when <b>a)</b> DSIT control strategy and <b>b)</b> DSIM control strategy adopted	70
5.3	Variation in solution inlet mass flow rate ( $m_{d,s,i}$ ) and dehumidifier solution inlet temperature ( $T_{d,s,i}$ ) at different ambient conditions	71
5.4	Variation in air cooling capacity ( $Q_{cc}$ ) at different ambient conditions	72
5.5	Variation in required dehumidified air sensible cooling ( $Q_{sen2}$ ) at different ambient conditions	74
5.6	Variation in regenerator solution inlet temperature and solution inlet mass flow rate at different ambient conditions	74
5.7	Variation in regenerator solution outlet temperature and air outlet temperatures at different ambient conditions	75
5.8	Variation in (a) required solution heat removal rate ( $Q_{rem}$ ), and (b) Chiller load ( $Q_{chiller}$ ) at different ambient conditions	77
5.9	Variation in solution heat addition rate ( $Q_{add}$ )	78
5.10	Variation in solution pressure drops in (a) dehumidifier ( $\Delta P_{d,s}$ ) (b) regenerator ( $\Delta P_{r,s}$ ) at different ambient conditions	79

5.11	Variation in (a) chiller load ( $Q_{chiller}$ ) (b) solution heat addition rate ( $Q_{add}$ ) at different ambient conditions when $C_r^*=1.5$ and 2.5	80
6.1	Psychrometric charts of LiCl, CaCl <sub>2</sub> , LiBr and KCOOH solutions at different concentrations	87
6.2	Psychrometric chart specifies dehumidifier air and solution conditions at $C_r^*=4, 3, 2.5, 2, 1.5$ & 1 and operating concentrations for (a) LiCl, (b) CaCl <sub>2</sub> , (c) LiBr and (d) KCOOH desiccant solutions	88
6.3	Psychrometric chart specifies regenerator air and solution conditions at $C_r^*=4, 3, 2.5, 2$ & 1.5 and operating concentration for (a) LiCl, (b) CaCl <sub>2</sub> , (c) LiBr and (d) KCOOH desiccant solutions	89
6.4	Heat capacity ratio ( $C_r^*$ ) vs. (a) air total cooling (sensible + latent cooling) achieved in the dehumidifier ( $Q_{cc}$ ) and (b) Required dehumidified air sensible cooling for each solution	90
6.5	Variation in required $Q_{add}$ at different $C_r^*$ for different solutions	91
6.6	Variation in (a) required solution heat removal rate ( $Q_{rem}$ ) and (b) Chiller load ( $Q_{chiller}$ ) at different $C_r^*$ and for different solutions	92
6.7	Heat capacity ratio ( $C_r^*$ ) vs. (a) solution pressure drop in dehumidifier and (b) solution pressure drop in regenerator for different solutions	93

6.8	Heat capacity ratio ( $C_r^*$ ) vs. <b>(a)</b> power consumption for solution pumping in dehumidifier channel and <b>(b)</b> power consumption for solution pumping in regenerator channel for different solutions	94
6.9	Psychrometric chart specifies dehumidifier solution and air conditions for <b>(a)</b> LiCl at $C_r^*=2.5$ , <b>(b)</b> CaCl <sub>2</sub> at $C_r^*=3.0$ , <b>(c)</b> LiBr at $C_r^*=2.5$ and <b>(d)</b> KCOOH at $C_r^*=2.5$ at different ambient conditions	95
6.10	Psychrometric chart specifies regenerator solution and air conditions for <b>(a)</b> LiCl at $C_r^*=2.5$ , <b>(b)</b> CaCl <sub>2</sub> at $C_r^*=3.0$ , <b>(c)</b> LiBr at $C_r^*=2.5$ and <b>(d)</b> KCOOH at $C_r^*=2.5$ at different ambient conditions	96
6.11	Variation in <b>(a)</b> required solution heat addition rate ( $Q_{add}$ ) and <b>(b)</b> Chiller load ( $Q_{chiller}$ ) at different ambient conditions	97
6.12	Variation in <b>(a)</b> solution pumping power for dehumidifier channel ( $P_{d,s}$ ) and <b>(b)</b> solution pumping power for regenerator channel ( $P_{r,s}$ ) at different ambient conditions	98

# Nomenclature

## Nomenclature

A	Heat and mass transfer area (m <sup>2</sup> )	m <sup>2</sup>
C	Solution concentration	-
c <sub>p</sub>	Specific heat at constant pressure	Jkg <sup>-1</sup> K <sup>-1</sup>
C <sub>r</sub> *	Heat capacity ratio	-
h	Enthalpy	J kg <sup>-1</sup>
H	Exchanger height	Mm
H*	Operating factor	-
h <sub>c</sub>	Convective heat transfer coefficient	W m <sup>-2</sup> °K
h <sub>m</sub>	Convective mass transfer coefficient	W m <sup>-2</sup> °K
h <sub>fg</sub>	Latent heat due to phase change	J kg <sup>-1</sup>
k	Thermal conductivity	W m <sup>-1</sup> °K
L	Length of channel	Mm
$\dot{m}$	Mass flow rate	kg s <sup>-1</sup>
NTU	Number of heat transfer units	-
NTU <sub>m</sub>	Number of mass transfer units	-
Nu	Nusselt number	-
Q	Transferred energy in heat/energy exchangers	W
R <sub>m</sub>	Membrane resistance	s m <sup>-1</sup>
RH	Relative humidity	-
T	Temperature	°C or °K
U	Overall heat transfer coefficient	W m <sup>-2</sup> °K
U <sub>m</sub>	Overall mass transfer coefficient	W m <sup>-2</sup> °K
V	Volume flow rate	m <sup>3</sup> s <sup>-1</sup>

w	Moisture content	$\text{kg}_{\text{water}} \text{kg}_{\text{air}}^{-1}$
X	Solution mass fraction	$\text{kg}_{\text{water}} \text{kg}_{\text{salt}}^{-1}$
p	Pressure	Pa

*Greek symbols*

$\Delta$	Thickness (mm)
$\xi$	Dimensionless temperature difference
$\Psi$	Dimensionless humidity ratio difference
$\varepsilon$	Effectiveness
$\Delta$	Differential between two quantities
$\mu$	Dynamic friction (Pa.s)
P	Power consumption (kW)

*Subscripts*

d	Dehumidifier
r	Regenerator
a	Air
i	Inlet
o	Outlet
s	Solution
m	Membrane
cc	Cooling capacity
sen	Sensible
lat	Latent
rem	Removal rate
add	Addition rate

LDAS	Liquid desiccant air system conditioning system
DBT	Dry bulb temperature(°c)
LAMEE	Liquid air membrane energy exchanger

# **Chapter 1**

## **Introduction**

### **1.1. Background**

Air conditioning demand is rising high with respect to time due to yearly raise in global temperatures caused primarily by industrial pollution, deforestation, heavy usage of automobiles and leakage of global warming potential and ozone depletion potential gases into the atmosphere. It is reported that air conditioning equipment for commercial buildings itself consumes 50-60% of total energy consumption of the buildings according to TERI (The energy and resources institute). Conventional vapor compression refrigeration systems (VCRS) serve this function which is energy intensive because of its overcooling of air for dehumidification and overheating of air to attain its supply condition. Energy consumption is even higher in most hot and humid climates. Desiccant material by virtue of its low vapour pressure can absorb the moisture from air thus it can handle latent heat independently and efficiently in humid climates. This property makes the desiccant air conditioning system as one of the best alternatives to independently handle the latent load in hot and humid climates and also to attain energy savings. Solid desiccant systems consists primarily a rotating wheel coated with desiccant salt absorbs the moisture from air when air is passing through the wheel. To independently handle the latent load and sensible load, few researchers working on hybrid solid desiccant - vapor compression air conditioning system [1]–[3]. But liquid desiccant systems have many advantages over solid desiccant systems

such as low pressure drop, high energy storage ability, higher dehumidification potential and requires low grade heat sources for regeneration[4]. Thus liquid desiccant air conditioning system (LDAS) considered as energy efficient technology for air dehumidification which independently handles the air latent load and required sensible cooling of air will be taken care by other systems like VCRS or indirect evaporative cooling system. LDAS is becoming attractive due to many advantages, such as effective utilization of low-grade heat sources, and less harm to the environments. This technology has been used in industrial and agricultural industries, such as moisture control in textile mills, post harvests and low-temperature crop drying in stores. It is playing a progressively prominent role in air conditioning systems [5].

There is voluminous literature survey available which is mainly focused on the different configurations of dehumidifier, performance (coefficient of performance, moisture removal rate, sensible effectiveness, latent effectiveness & total effectiveness) investigation of dehumidification system and regeneration system at different air & solution conditions and performance comparison of LAMEE by using different desiccant solutions. Identification of suitable desiccant material for a given LDAS application requires special attention in design of energy efficient system. Research in this direction is mainly concentrated on the influence of different desiccant solutions at different operating parameters on dehumidification and regeneration performance considering dehumidification rate, effectiveness and COP as the performance indices. All their studies are mainly attentive to the influence of desiccant solution on dehumidifier/regenerator performance but not on other primary components of LDAS. This analysis is not helpful in choosing the right desiccant material since impact of desiccant solution on solution pumping power, solution heater load, solution cooler load and chiller load are not taken into consideration. This research gap motivates us to study on the identification of suitable liquid desiccant material at optimum concentration and heat capacity ratio (mass flow rate) with solution heater load, solution cooler load and chiller load as primary performance indices. This study helps the researchers in designing the energy efficient desiccant air conditioning system for a given LDAS air conditioning application.

The objectives in this study are listed as below

### **1.2. Objectives:**

- To study and identify the suitable combination of desiccant solution operating parameters (concentration and heat capacity ratio) for energy efficient liquid desiccant air conditioning system.
- To study the two desiccant solution control strategies to suit required latent load at different ambient conditions and to find optimum control strategy.
- To study the selection methodology for choosing the energy efficient desiccant solution among commonly used potential desiccant solution for a given load.

### **1.3. Scope**

- a. Design the system component specifications and model the analytical solution for the governing equations and its validation.
- b. For a given desiccant solution, find the behavior of thermal energy requirements of the system at different operating parameters for a given air conditioning application.
- c. Identify the suitable desiccant solution at optimum operating parameters for a given air conditioning application.

### **1.4. Thesis structure**

Chapter 2 presents the detailed literature survey which describes the efforts by the other researchers in this field. Chapter 3 explains the system component specifications, modelling the analytical solution for governing equations and performance indices. Validation of considered analytical model is also included in chapter 3. Chapter 4 presents the investigation of effect of operating parameters on the thermal energy requirements for the given liquid desiccant air conditioning system application. This chapter explains the behavior of thermal energy requirements for the system such as solution heater load, solution cooler load and chiller load are analyzed at different operating parameters (concentration and heat capacity ratio). This chapter

concludes that system thermal energy requirements decreases with increase in solution concentration as well as with decrease in heat capacity ratio and concentration for a given desiccant solution. It is known that frequent change in ambient conditions requires precise control of the desiccant solution operating parameters to suit the required conditioned space load. Chapter 5 delineates the selection approach of efficient control strategy for a given air conditioning application which leads to energy savings as well as thermal comfort. Chapter 6 explains the methodology for choosing the suitable desiccant solution among commonly used potential solutions such as LiCl, CaCl<sub>2</sub>, LiBr and KCOOH solutions at optimum heat capacity for energy efficient membrane based liquid desiccant air conditioning system (LDAS). Chapter 7 outlines the key conclusions of this study and recommendations for future work.

## **Chapter 2**

### **Literature survey**

This study focuses on the methodology to identify the suitable liquid desiccant at optimum operating parameters for the design of energy efficient liquid desiccant air conditioning system. This also includes the selection methodology of efficient desiccant solution control strategy to suit the conditioned load which varies according to the ambient condition. Thus this literature part is divided into two sections one of which addresses fundamental understanding of different desiccant material, desiccant air conditioning, and different system configurations while the other sections addresses the different desiccant solution control strategies, effect of different desiccant materials and different operating parameters on the system performance.

#### **2.1. Fundamental understanding of different desiccant materials, liquid desiccant air conditioning system, different system configurations**

Before go through the detailed literature survey on the efforts carrying out on the performance improvement of liquid desiccant air conditioning system, it is required to have basic understanding of this system and its components. This section thus addresses the fundamental understanding of different desiccant materials, desiccant air conditioning function, different types of system configurations and performance parameters used in this field.

Desiccant air conditioning principle was introduced nearly 80 years back in 1930s. Desiccant materials have affinity to absorb the moisture from the air where driving force is difference between vapor pressures of air and desiccant material. This natural property of desiccant

materials made them to adopt in the alternative dehumidification system/ air conditioning system. As long as the desiccant surface vapor pressure is lesser than that of the ambient vapor pressure, desiccant absorbs the moisture from the air. Once the desiccant material is saturated and reached the equilibrium in vapor pressure with ambient air, moisture absorption stops. In order to reuse the desiccant material, it has to reject the moisture which it absorbed. To achieve it, its vapor pressure has to be raised which is done by heating it so that it rejects the moisture to the ambient air/ room return air supplied over the desiccant material. Both solid & liquid desiccants are employed in industries for dehumidification.

### 2.1.1. Solid desiccant material and its function in dehumidification system

Solid desiccant is as hygroscopic salt which has high affinity for moisture. Solid desiccant materials includes silica gel, LiCl salt, activated alumina, molecular sieve etc. Solid desiccant air conditioning system consists primarily a rotating wheel coated with solid desiccant powder absorbs the moisture from the air when it passes through the wheel on the dehumidification side as indicated in schematic diagram (Fig. 1.1).

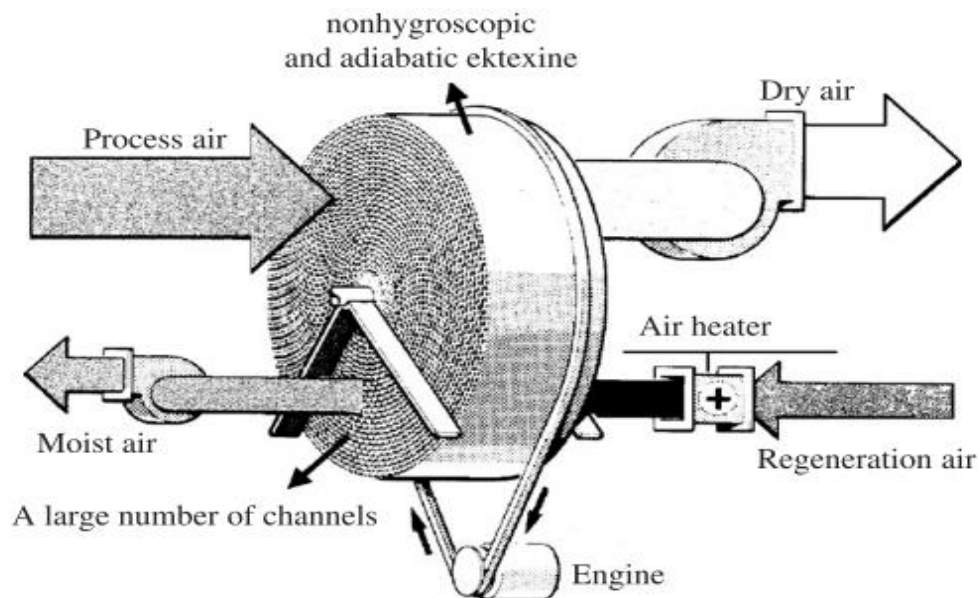


**Fig. 1.1:** Schematic figure of rotary desiccant wheel [6]

Air gets dehumidified and which is to be sensibly cooled to meet the required supply condition. This can be done by coupling the solid desiccant air conditioning system with the sensible heat exchanger/ evaporative cooler. To independently handle the latent load and sensible load, few researchers working on hybrid solid desiccant vapor compression air conditioning system[2], [3], [7]–[9]. To reconcentrate the desiccant wheel, hot air is passed through the regeneration side of the rotating wheel where desiccant desorbs the moisture to the exhaust air due to vapor pressure difference. Thermal energy required for regeneration of rotary desiccant wheel is supplied either by electrical heater or solar/waste heat.

Even though solid desiccant materials can be used for dehumidification applications, but its use is limited compared to liquid desiccant materials. This is since liquid desiccant systems have many advantages over solid desiccant systems such as low pressure drop, high energy storage ability, higher dehumidification potential, flexibility for using multistage dehumidifiers with single regenerator, and requires low grade heat sources for regeneration. Thus liquid desiccant air conditioning system (LDAS) considered as energy efficient technology for air dehumidification which independently handles the air latent load and required sensible cooling of air will be taken care by other systems like VCRS or indirect evaporative cooling system.

### **2.1.2. Liquid desiccant material and its function in dehumidification system**

Liquid desiccants includes glycols and solutions of halide salts such as lithium chloride (LiCl), calcium chloride (CaCl<sub>2</sub>), lithium bromide (LiBr), potassium formate (KCOOH), triethylene glycol and mixture of salts. The strength of a liquid desiccant can be measured by its equilibrium vapor pressure, which is water vapor pressure that is in equilibrium with liquid desiccant material. The vapor pressure exponentially increases with the temperature of the solution and also increases as the water is absorbed by the desiccant solution. The behavior of liquid desiccant can be easily controlled by varying its temperature or concentration or both. A good liquid desiccant should have large saturation absorption capacity, low regeneration temperature, non-volatile, non-corrosive, non-toxic, non-flammable, low viscosity, high heat transfer, inexpensive and

stable. Thus liquid desiccant air conditioning system (LDAS) considered as energy efficient technology for air dehumidification which independently handles the air latent load and required sensible cooling of air will be taken care by other systems like VCRS or indirect evaporative cooling system. LDAS becoming attractive due to many advantages, such as effective utilization of low-grade heat sources, and less harm to the environments. This technology has been used in industrial and agricultural industries, such as moisture control in textile mills, post harvests, and low-temperature crop drying in stores. It is playing a progressively prominent role in air conditioning systems for hot and humid climates.

The earliest used liquid desiccant is Triethylene glycol but its use is limited due to its high viscous and volatile nature [10]. Halide salt solutions such as LiBr and LiCl solutions can dry air to 6% and 15% relative humidity, respectively but these solutions are naturally corrosive. Halide salts are relatively expensive in nature[11].

Formate salts are observed less viscous in nature. Even though potassium formate is a relatively weaker desiccant as compared to LiCl or LiBr but it can dry the air below 30% relative humidity and it can be a good alternative desiccant for many applications. A good and cost effective alternative to LiCl is  $\text{CaCl}_2$  but it is a weak desiccant as compared to LiCl.  $\text{CaCl}_2$  solution of 42% concentration will dry air to about 35% RH while a 43% LiCl solution can dry air to a 15% RH. Morillon et al. [12] measured the vapor pressures  $\text{CaCl}_2$ , LiCl, and LiBr solutions. Although  $\text{CaCl}_2$  salt is readily available and the cheapest desiccant but it has high vapor pressure at the same temperature and same concentration than other halide salts. Ertas et al. [13] proposed a low cost composite desiccant as an alternative to high cost LiCl which is a mixture of LiCl and  $\text{CaCl}_2$ . The  $\text{CaCl}_2$  has 20 times lower cost as compared to LiCl. They showed that 43% solution of the 50/50 mixture of these two desiccants will behave like 40% of pure LiCl. It may be noted that 43% concentration  $\text{CaCl}_2$  solution by weight will have the same properties as the solution of 34% LiCl.

A number of composite desiccant materials have been developed in the past few years to improve their performance. Aristov et al. [14] have developed composite desiccant materials

compromising of silica gel/SiO<sub>2</sub> and inorganic salt (CaCl<sub>2</sub>, LiBr, SrCl<sub>2</sub>, and NaSO<sub>4</sub>). Their results showed that these composite materials have lower desorption temperature.

**2.1.3. Dehumidifier/regenerator (energy exchanger):** Dehumidifier/ regenerator is a solution-air enthalpy exchanger where moisture is absorbed by desiccant or moisture removed from desiccant based on the vapor difference between desiccant and air. According to type of solution-air surface contactors, dehumidifiers/regenerator can be categorized into direct solution-air contact based energy exchangers and indirect solution-air contact based energy exchangers. Direct solution-air contact based energy exchangers includes packed type, liquid film desiccant type and spray tower pad type while the indirect solution-air contact based energy exchangers includes membrane based energy exchanger.

#### **2.1.3.1. Direct solution-air contact based energy exchangers**

In this type energy exchangers, desiccant solution falls from nozzles/ distribution system placed at top of the tower through gravity and air passes from bottom of the dehumidifier for counter flow type configurations whereas it passes across the solution flow direction (perpendicular) in cross flow configurations. The air gets contacted with desiccant and moisture absorbed by the desiccant due to the vapor pressure difference. Air gets heated by losing its moisture content which raises the solution temperature. This process is nearly constant enthalpy process follows adiabatic line of ambient air condition. Moisture absorption potential got reduced for desiccant solution as the process continues because of its increase in temperature as well as reduction of its solution concentration. Therefore the targeted dehumidification cannot be achieved. To overcome this drawback internally cooled dehumidifiers are introduced in which cooling water flows in the tubes of dehumidifier which absorbs heat from solution & air and makes the process nearly isothermal. Moisture absorbed desiccant solution gets diluted at the outlet of dehumidifier. To continue this process desiccant solution has to be concentrated which can be done by removing moisture content contained by it. Solution will lose moisture content to ambient air if the solution equilibrium vapor pressure is higher than the ambient air. For achieving this, heat source like

solar energy/ waste heat energy/ electric heater/ boiler can be used which heats the solution until required vapor pressure is achieved. Hot solution will be sent to regenerator where solution gets contacted with ambient air and loses its moisture to air. Afterwards, concentrated hot solution has to be cooled to initial dehumidifier supply temperature to continue the process.

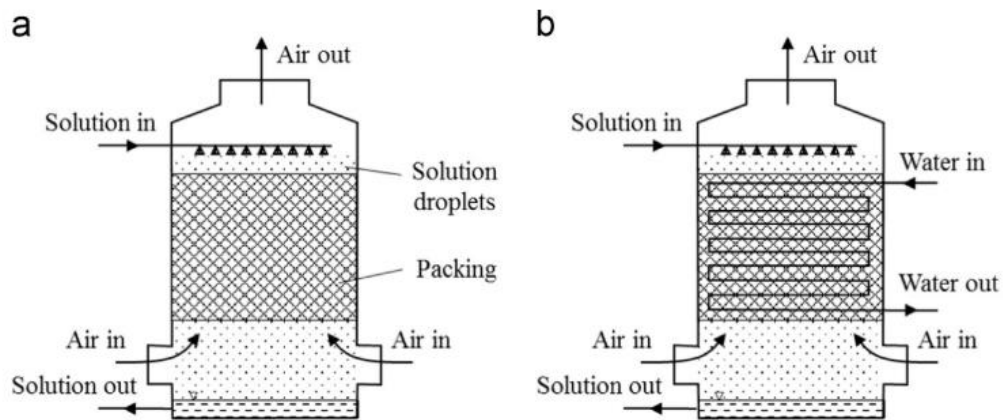


Fig 1.2. Conceptual schematics for (a) adiabatic and (b) isothermal packed beds [15]

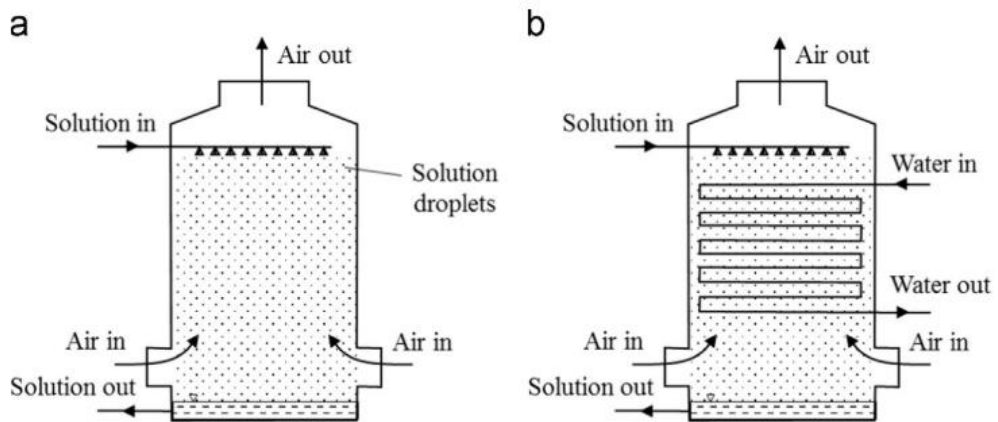
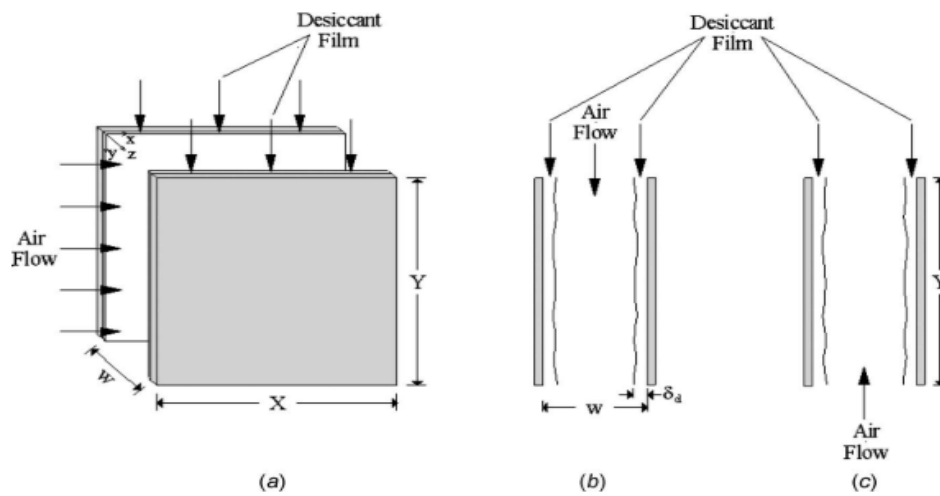


Fig 1.3. Conceptual schematics for (a) adiabatic and (b) isothermal spray towers [15].

Figs. 1.2 shows the adiabatic and isothermal (internal cooling) packed bed type energy exchanger [15]. In these exchangers, solution distributed from the top and flows over the packing and where solution gets contacted with air which is flowing from bottom of the bed/ across the bed. These exchangers can act as either dehumidifier or regenerator based on the vapor pressure difference between solution and air. When the solution has lesser vapor pressure than air, solution absorbs moisture from the air and also gets heated due to the phase change heat. Due to this solution heating, solution absorption potential decreases. To prevent this, isothermal energy exchangers are introduced where cooling water flowing in the tubes continuously cools the solution such that its dehumidification potential will not decrease. Bansal et al. [16] compared the experimental performances of both type dehumidifiers. It was found that the effectiveness of the internally-cooled packed bed is 28–45% higher than the effectiveness of the adiabatic packed bed. Entrainment of liquid droplets with the air stream (called carryover) is a drawback of the packed bed design especially when it is operated under high flow rates. Thus, a mist eliminator is to be installed at the air exit to capture any entrained desiccant droplets.

Fig. 1.3 shows the adiabatic and isothermal (internal cooling) spray pad type energy exchanger [15]. In these exchangers, the desiccant solution is sprayed as small droplets from distributors located at the top of the spray tower. The heat and mass transfer occurs at the air-solution interface. Unlike the packed-bed design, no contact surfaces are used to aid the solution distribution in the spray tower. Risk of solution carryover with the supply air is more in spray pad tower compared to packed bed due to larger contact interface area and absence of packing. Providing the internal cooling in the spray tower leads to significant (e.g. 20%) enhancement in its effectiveness as in packed bed tower [17].



**Fig 1.4:** Falling film type energy exchanger schematic for (a) crossflow (b) parallel and (c) counter flow arrangements[18]

There are few more direct contact based energy exchangers in which falling film type is also one of them used for dehumidification/regeneration. In the falling-film design as shown in fig 1.4, solution film is distributed over plates or tubes, and the air flows over the solution film[18]. Lower air-side pressure drop compared to the commonly used packed bed is one of the main advantages. Also, there is a lower risk of solution droplets carryover in this design compared to the spray tower design.

These direct contact based energy exchangers can also be categorized based on the air stream flow direction which are parallel flow, counter flow and cross flow configurations. It was observed from that the counter flow configuration has the highest effectiveness under dehumidification and regeneration conditions, compared to other configurations[19].

Desiccant droplets carryover with supply air is a common problem with direct-contact dehumidifiers/regenerators, and may be very noticeable at high solution and air flow rates. By installing mist eliminator at the air exit, it can be eliminated which results in additional air side pressure drop and raises the operating and initial costs. To resolve these problems, indirect

contact based energy exchangers are introduced which completely eliminates this carryover problem.

### 2.1.3.2. Indirect solution-air contact based energy exchangers

These are recent developed desiccant dehumidifiers/regenerators using predominantly in LDAS. Isetti et al. [21] first time introduced membrane based energy exchanger where membrane is impermeable to liquid but not to vapor, to act as a porous barrier between solution and moist air. Later, several researchers working on different types of this membrane based systems for enhancing the performance. As shown in Fig. 1.5, air and solution streams in this type of configurations are separated by a hydrophobic semi permeable membrane which permits only

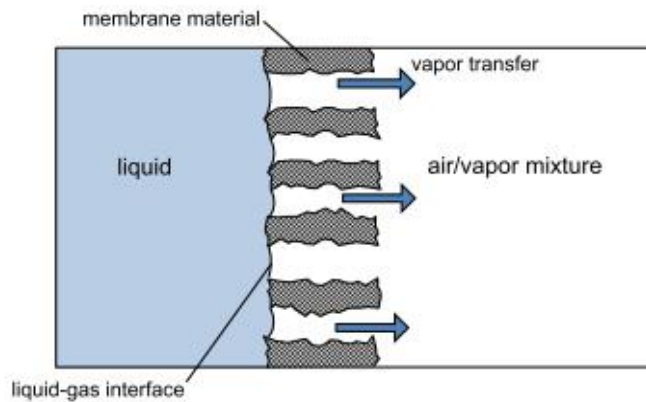


**Fig. 1.5.** A conceptual representation for moisture transfer between air and liquid streams through a semi permeable hydrophobic membrane[20]

water vapor but not liquid through it[20]. Due to this membrane characteristic, desiccant droplets carryover problem can be completely avoided in this design. Different types of indirect contact based systems are there in which one of them primarily used for LDAS is liquid-to-air membrane energy exchanger (LAMEE). LAMEEs are categorized into two types which are flat plate LAMEE and hollow fiber LAMEE.

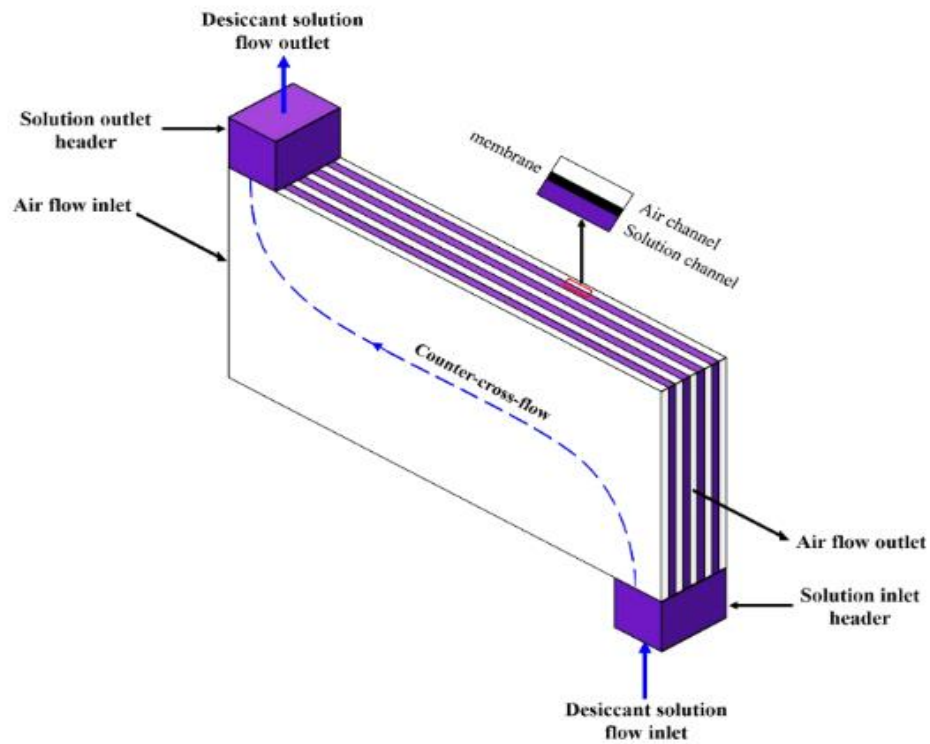


**Fig 1.6.** Flat plate LAMEE configuration[22]

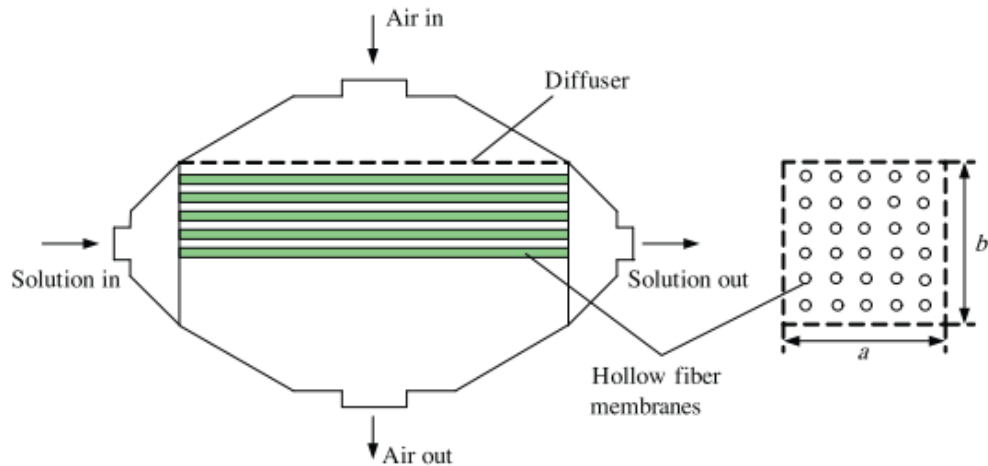


**Fig 1.7.** Hollow fiber LAMEE configuration[23]

In flat plate LAMEE, air and solution flows in alternative rectangular channels which are partitioned by a hydrophobic membrane. Fig 1.6 shows the counter flow flat plate LAMEE [22]. On the other hand, hollow fiber LAMEE design is similar to shell and tube heat exchanger, where solution flows in hollow fiber semi permeable membrane tubes and air flows outside the tubes within the shell (Fig.1.7 ) [23]. As mentioned earlier, to enhance the dehumidification potential, internally cooled flat plate LAMEEs are also introduced, where cooling water tubes are inserted in the solution channels to maintain the solution temperature in the operating limits[24].

So far, different types of desiccant materials, dehumidifier/ regenerator configurations and their functioning are discussed. Research in this field is predominantly concentrated on the effect of different operating parameters such as desiccant material, desiccant solution parameters and air parameters on the dehumidification/regeneration performance. Performance indices considered to analyze the dehumidifier/regenerator performance are effectiveness, moisture removal rate and thermal coefficient of performance (ratio of attained cooling load in dehumidifier to the heat supplied to the regenerator).

## **2.2. Effect of desiccant solution and air operating parameters on performance**

M. Radhwan et al.[25] did a parametric study on performance of counter flow packed bed dehumidifier/regenerator with  $\text{CaCl}_2$  solution as liquid desiccant. It is found that during the dehumidification process the desiccant solution temperature is increased along the bed when both air and solution are have the same temperature and this raise in temperature is proportional to the air inlet humidity ratio. The results also indicated that the desiccant solution inlet temperature has a strong effect on the bed performance along the bed during both dehumidification and regeneration while air inlet temperature has a negligible effect during the regeneration process. A. Ertas et.al [26] investigated the effect of desiccant solution temperature, concentration and flow rate on the performance of counter flow packed regeneration tower at different ambient conditions. Desiccant solution considered in their study is a mixture of 50% LiCl Solution and 50%  $\text{CaCl}_2$  solution by weight. It is seen that COP of a LDAS is lower in hot and humid climates than in moderate climates. The change in desiccant solution concentration in regenerator is a strong function of solution inlet temperature, and a weak function of air inlet temperature.

Isetti et al. [21] theoretically and experimentally dealt with a new approach where they used a membrane, impermeable to liquid but not to vapor, to act as a porous barrier between solution and moist air. They found that considerable moisture transfer between solution and air flowing across the membrane can be achieved and re-concentration of the liquid desiccant can be efficiently carried out in a membrane desorber.

Fumo et.al [27] experimentally as well as mathematically studied the influence of design variables such as air and desiccant solution flow rates, air temperature and humidity, and desiccant solution temperature and concentration on the performance of packed tower dehumidifier and regenerator with LiCl solution as desiccant solution. They observed that dehumidification process is greatly influenced by desiccant solution concentration and flow rate, air flow rate and air humidity whereas regeneration rate is strongly influenced by desiccant

solution and concentration, air flow rate. Both experimental results and simulation results are in good agreement.

Yonggao et.al [28] experimentally studied the effects of the cooling water temperature, the air flow rate and the desiccant solution temperature on the internally cooled plate fin based dehumidifier performance and the cooling efficiency (ratio of actual solution temperature difference to the maximum solution temperature difference). The results indicated that the cooling efficiency decreased with the increasing of the cooling water temperature and both low desiccant solution temperature and internally cooling leads to better dehumidification performance. Effects of the air flow rate and the desiccant inlet temperature on internally heated regeneration performance are also discussed and compared with the performance of adiabatic regeneration process. It was found that the regeneration efficiency of internally heated regeneration was higher than that of the adiabatic regeneration. Yonggao et.al [29] also presented a mathematical model to predict the performance of this internally cooled plate type dehumidifier/regenerator and compared with the experimental results. It is observed that the errors were within 5% and indicated acceptable accuracy.

Khizir Mahmud et. al [30] tested  $MgCl_2$  based Run around membrane energy exchanger (RAMEE) which consists of two LAMEEs one for dehumidification and other for regeneration under different operating parameters in both summer and winter conditions. During summer test conditions, system total effectiveness (actual change in air enthalpy to maximum change air enthalpy during dehumidification) increases with increasing desiccant solution flow rate, but decreases as the air flow rate increases. Under winter test conditions, the total effectiveness varies little with variation in the air and desiccant solution flow rates.

Qiu et. al [31] experimentally examined the performance of potassium formate (HCOOK) based novel dehumidifier under the different parameters such as air flow rate, air relative humidity (RH) and desiccant solution concentration. It is noticed that lower air flow rate leads to high dehumidification rate but in a practical application, the optimum air flow rate has to be

determined considering RH and energy saving requirements into account. The air inlet RH has a large effect on system performance. The drop in RH could be over 25% using strong HCOOK solution to dehumidify highly humid air (>75% RH). However, it does not dehumidify efficiently the air with a RH lesser than 43% even if strong HCOOK desiccant solution is used.

Zhang et.al [32] investigated the effect of air velocity and desiccant solution flow rate on the performance of packed column dehumidifier/regenerator using lithium chloride solution as a liquid desiccant. They observed that increasing the flow rate of either the desiccant solution or air will improve the mass transfer rate in dehumidifier/regenerator. And also it is found that higher desiccant solution temperature resulted in lower overall mass transfer coefficient.

Hemingson et.al [33] numerically studied the steady state performance of RAMEE under wide range of outdoor air conditions. Their results indicate that heat transfer effects latent performance and moisture transfer effects the sensible performances in the RAMEE. This is because, humidity ratio of the desiccant solution is temperature dependent and the latent energy is released/absorbed as the water phase change occurs.

Zhang et.al [34] deduced analytical solution to heat and mass transfer in hollow fiber membrane contactors for LDAS. The model is validated by experiments and found that it can provide convenient accurate tool for component design and optimization. With the model, the effects of varying operating conditions on LiCl based system performance are investigated and it is noticed that the sensible and moisture effectiveness decrease with increase in air flow rates. This is due to decrease in total number of transfer units NTU (which decreases the heat/mass transfer area) with increase air flow rate. Thus NTU is found as dominant factor which affects the heat/mass transfer performance of the dehumidifier. Pahlavanzadeh et.al [35] theoretically and experimentally investigated effect of various operating parameters on number of mass transfer units  $NTU_m$  for LiCl based packed bed column dehumidifier. They observed that increase of  $NTU_m$  causes enhanced performance of the system. With their study, it is found that  $NTU_m$  can be raised by increase in dimension and porosity of the packed bed columns, increasing the mass flow rate, temperature,

and humidity ratio of the air and reducing the mass flow rate, temperature and concentration of the desiccant solution.

Ghadiri Moghaddam et.al [36] experimentally and numerically investigated the effect of heat and mass transfer directions for the air and desiccant solution flows, and the effect of different desiccant solution types and concentrations on the LAMEE effectiveness. It is found that sensible effectiveness increases with solution to air heat capacity ratio ( $C_r^*$ ) for the cooling and dehumidification process. They also noticed that varying concentration is one way to control air outlet humidity ratio.

Abdel-Salam et.al [37] conducted parametric study on the steady state performance of membrane based LDAS using TRNSYS energy simulation platform. Results indicate that the dehumidification rate can be effectively controlled by regulating the temperatures of the desiccant solution entering the regenerator and dehumidifier. Increasing  $C_r^*$  is favorable for the cooling capacity and system COP, especially when  $C_r^*$  increases from 2 to 4. According to the results, they recommended that the NTU and  $C_r^*$  are to be within 5–10 and 3–5, respectively.

Kassai et.al [38] numerically investigated the influence of desiccant solution flow rate ( $C_r^*$ ) and regenerator air inlet temperature on the dehumidifier air outlet humidity ratio for the RAMEE system. They reported that until  $C_r^* < 1$ , increase in regenerator air inlet temperature leads to enhancement in dehumidification rate. The reason is that the solution concentration change increases when the regenerator air inlet temperature increases which causes to better dehumidification rate. But at  $C_r^* > 1$ , regenerator air inlet temperature shows negative impact on dehumidification capacity. Thus, heating the regenerator air flow is not recommended to enhance the dehumidification rate. Kassai [39] also investigated the effect of  $C_r^*$  (less than 1) on the steady state performance of LAMEE for winter conditions. It is reported that total effectiveness of the LAMEE decreases with  $C_r^*$  in the mentioned range.

G. Ge et.al [40] experimentally and analytically investigated the influences of the different dependent operating parameters on the moisture flux ratio (ratio between the actual moisture removal rate (MRR) with respect to the membrane overall mass transfer conductance) and sensible and latent

effectiveness of LAMEEs used as dehumidifier and regenerator. In their study, LiCl solution is used as desiccant solution and operating parameters considered are air and solution inlet parameters, NTU,  $C_r^*$ , solution operating ratio (it characterizes the closeness of the solution concentration to the solution thermodynamic saturation conditions at the solution temperature), etc. in the selected range. It is found that air flow rate, air humidity ratio, desiccant solution temperature, and solution concentration are most influential parameters on moisture exchange rate in dehumidifier and regenerator. In addition to these parameters, solution flow rate also considerably influences regeneration performance. They also reported that NTU and  $C_r^*$  directly influence the performance parameters considered in their study.

Mohan et.al [41] examined the effect of varying room air temperature and specific humidity on the performance of the hybrid liquid desiccant vapor compression system where packed column used as dehumidifier and regenerator. LiCl considered as desiccant material and the solution to air flow ratio considered very low (0.01). They found that increase of air temperature reduces dehumidification rate and regeneration rate of liquid desiccant. On the other hand, an increase of room specific humidity enhances dehumidification rate as well as regeneration rate of the desiccant solution. Ahn et. al [42] conducted series of field tests on LiCl based hybrid liquid desiccant system and observed that the cooling capacity dropped with increase in ambient temperature, while it increased as ambient humidity increased. The COP also observed to be increased with increase in ambient humidity.

Bai et al. [43] experimentally investigated the impacts of concentration, solution to air mass flow rate ratio, solution inlet temperature and NTU on  $\text{CaCl}_2$  based membrane based liquid desiccant dehumidification system performance. They noticed that both the total and latent effectiveness increase with concentration, whereas nearly no difference is observed in the sensible effectiveness. They also found that all effectiveness can be enhanced by reducing solution inlet temperature.

Sabek et.al [44] carried out numerical investigation to find the impact of air and desiccant solution properties on the LiCl based LAMEE . They noticed that the optimal inlet air and

desiccant liquid velocities enhance heat and mass transfer rates as well as the sensible, latent and total effectiveness. The inlet air humidity ratio and is found to have a great impact on the mass and heat transfer rates in the LAMEE which increase under high values.

Wang et. al [45] analyzed the coupled heat and mass transfer process in a counter-flow adiabatic structured packed tower with the air inlet humidity ratio varying broadly from 20 g/kg air to 16 g/kg air using KCOOH solution as the desiccant solution. The moisture removal rate within dehumidifier increases with the air inlet humidity ratio and the increasing trend becomes gradually flat when the liquid-air flow rate ratio is low. The optimal liquid-air flow rate ratio is about 0.6– 1.0 when the air inlet humidity ratio is 30 g/kg air, and is about 2.5–3.5 when the air inlet humidity ratio is 13 g/kg air. In high humid conditions, the dehumidification rate is more significantly influenced by the liquid-air flow rate ratio and less influenced by the desiccant concentration and temperature compared with the low humidity conditions.

The literature survey so far done shows that numerous studies are focused on the effect of various operating parameters (ambient air conditions, solution to air mass flow rate ratio, concentration, solution inlet temperature and number of heat transfer units (NTU)) on the energy exchanger performance (dehumidifier or regenerator) for a given desiccant solution. It is observed that dehumidification rate as well as regeneration rate is greatly influenced by NTU, solution inlet temperature, solution flow rate, solution concentration, air temperature, air humidity ratio and air flow rate irrespective of desiccant solution. In addition to this, few more studies have addressed the effect of desiccant material at respective operating parameters on the performance of dehumidifier/regenerator/ overall system (LDAS).

### **2.3. Effect of desiccant material on performance of dehumidifier/regenerator**

Lof in 1955 introduced first liquid desiccant driven air conditioning system with triethylene glycol (TEG) aqueous solution as the liquid desiccant [46]. However, it is gradually substituted by some salt solutions which are LiCl aqueous solution and LiBr aqueous solution because

boiling temperatures of water and TEG (temperature difference between solution and air is 200°C at atmospheric pressure) are too close that the organic ingredient may vaporize into the processed air. Even though TEG is not toxic, the organic ingredient in the supply air stream makes it unacceptable for practical use in air conditioning [27]. Compared with glycol desiccant solutions, salt solutions (LiCl, CaCl<sub>2</sub> or LiBr solution) won't evaporate into air under ambient conditions. The drawback of the salt solutions is their corrosive nature.

The physical properties of some desiccant solutions, including LiCl, LiBr and CaCl<sub>2</sub> solutions, have been examined by many researchers [47], [48]. Among them, CaCl<sub>2</sub> solution is cheapest but it has the poor moisture absorption potential because of its high vapor pressure at a given operating temperature whereas LiBr solution is the costliest. Longo et. al [49] observed that KCOOH solution compared to LiCl and LiBr solutions is poor in dehumidification performance (low moisture absorption potential) whereas it performs better in regeneration tests (more % change in solution concentration) at typical operating conditions. However, KCOOH is less corrosive and expensive. Afshin et. al [50] investigated several possible desiccant solutions (LiBr, LiCl, CaCl<sub>2</sub> and MgCl<sub>2</sub> solutions) to find the best suitable desiccant solution to be used in a run-around membrane energy exchanger (RAMEE). They dealt effect of desiccant on total effectiveness, operating cost and pumping energy and also discussed the risk of crystallization.

Liu et. al [51] compared mass transfer performance of two frequently used desiccant solutions, LiCl solution and LiBr solution which have same solution temperature and vapour pressures. Their results revealed that LiCl solution gives better mass transfer performance than that of LiBr solution in dehumidification process while LiBr solution gives better mass transfer performance than LiCl solution in the regeneration process. And also they concluded that the system COPs (ratio of achieved cooling capacity in dehumidifier to the heat supplied to the regenerator) using LiCl or LiBr solution are found similar, however, LiCl initial cost is 18% lesser than that of LiBr solution in the present Chinese market. Koronaki et al. [52] theoretically studied the heat and mass transfer performance in counter flow through structured packing at different parameters of LiCl, LiBr and CaCl<sub>2</sub> solutions. It was observed that that the moisture removal rate increasing

with rising desiccant solution inlet concentration, air inlet humidity ratio, air and desiccant solution flow rate; dropping with desiccant solution inlet temperature; and was nearly no variation with air inlet temperature. The study has also revealed that LDAS using LiCl solution seem to have superior performance than those using CaCl<sub>2</sub> and LiBr solutions, under the same working conditions. Ghadiri Moghaddam et al. [36] studied the influence of LiCl and MgCl<sub>2</sub> solutions at three different concentrations on the liquid to air membrane energy exchanger (LAMEE) performance. 10% maximum variance is found for the LAMEE total effectiveness with the different operating conditions. And also the results indicate that both the salt solutions and concentration influence the LAMEE effectiveness, and varying the concentration is one way to regulate the supply air outlet humidity ratio. Gurubalan et. al [53] numerically investigated the impact of operating parameters in the LAMEE using different desiccant solutions such as LiBr, LiCl and CaCl<sub>2</sub> solutions for hot and humid ambient conditions. Their results indicate that the LAMEE can attain an enhanced dehumidification rate at high air flow rates and also with LiCl solution.

Most of these studies are concentrated on the influence of different desiccant solutions on dehumidification and regeneration performance considering dehumidification rate, effectiveness and COP as the performance indices. From the literature survey, it is observed that research is mainly concentrated on effect of desiccant material type, its operating parameters and air parameters on the dehumidification/ regeneration performance.

#### **2.4. Research gap and motivation**

It is well known that ambient condition and room supply conditions are prerequisites to design air conditioning system for a building. Hence, it is necessary to study the system performance for a given ambient condition (peak) and required room supply condition. Accordingly, for a given air conditioning application, we choose refrigerant type, mass flow rate, evaporator inlet temperature and condenser inlet temperature at peak ambient condition and required room supply condition for conventional air conditioning system. In the same manner, suitable liquid desiccant and its

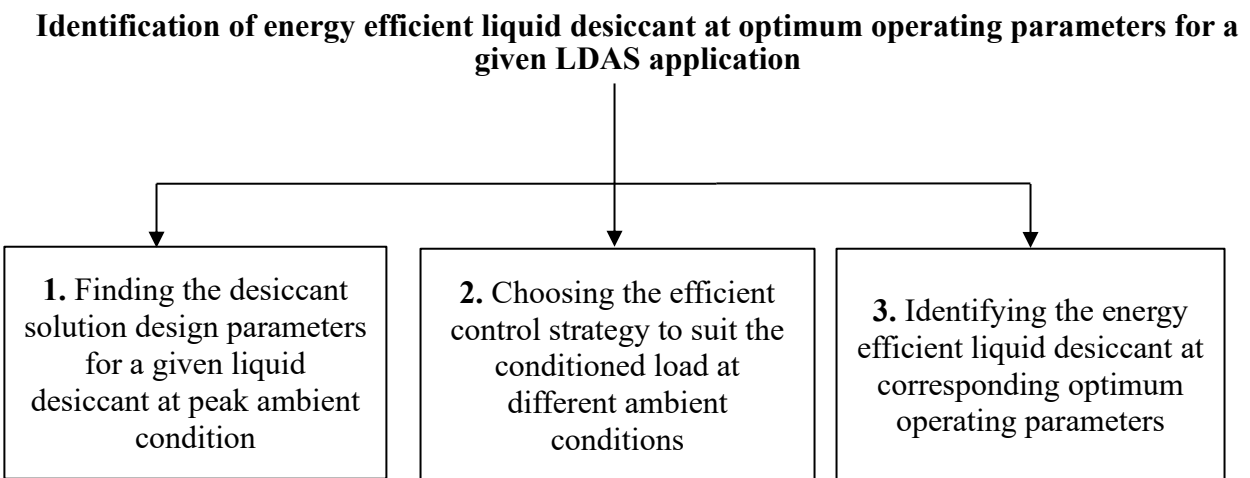
design parameters (mass flow rate, concentration, and inlet temperature) are to be chosen while designing LDAS for an air conditioning application. As so far, no study in the literature has addressed the methodology to identify suitable liquid desiccant and its design parameters for LDAS application. LDAS design includes system components design as well as selection of suitable liquid desiccant solution and its design parameters which are to be considered at peak ambient condition. Few studies are focused on the design of optimum dimensions of flat plate LAMEE channel but not addressed the choosing of energy efficient desiccant material and its operating parameters[54]. This motivates us to present the methodology to identify the suitable energy efficient liquid desiccant at corresponding optimum operating parameters for a given air conditioning application.

It is known that any liquid desiccant at different combinations of operating parameters (heat capacity ratio, concentration and temperature) can achieve required dehumidification rate for a given ambient condition. But suitable liquid desiccant at corresponding optimum operating parameters only can attain energy savings. Therefore to find the right liquid desiccant and corresponding optimum operating parameters for energy efficient LDAS, this study has been divided in to three sections as shown below.

Several works have been done on the influence of different air/solution parameters on dehumidifier/regenerator performance considering effectiveness and moisture removal rate as performance indices. In all their works, how the operating parameters effects the dehumidification rate and effectiveness have been investigated. But this approach is not suitable to design LDAS for an air conditioning application since optimum (design) solution parameters have to be chosen based on other LDAS primary component loads which are the solution heater load, solution cooler load and chiller load but not on the performance of dehumidifier/regenerator. This is due to fixed dehumidification load to be considered at peak ambient condition. Thus, to find the optimum parameters for a given solution, it is required to analyze the effect of different operating parameters of corresponding solution on the solution heater, solution cooler, chiller loads and solution pressure drop to attain the fixed

dehumidification rate at fixed ambient condition. Based on these outcomes, optimum operating parameters (design parameters) will be established for the given desiccant solution. In addition to this, control performance of LDAS has also to be studied since frequent change in ambient conditions requires precise control of the desiccant solution operating parameters (for a given solution) to suit the required conditioned space load. Efficient desiccant solution control strategy will be determined from this objective. With the optimum range of operating parameters and efficient desiccant solution control strategy, influence of desiccant material type (commonly used liquid desiccants) on the mentioned performance indices will be analyzed.

As explained above, this study has been divided into three sections (objectives) which are shown below.



This study will be beneficial for LDAS designers in choosing the appropriate desiccant solution at optimum concentration and heat capacity for an energy efficient membrane based LDAS.

## **2.5. Objectives of thesis**

The following objectives are studied in this thesis.

- To study and identify the suitable combination of desiccant solution operating parameters for energy efficient liquid desiccant air conditioning system.
- To analyze the two desiccant solution control strategies and choose efficient control strategy to suit the required latent load at different ambient conditions.
- To identify the energy efficient desiccant solution among commonly used potential desiccant solution for a given AC application.

## **Chapter 3**

### **System description and solution procedure**

#### **3.1. System description and control volume modelling**

LDAS comprises of mainly 4 components namely dehumidifier, solution heater, regenerator and solution cooler as shown in Fig. 3.1. Counter-flow type LAMEEs of the equal size are considered as dehumidifier and regenerator in this study. As indicated in fig. 3.2a, LAMEE comprises of series of alternate solution and air channels separated by membrane which is impermeable to liquid but not water vapor. As the solution and air output parameters at each channel outlet in full scale LAMEE will be same, control volume has been chosen in full scale LAMEE to find the output parameters at different solution operating conditions.

Control volume which covers half width air channel, membrane and half width solution channel of full scale LAMEE has been chosen to investigate the heat and mass transfer processes at each given solution inlet condition. As shown in fig. 3.2b, in this control volume, channel widths and

mass flow rates only need to be reduced to half in magnitude and two exterior walls considered as adiabatic walls. Accordingly flow rates are halved for each channel. Since the air velocity in air channel is considered 2.4m/s, air flow rate becomes 28 Cfm (Cubic feet/min) as per the considered channel dimensions for full scale LAMEE. As a result, air flow rate in air channel for control volume becomes 14 Cfm. Control volume dimensions are indicated in Table 3.1

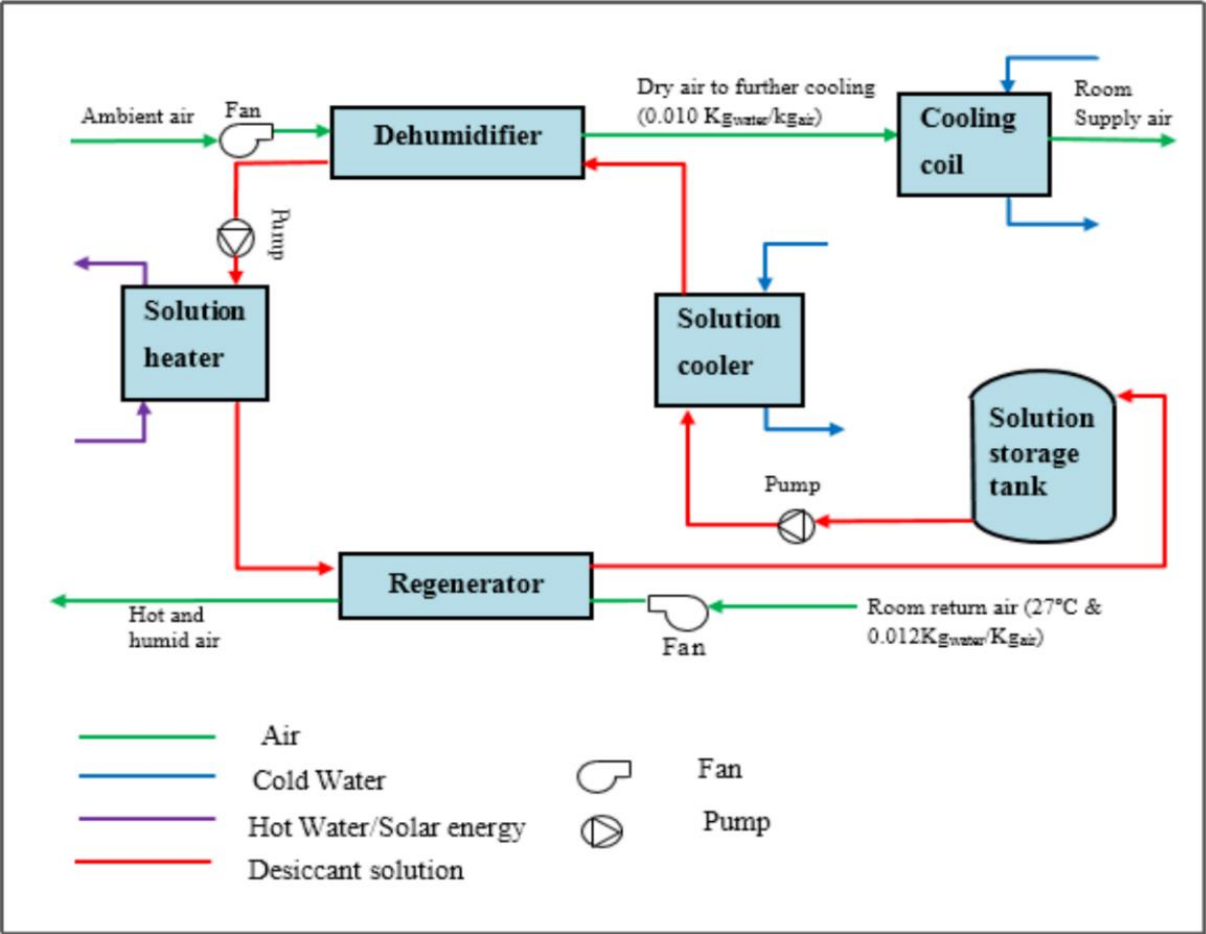


**Fig. 3.1:** Schematic diagram of LDA

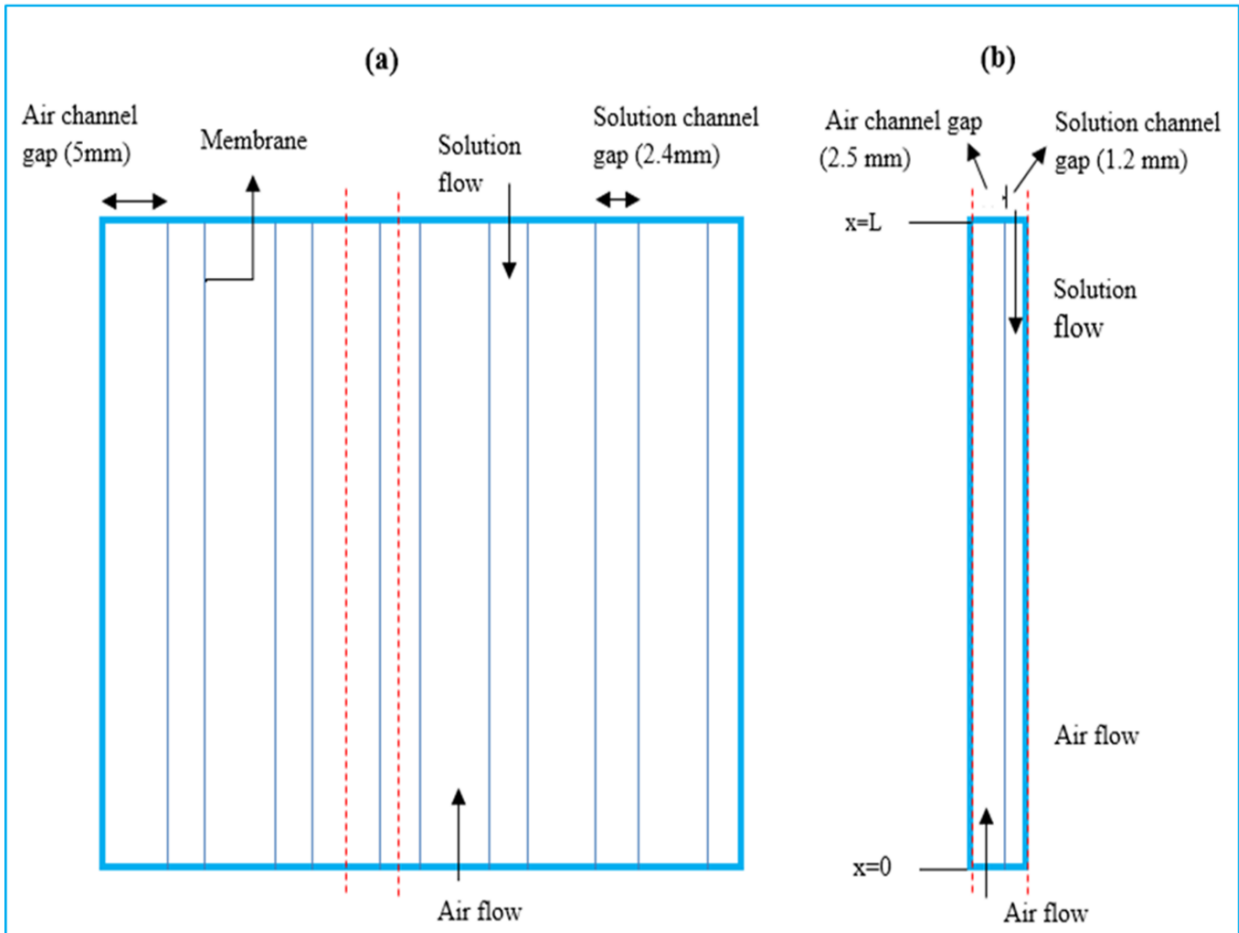


**Fig. 3.2.** Sectional plan views of (a) Full scale LAMEE and (b) Control volume

Table 3.1. Specifications of LAMEE control volume

Parameter	Value	unit
LAMEE length x height (L x H)	1800 x 1000	mm x mm
Air channel width ( $\delta_a/2$ )	2.5	mm
Solution channel width ( $\delta_s/2$ )	1.2	mm
Membrane thickness ( $\delta_m$ )	0.265	mm
Number of transfer units (NTU)	6	--
Air mass flow rate ( $m_a$ )	0.00812	kg s <sup>-1</sup>
Membrane thermal conductivity, $k_m$	0.065	(W m <sup>-1</sup> )
Membrane water vapor resistance, $R_m$ [55]	24	(s m <sup>-1</sup> )

### 3.2. Solution procedure

The objective of the study is to present the methodology to identify the energy efficient liquid desiccant at optimum operating parameters for a given air conditioning application. To accomplish the objective, this study is divided in to three sub-objectives (chapters 4, 5 and 6).

Initially, at fixed dehumidification rate and given peak ambient condition, LDAS performance has been examined at the different combination of solution parameters for a given desiccant solution. The performance indices considered in this study are solution pressure drop, required solution heat addition rate, required solution heat removal rate, and required chiller load (to sensibly cool the concentrated solution leaving regenerator and dehumidified air leaving dehumidifier). By analyzing these performance indices, optimum design solution parameters (design parameters) can be chosen for energy efficient LDAS.

However, for a specific air conditioning application, it requires the proper control of the desiccant solution parameters to suit the variations in space load due to frequent variation in ambient conditions which leads to energy savings and thermal comfort. Thus, methodology to choose the efficient solution control strategy (dehumidifier solution inlet temperature (DSIT) control

strategy/ dehumidifier solution inlet mass flow rate (DSIM) control strategy) has been studied later.

Finally, influence of commonly used potential desiccant solutions such as *LiCl*, *CaCl<sub>2</sub>*, *LiBr* and *KCOOH* solutions at their optimum operating parameters (design parameters) on mentioned performance indices will be studied. Subsequently, performance indices will be analyzed at different ambient conditions also for corresponding solutions by adopting efficient desiccant solution control strategy. Based on these outcomes, energy efficient liquid desiccant at corresponding optimum operating parameters can be selected for a specific air conditioning application.

Table 3.2. Air ambient parameters (Mumbai summer peak condition) and other required parameters

Air conditions	Air parameters	
Ambient peak condition	$T_{amb} = 35^{\circ}\text{C}$ (DBT)	$w_{amb} = 0.031 \text{ kg}_{\text{water}} \text{ kg}_{\text{air}}^{-1}$
Supply air condition	$T_{sup} = 15^{\circ}\text{C}$ (DBT)	$w_{sup} = 0.010 \text{ kg}_{\text{water}} \text{ kg}_{\text{air}}^{-1}$
Room condition	$T_{room} = 25^{\circ}\text{C}$ (DBT)	$w_{room} = 0.012 \text{ kg}_{\text{water}} \text{ kg}_{\text{air}}^{-1}$ ( $RH_{sup} = 50\%$ )
Air flow rate	$m_a = (28/2) \text{ Cfm} = 14 \text{ Cfm} = 0.00812 \text{ kg s}^{-1}$	

100% fresh air supply has been chosen as air conditioning application in this study. Mumbai summer peak parameters are considered as inlet air condition for dehumidifier LAMEE as the air is most hot and humid. Room return air which is  $27^{\circ}\text{C}$  Dry bulb temperature (considered  $2^{\circ}\text{C}$  greater than room condition) and  $w_{room} = 0.012 \text{ kg}_{\text{water}} \text{ kg}_{\text{air}}^{-1}$  is utilized as supply air for regenerator LAMEE since it is relatively drier and cooler than ambient air. Both air flow rate and supply point are considered to be fixed as indicated in Table 3.2. Air inlet condition (mass flow

rate, temperature, humidity ratio) at dehumidifier inlet is fixed at each different solution condition. Since air heat capacity is fixed,  $C_r^*$  directly refers to solution heat capacity.

Considering fixed air outlet humidity ratio at dehumidifier LAMEE exit ( $0.010 \text{ kg}_{\text{water}} \text{ kg}_{\text{air}}^{-1}$ ), required dehumidifier solution inlet temperature at each solution condition which attains required dehumidification rate will be found by trial and error method. Accordingly, variations in solution outlet concentration, solution mass flow rate, solution outlet temperature and air temperature at LAMEE exit will be found out. To achieve the solution outlet concentration at regenerator LAMEE exit equal to the solution inlet concentration at dehumidifier LAMEE entry, required regenerator solution inlet temperature will be found. Subsequently, variations in solution outlet temperature, air outlet temperature and air outlet humidity at regenerator exit will be found out.

Based on these outcomes, the performance indices specified in section (3.3) will be established from which LDAS performance can be analyzed. Zhang's Analytical model [20] has been adopted to determine the required solution and air parameters of LAMEE. Aqueous *LiCl* solution has been considered as liquid desiccant solution in this study for which required thermo-physical properties taken from the correlations established by Manuel R. Conde [28].

### **3.3. Assumptions**

The below assumptions are considered in this study

- (i) Heat and moisture transfer exchanges take place only between air and solution streams.
- (ii) Both solution and air flows are fully developed laminar flows.
- (iii) Air condensation effect in LAMEE has been ignored in the present study.
- (iv) Membrane maldistribution in the LAMEE is ignored.
- (v) Phase change heat (loss or gain) at the air-solution interface occurs only on the liquid side.
- (vi) Heat and moisture transfer in flow direction are assumed negligible in both channels.

- (vii) Thermal diffusivity as well as mass diffusivity considered as constant in the axial direction of the air and solution channels

### 3.4. Governing equations for air and solution

Steady-state energy and mass conservation equations for each fluid (air and solution) in a LAMEE (same for both dehumidifier and regenerator) are as follows (Eqs. 1-4) [56].

$$\frac{\dot{m}_a}{H} c_{p,a} \frac{dT_a}{dx} + U(T_a - T_s) = 0 \quad (1)$$

$$\frac{\dot{m}_s}{H} c_{p,s} \frac{dT_s}{dx} - U(T_a - T_s) - U_m h_{fg} (w_a - w_s) = 0 \quad (2)$$

$$\frac{\dot{m}_a}{H} \frac{dw_a}{dx} + U_m (w_a - w_s) = 0 \quad (3)$$

$$\frac{\dot{m}_{salt}}{H} \frac{dX_s}{dx} - U_m (w_a - w_s) = 0 \quad (4)$$

Where  $H$ ,  $\dot{m}_a$ ,  $\dot{m}_{salt}$ ,  $X_s$ ,  $U$  and  $U_m$  are height of LAMEE, mass of air, mass of salt, solution mass fraction, overall heat and mass transfer coefficients which are expressed as follows (Eqs. 5-8)

$$\dot{m}_{salt} = \frac{\dot{m}_s}{1 + X_s}; \quad (5)$$

$$X_s = \frac{1 - C_s}{C_s} \quad (6)$$

Where  $C$  = salt concentration

$$U = \left( \frac{1}{h_{c,a}} + \frac{\delta_m}{k_m} + \frac{1}{h_{c,s}} \right)^{-1} \quad (7)$$

$$U_m = \left( \frac{1}{h_{m,a}} + R_m + \frac{1}{h_{m,s}} \right)^{-1} \quad (8)$$

where  $h_{c,s}$  and  $h_{c,a}$  are convection heat transfer coefficients of solution and air and  $h_{m,s}$  and  $h_{m,a}$  are convection mass heat transfer coefficients of solution and air which are defined as below. And  $\delta_m$ ,  $k_m$  and  $R_m$  are membrane thickness, membrane thermal conductivity, and membrane water vapor resistance respectively.

Since  $h_{m,s}$  is comparatively much higher than  $h_{m,a}$  which does not make any difference in  $U_m$  value, it can be ignored in the formulation. Therefore Eq. 8 becomes

$$U_m = \left( \frac{1}{h_{m,a}} + R_m \right)^{-1} \quad (9)$$

When the flow between two infinite rectangular parallel plates with constant heat flux across one wall and insulated (adiabatic) on another wall is fully developed laminar, the Nusselt number ( $Nu$ ) is assumed to be 5.39 [57], and it is used to determine the convective heat transfer coefficient by the definition

$$h_c = \frac{Nu.k}{D} \quad (10)$$

with this, convective mass transfer coefficient can be calculated by using below definition (Eq. 11)

$$h_m = \frac{h}{c_p} Le^{\left(\frac{-2}{3}\right)} \quad (11)$$

where  $Le$  is Lewis number which is defined as the ratio of thermal and mass diffusivities

Please note that thermal diffusivity as well as mass diffusivity are considered as constant in the axial direction of the air and solution channels.

It is known that thermal and mass diffusivities of water vapor in air varies with temperature. But, the Lewis number is approximately equal to one for water vapor in air. Thus, Lewis number term can be excluded in the eq.11.

Eqs. (1) - (4) are the governing differential equations for heat and moisture transfer in the module. They can be solved by finite difference iterations, with known heat mass transport properties. However they are difficult for common engineers to use. In contrast, analytical solutions for above differential equations will be convenient and helpful for common designers to use.

To simplify the governing equations, Zhang's Analytical model [34] has been adopted to estimate the required air and solution parameters of LAMEE. Normalized equations for the governing equations (Eqs. 1-4) which applicable to both dehumidifier and regenerator LAMEEs as followed (Eqs. 10-13) [14] can be used.

$$\frac{dT_a^*}{dx^*} = NTU (T_s^* - T_a^*) \quad (12)$$

$$\frac{dT_s^*}{dx^*} = \frac{NTU}{C_r^*} (T_s^* - T_a^*) + \frac{H^*}{C_r^* \cdot c_{p,a}} \frac{dw_a^*}{dx^*} \quad (13)$$

$$\frac{dw_a^*}{dx^*} = NTU_m (w_s^* - w_a^*) \quad (14)$$

$$\frac{dw_s^*}{dx^*} = 2501 \frac{E_T}{H_*} \frac{dT_s^*}{dx^*} \quad (15)$$

Where  $T^*$ ,  $w^*$  and  $x^*$  are dimensionless parameters which are defined as below

Dimensionless parameters for dehumidifier LAMEE are as follows (Eqs.16-19)

$$\text{Dimensionless temperature, } T^* = \frac{T - T_{d,a,i}}{T_{d,s,i} - T_{d,a,i}} ; \quad (16)$$

$$\text{Dimensionless humidity ratio, } w^* = \frac{w - w_{d,a,i}}{w_{d,s,i} - w_{d,a,i}} ; \quad (17)$$

$$\text{Dimensionless length, } x^* = \frac{x}{L} \quad (18)$$

$$H^* \text{ is an operating factor, } H^* = 2501 \frac{w_{d,s,i} - w_{d,a,i}}{T_{d,s,i} - T_{d,a,i}} \quad (19)$$

Dimensionless parameters for regenerator LAMEE are as follows (Eqs.20-23)

$$\text{Dimensionless temperature, } T^* = \frac{T - T_{r,a,i}}{T_{r,s,i} - T_{r,a,i}} ; \quad (20)$$

$$\text{Dimensionless humidity ratio, } w^* = \frac{w - w_{r,a,i}}{w_{r,s,i} - w_{r,a,i}} \quad (21)$$

$$\text{Dimensionless length, } x^* = \frac{x}{L} \quad (22)$$

$$H^* \text{ is an operating factor, } H^* = 2501 \frac{w_{r,s,i} - w_{r,a,i}}{T_{r,s,i} - T_{r,a,i}} \quad (23)$$

where  $T_{d,a}$  and  $w_{d,a}$  are the bulk temperature and humidity ratio of the air, and  $T_{d,s}$  and  $w_{d,s}$  are the bulk temperature and equilibrium humidity ratio of the salt solution in dehumidifier LAMEE.  $T_{r,a}$  and  $w_{r,a}$  are the bulk temperature and humidity ratio of the air, and  $T_{r,s}$  and  $w_{r,s}$  are the bulk temperature and equilibrium humidity ratio of the salt solution in Regenerator LAMEE. The  $i$  and  $o$  represents inlet and outlets of dehumidifier/ regenerator.  $L$  represents length of LAMEE channels (same for both LAMEEs).

And below remaining all formulations are same for both LAMEEs which are defined as (Eqs. 24-27)

$$\text{Heat capacity ratio, } C_r^* = \frac{m_s c_{p,s}}{m_a c_{p,a}} ; \quad (24)$$

$$\text{Slope of equilibrium iso-concentration line, } E_T = \left( \frac{dw_s}{dT_s} \right) \quad (25)$$

$$\text{Number of Transfer Units, } NTU = \frac{U A}{\left( m c_p \right)_{min}} = \frac{U A}{\left( m_a c_{p,a} \right)} \quad (26)$$

$$\text{Number of Mass Transfer Units, } NTU_m = \frac{U_m A}{m_a} \quad (27)$$

Where  $A$ = Air- Desiccant solution interface area

Analytical solution: Equations (12), (13) and (14), (15) are the governing differential equations for heat and moisture transfer in the module. Subtracting Eq. (12) from (13) yields

$$\frac{d(T_s^* - T_a^*)}{dx^*} = \frac{NTU}{C_r^*} (T_s^* - T_a^*) + \frac{H^*}{C_r^* \cdot c_{p,a}} \frac{dw_a^*}{dx^*} - NTU (T_s^* - T_a^*) \quad (28)$$

Substituting eq.(14) in eq.(28), it becomes

$$\frac{d(T_s^* - T_a^*)}{dx^*} = \left(\frac{1}{C_r^*} - 1\right) NTU (T_s^* - T_a^*) + \frac{H^*}{C_r^* \cdot c_{p,a}} NTU_m (w_s^* - w_a^*) \quad (29)$$

Subtracting eq. (14) from eq. (15) yields

$$\frac{d(w_s^* - w_a^*)}{dx^*} = 2501 \frac{E_T}{H_*} \frac{dT_s^*}{dx^*} - NTU_m (w_s^* - w_a^*) \quad (30)$$

Substituting eqs.(13) and (14) in eq.(30), it becomes

$$\frac{d(w_s^* - w_a^*)}{dx^*} = NTU_m \left(1 - 2501 \frac{H^*}{C_r^* \cdot c_{p,a}}\right) (w_s^* - w_a^*) - 2501 \frac{E_T}{H_*} \frac{NTU}{C_r^*} (T_s^* - T_a^*) \quad (31)$$

Inorder to simplify the eqs. (29) and (31), we define

$$\xi = (T_s^* - T_a^*) \quad (32)$$

$$\psi = (w_s^* - w_a^*) \quad (33)$$

Then the governing differential Eqs. (29) and (31) will transformed into

$$\frac{d\xi}{dx^*} = a_{11}\xi + a_{12}\psi \quad (34)$$

$$\frac{d\psi}{dx^*} = a_{21}\xi + a_{22}\psi \quad (35)$$

With constatnts

$$a_{11} = \left(\frac{1}{C_r^*} - 1\right) NTU \quad (36)$$

$$a_{12} = \frac{H^*}{C_r^* \cdot c_{p,a}} NTU_m \quad (37)$$

$$a_{21} = -2501 \frac{E_T}{H_*} \frac{NTU}{C_r^*} \quad (38)$$

$$a_{22} = NTU_m \left(1 - 2501 \frac{H^*}{C_r^* \cdot c_{p,a}}\right) \quad (39)$$

The set of eqs. (34) and (35) have analytical solutions in the form as shown below

$$\xi = C_1 e^{\lambda_1 x^*} + C_2 e^{\lambda_2 x^*} \quad (40)$$

$$\psi = -K_1 C_1 e^{\lambda_1 x^*} + K_2 C_2 e^{\lambda_2 x^*} \quad (41)$$

The roots of the characteristic Eqs. of (34) and (35) are given as

$$\lambda_{1,2} = \frac{(a_{11} + a_{22}) \pm \sqrt{(a_{11} + a_{22})^2 - 4(a_{11}a_{22} - a_{12}a_{21})}}{2} \quad (42)$$

By satisfying the general set of Eqs. (40) and (41) to Eq. (34), the coefficients of  $K_1$  and  $K_2$  are given as

$$K_1 = \frac{a_{11} - \lambda_1}{a_{12}} \quad (43)$$

$$K_2 = \frac{-a_{11} + \lambda_2}{a_{12}} \quad (44)$$

Similarly, by satisfying the general set of Eqs. (40) and (41) to Eq. (35), the coefficients of  $K_1$  and  $K_2$  are given as

$$K_1 = \frac{a_{21}}{a_{22} - \lambda_1} \quad (45)$$

$$K_2 = \frac{a_{21}}{\lambda_2 - a_{22}} \quad (46)$$

Either Eqs. (43), (44) or (45), (46) can be applied. In this study, Eqs.(43) and (44) are used

### 3.4.1. For dehumidifier

$$\text{At } x^* = 0, T_{d,a,i}^* = 0; w_{d,a,i}^* = 0 \quad (47)$$

Eqs. (40) and (41) become

$$\xi = T_{d,s,o}^* - T_{d,a,i}^* = T_{d,s,o}^* = C_1 + C_2 \quad (48)$$

$$\psi = w_{d,s,o}^* - w_{d,a,i}^* = w_{d,s,o}^* = -K_1 C_1 + K_2 C_2 \quad (49)$$

$$\text{At } x^* = 1, T_{d,s,i}^* = 1; w_{d,s,i}^* = 1 \quad (50)$$

Eqs. (40) and (41) become

$$\xi = T_{d,s,i}^* - T_{d,a,o}^* = 1 - T_{d,a,o}^* = C_1 e^{\lambda_1} + C_2 e^{\lambda_2} \quad (51)$$

$$\psi = w_{d,s,i}^* - w_{d,a,o}^* = 1 - w_{d,a,o}^* = -K_1 C_1 e^{\lambda_1} + K_2 C_2 e^{\lambda_2} \quad (52)$$

Further, integrating Eq. (15) from  $x^* = 0$  to 1 which yields

$$w_{d,s,o}^* - w_{d,s,i}^* = 2501 \frac{E_T}{H_*} (T_{d,s,o}^* - T_{d,s,i}^*) \quad (53)$$

Overall heat balance equation in the LAMEE can be written as

$$\dot{m}_s c_{p,s} (T_{d,s,i} - T_{d,s,o}) = \dot{m}_a c_{p,a} (T_{d,a,o} - T_{d,a,i}) + \dot{m}_a h_{fg} (w_{d,a,o} - w_{d,a,i}) \quad (54)$$

Normalizing the above equation to

$$T_{d,s,i}^* - T_{d,s,o}^* = \left(\frac{1}{C_r^*}\right)(T_{d,a,o}^* - T_{d,a,i}^*) + \left(\frac{H^*}{c_{p,a} \cdot C_r^*}\right)(w_{d,a,o}^* - w_{d,a,i}^*) \quad (55)$$

Substituting Eqs. (48) to (52) into Eqs. (53) and (55) respectively then

Eq. (53) becomes

$$(K_1 + 2501 \frac{E_T}{H_*})C_1 + (2501 \frac{E_T}{H_*} - K_2)C_2 + (1 - 2501 \frac{E_T}{H_*}) = 0 \quad (56)$$

Eq. (55) becomes

$$\left(1 - \frac{1}{C_r^*} e^{\lambda_1} - \frac{H^*}{c_{p,a} \cdot C_r^*} K_1 e^{\lambda_1}\right)C_1 + \left(1 + \frac{1}{C_r^*} e^{\lambda_2} - \frac{H^*}{c_{p,a} \cdot C_r^*} K_2 e^{\lambda_2}\right)C_2 + \left(\frac{1}{C_r^*} - 1\right) = 0 \quad (57)$$

Eqs. (56) and (57) can be written in the following form as

$$b_{11}C_1 + b_{12}C_2 + b_{13} = 0 \quad (58)$$

$$b_{21}C_1 + b_{22}C_2 + b_{23} = 0 \quad (59)$$

Where the coefficients in the equations are

$$b_{11} = K_1 + 2501 \frac{E_T}{H_*} \quad (60)$$

$$b_{12} = 2501 \frac{E_T}{H_*} - K_2 \quad (61)$$

$$b_{13} = 1 - 2501 \frac{E_T}{H_*} \quad (62)$$

$$b_{21} = 1 - \frac{1}{C_r^*} e^{\lambda_1} - \frac{H^*}{c_{p,a} \cdot C_r^*} K_1 e^{\lambda_1} \quad (63)$$

$$b_{22} = 1 + \frac{1}{C_r^*} e^{\lambda_2} - \frac{H^*}{c_{p,a} \cdot C_r^*} K_2 e^{\lambda_2} \quad (64)$$

$$b_{23} = \frac{1}{C_r^*} - 1 \quad (65)$$

Algebraic solution of the set of Eqs. (58) and (59) are

$$C_1 = \frac{b_{13}b_{22} - b_{12}b_{23}}{b_{12}b_{21} - b_{11}b_{22}} \quad (66)$$

$$C_2 = \frac{b_{11}b_{23} - b_{13}b_{21}}{b_{12}b_{21} - b_{11}b_{22}} \quad (67)$$

At this step, the analytical solution of Eqs. (34) and (35) are obtained. With these coefficients, air outlet temperature and humidity can be calculated.

$$T_{d,a,o}^* = 1 - C_1 e^{\lambda_1} - C_2 e^{\lambda_2} \quad (68)$$

$$w_{d,a,o}^* = 1 + K_1 C_1 e^{\lambda_1} - K_2 C_2 e^{\lambda_2} \quad (69)$$

solution outlet temperature and humidity can also be calculated from Eqs. (48) and (49)

### 3.4.2. For regenerator

In the same manner explained in section 3.4.1 for dehumidifier, air and solution outlet conditions for regenerator also can be determined.

### 3.5. Performance indices

With the air and solution output parameters for dehumidifier and regenerator determined in section 3.4, following performance indices can be established.

➤ **Cooling capacity (air cooling load attained in dehumidifier)**

It can be defined as

$$Q_{cc} = Q_{sen} + Q_{lat} = \dot{m}_a (h_{d,a,i} - h_{d,a,o}) \quad (70)$$

Where  $Q_{sen}$  (Air sensible cooling attained in dehumidifier) =  $\dot{m}_a c_{p,a} (T_{d,a,o} - T_{d,a,i})$ ,

$Q_{lat}$  (Air latent cooling attained in dehumidifier) =  $\dot{m}_a h_{fg} (w_{d,a,i} - w_{d,a,o})$

$\dot{m}_a$  = air mass flow rate,  $c_{p,a}$  = air specific heat,  $T_{d,a,i}$  and  $T_{d,a,o}$  = Air temperatures at dehumidifier inlet and outlets,  $w_{d,a,i}$  and  $w_{d,a,o}$  = Air humidity contents at dehumidifier inlet and outlets,  $h_{fg}$  = Phase change heat = 2501 kJ kg<sup>-1</sup> and  $h_{d,a,o}$  &  $h_{d,a,i}$  = Air enthalpy at dehumidifier outlet and inlets

➤ **Desiccant solution pressure drop**

It can be defined as follows

$$\Delta p_s \text{ (Pa)} = \frac{f_s L V_s^2 \rho_s}{2D_s} \quad (71)$$

$f_s = \frac{64}{\text{Re}}$  as flow is laminar, where  $f_s$  = friction factor,

Re = Reynolds's number =  $\frac{\rho_s V_s D_s}{\mu_s}$

$\rho_s$  = solution density,  $V_s$  = Solution average velocity,  $D_s$  = Solution channel hydraulic diameter  $\mu_s$  = Solution dynamic friction,  $L$  = length of channel

➤ **Required solution heat removal rate for solution cooling**

It is written as

$$Q_{rem} = \dot{m}_s c_{p,s} (T_{r,s,o} - T_{d,s,i}) \quad (72)$$

where  $\dot{m}_s$  = solution mass flow rate,  $c_{p,s}$  = Solution specific heat,

$T_{d,s,i}$  = temperature of solution at dehumidifier inlet

$T_{r,s,o}$  = temperature of solution at regenerator outlet

➤ **Required solution heat addition rate for solution heating**

It is given by

$$Q_{add} = \dot{m}_s c_{p,s} (T_{r,s,i} - T_{d,s,o}) \quad (73)$$

$T_{r,s,i}$  = temperature of solution at regenerator inlet

➤ **Required sensible cooling for dehumidified air to meet supply condition ( $T_{sup}$ )**

It is given by

$$Q_{sen2} = \dot{m}_a c_{p,a} (T_{sup} - T_{d,a,o}) \quad (74)$$

where  $T_{sup}$  = Required air temperature at supply condition (Table 2)

$T_{d,a,o}$  = Air temperature at dehumidifier outlet

➤ **Chiller load for sensible cooling of hot concentrated solution and dehumidified air**

It refers to

$$Q_{chiller} = Q_{rem} + Q_{sen2} \quad (75)$$

➤ **Power consumption for solution pumping**

$$P_s (kW) = \frac{\dot{m}_s \Delta p_s * 0.001}{\rho_s} \quad (76)$$

### 3.6. Boundary conditions

#### Dehumidifier boundary conditions

Since main objective of this study is to achieve same dehumidification rate at different operating conditions, moisture content at dehumidifier air outlet ( $w_{a,d,o}$ ) has to be fixed which is  $0.01 \text{ kg}_{\text{water}} \text{ kg}_{\text{air}}^{-1}$ .

$$\begin{aligned}
 T_a(x=0) &= T_{amb} = T_{d,a,i} ; & T_a(x=L) &= T_{d,a,o} ; \\
 w_a(x=0) &= w_{amb} = w_{d,a,i} ; & w_a(x=L) &= w_{d,a,o} = 0.01 \text{ kg}_{\text{water}} \text{ kg}_{\text{air}}^{-1} \\
 T_s(x=0) &= T_{d,s,o} ; & T_s(x=L) &= T_{d,s,i} \\
 w_s(x=0) &= w_{d,s,o} ; & w_s(x=L) &= w_{d,s,i} \\
 C(x=0) &= C_{d,s,o} ; & C(x=L) &= C_{d,s,i}
 \end{aligned}$$

Non-dimensional form of boundary conditions are as follows

$$\begin{aligned}
 T_a^*(x=0) &= 0 ; & T_a^*(x=L) &= \xi_{sen,d} \\
 w_a^*(x=0) &= 0 ; & w_a^*(x=L) &= \xi_{lat,d} \\
 T_s^*(x=L) &= T_{d,s,i} = 1 ; & w_s^*(x=L) &= w_{d,s,i} = 1
 \end{aligned}$$

#### Regenerator boundary conditions

$$\begin{aligned}
 T_a(x=0) &= 27^\circ\text{C}; & T_a(x=L) &= T_{r,a,o} \\
 w_a(x=0) &= 0.012 \text{ kg}_{\text{water}} \text{ kg}_{\text{air}}^{-1}; & w_a(x=L) &= w_{r,a,o} \\
 T_s(x=0) &= T_{r,s,o} ; & T_s(x=L) &= T_{r,s,i} \\
 w_s(x=0) &= w_{r,s,o} ; & w_s(x=L) &= w_{r,s,i}
 \end{aligned}$$

Since solution concentration at regenerator inlet will be the same as solution concentration at dehumidifier outlet and also solution concentration at dehumidifier inlet will be the same as solution concentration at regenerator outlet, concentration at regenerator boundaries becomes as

$$C(x=0) = C_{r,s,o} = C_{d,s,i}; \quad C(x=L) = C_{r,s,i} = C_{d,s,o}$$

Non-dimensional form of boundary conditions are as follows

$$T_a^*(x=0) = 0; \quad T_a^*(x=L) = \xi_{sen,r}$$

$$w_a^*(x=0) = 0; \quad w_a^*(x=L) = \xi_{lat,r}$$

$$T_s^*(x=L) = T_{r,s,i} = 1; \quad w_s^*(x=L) = w_{r,s,i} = 1$$

As mentioned in this section, solution & air temperatures at dehumidifier & regenerator channel outlets ( $T_{d,s,o}$ ,  $T_{r,s,o}$ ,  $T_{d,a,o}$  &  $T_{r,a,o}$ ) and solution & air moisture content at dehumidifier & regenerator solution outlets ( $w_{d,s,o}$ ,  $w_{r,s,o}$ ,  $w_{d,a,o}$ ,  $w_{r,a,o}$ ) are the output parameters which vary in x-direction. Considering the mentioned pre-defined boundary conditions, these output parameters were determined analytically.

Sections 4.2.1 and 4.2.2 explained about the variation in these parameters along the x-direction

### 3.7. Validation of the current analytical model

**Table 3.3:** Ambient test conditions considered in the experiment [58]

Test	Air parameters
F1	$T_{a,i} = 38.8^\circ\text{C}$ (DBT); $w_{a,i} = 0.0214 \text{ kg}_{\text{water}} \text{ kg}_{\text{air}}^{-1}$
F2	$T_{a,i} = 35.4^\circ\text{C}$ (DBT); $w_{a,i} = 0.0160 \text{ kg}_{\text{water}} \text{ kg}_{\text{air}}^{-1}$
F3	$T_{a,i} = 36.3^\circ\text{C}$ (DBT); $w_{a,i} = 0.0176 \text{ kg}_{\text{water}} \text{ kg}_{\text{air}}^{-1}$
F4	$T_{a,i} = 35.4^\circ\text{C}$ (DBT); $w_{a,i} = 0.0210 \text{ kg}_{\text{water}} \text{ kg}_{\text{air}}^{-1}$

As mentioned earlier, control volume has been considered in this study with which full scale LAMEE performance can be estimated. At given ambient test conditions as indicated in Table 3.3, current considered model is validated with existed experiment results published by [58].

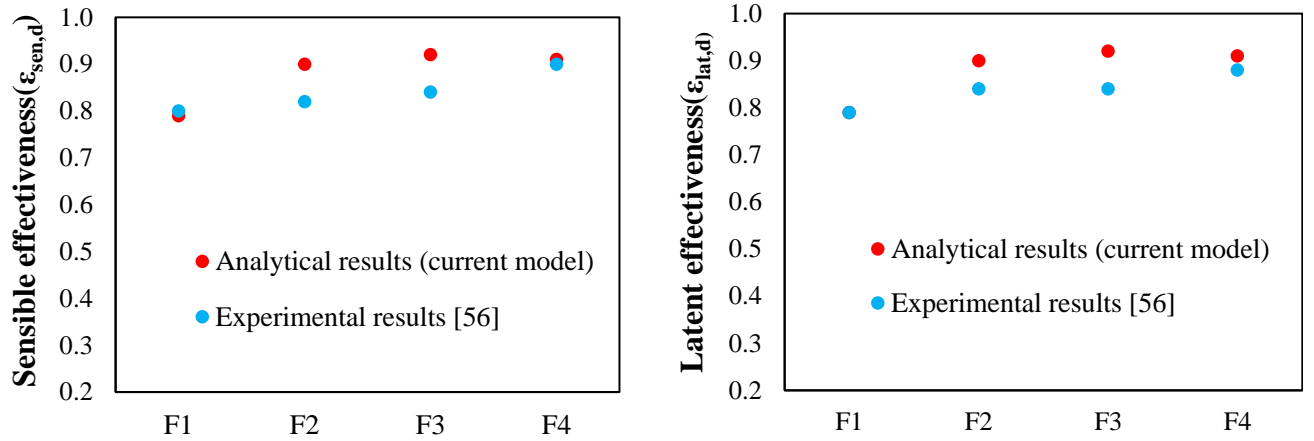


**Fig. 3.3.** Comparison of  $\varepsilon_{sen}$  and  $\varepsilon_{lat}$  obtained from current analytical model with existing experimental and numerical results at different ambient conditions (F1-F4)

It is observed from Fig. 3.3 that the analytical results obtained for this control volume are in acceptable agreement with that of full scale LAMEE. Dehumidifier's sensible effectiveness ( $\varepsilon_{sen,d}$ ) and latent effectiveness ( $\varepsilon_{lat,d}$ ) obtained from the current model are accurate within an error of 1 to 5% and 1 to 9% to that of original numerical and experimental results respectively (Fig. 3.3). As the results are in acceptable range (since variation in the results is below 10%), the current model is acceptable and can be used to predict the outlet parameters in this study.

- Sensible effectiveness for dehumidifier LAMEE is given by Eq. 77 as follows

$$\xi_{sen,d} = \frac{T_{d,a,o} - T_{d,a,i}}{T_{d,s,i} - T_{d,a,i}} \quad (77)$$

- Latent effectiveness for dehumidifier LAMEE is given by Eq. 78 as follows

$$\xi_{lat,d} = \frac{W_{d,a,o} - W_{d,a,i}}{W_{d,s,i} - W_{d,a,i}} \quad (78)$$

## **Chapter 4**

### **Identification of optimum desiccant solution parameters for a given liquid desiccant**

#### **4.1. Methodology**

The objective of the thesis is to choose suitable potential liquid desiccant at corresponding optimum operating parameters for a given air conditioning application. As mentioned earlier that, first step to achieve the objective is to find the optimum solution operating parameters for a given liquid desiccant. This chapter addresses this sub-objective of the thesis.

It is well known that ambient condition and room supply conditions are prerequisites to design air conditioning system for a building. Hence, it is necessary to study the system performance for a given ambient condition and required room supply condition. Suitable combination of desiccant solution parameters may achieve the required dehumidification rate for a given ambient condition. To meet the required humidity ratio, other components of the LDAS like regenerator,

solution heater, solution cooler and economizer play a significant role. Hence, varying the dehumidifier solution parameters will have an effect on the performance of all these components. In this chapter, at fixed dehumidification rate and given ambient condition, LDAS performance has been examined at the different combination of solution parameters. The performance indices considered are solution pressure drop, required solution heat addition rate, and required chiller load (to sensibly cool the concentrated solution leaving regenerator and dehumidified air leaving dehumidifier). By analyzing these performance indices, optimum design solution parameters can be chosen for energy efficient LDAS. The analysis made in this chapter helps LDAS designers in selecting the suitable solution design parameters which could attain energy savings and also required chiller design capacity can be estimated.

To supply cool and dry air to the conditioned room, initially, the ambient air (100% fresh air) has to be dehumidified with the use of LDAS to required humidity content and then it has to be sensibly cooled to supply air condition by another method (VCRS system/ indirect evaporation cooling system). Different concentrated solutions at different heat capacities and temperatures can be employed in LDAS to dehumidify the ambient air to same required humidity point, but air might reach different temperatures. Selection of suitable solution operating parameters plays a vital role in the design of an energy efficient LDAS which leads to energy savings. In this chapter, LiCl solution has been considered as liquid desiccant.

Since solution concentration and its heat capacity are prominent factors to affect the LDAS performance, various combinations of different heat capacities ( $C_r^* = 2.5, 3, 4$  and  $5$ ) and different concentrations ( $C_s = 0.25, 0.3, 0.35$  and  $0.4$ ) are considered to analyze the system performance by fixing the air outlet humidity ratio at dehumidifier LAMEE exit as  $0.010 \text{ kg}_{\text{water}} \text{ kg}_{\text{air}}^{-1}$ . LDAS performance is evaluated at 16 different solution combinations which are listed in Table 4.1 as below.

Table 4.1. Different combinations of solution parameters (16 nos)

S no	Heat capacity ratio, $C_r^*$	Concentration, $C_s$
1		$C_s = 0.25$
2		$C_s = 0.30$
3	$C_r^* = 2.5$	$C_s = 0.35$
4		$C_s = 0.40$
5		$C_s = 0.25$
6		$C_s = 0.30$
7	$C_r^* = 3.0$	$C_s = 0.35$
8		$C_s = 0.40$
9		$C_s = 0.25$
10		$C_s = 0.30$
11	$C_r^* = 4.0$	$C_s = 0.35$
12		$C_s = 0.40$
13		$C_s = 0.25$
14		$C_s = 0.30$
15	$C_r^* = 5.0$	$C_s = 0.35$
16		$C_s = 0.40$

Analytical model developed by [34] has been adopted to evaluate the required air and solution outputs of dehumidifier/ regenerator. Aqueous *LiCl* solution properties have been taken from the correlations established by [47]. Based on this correlations, *LiCl* psychrometric chart has been made and *LiCl* iso-concentration lines are indicated as shown in Figure 4.1.

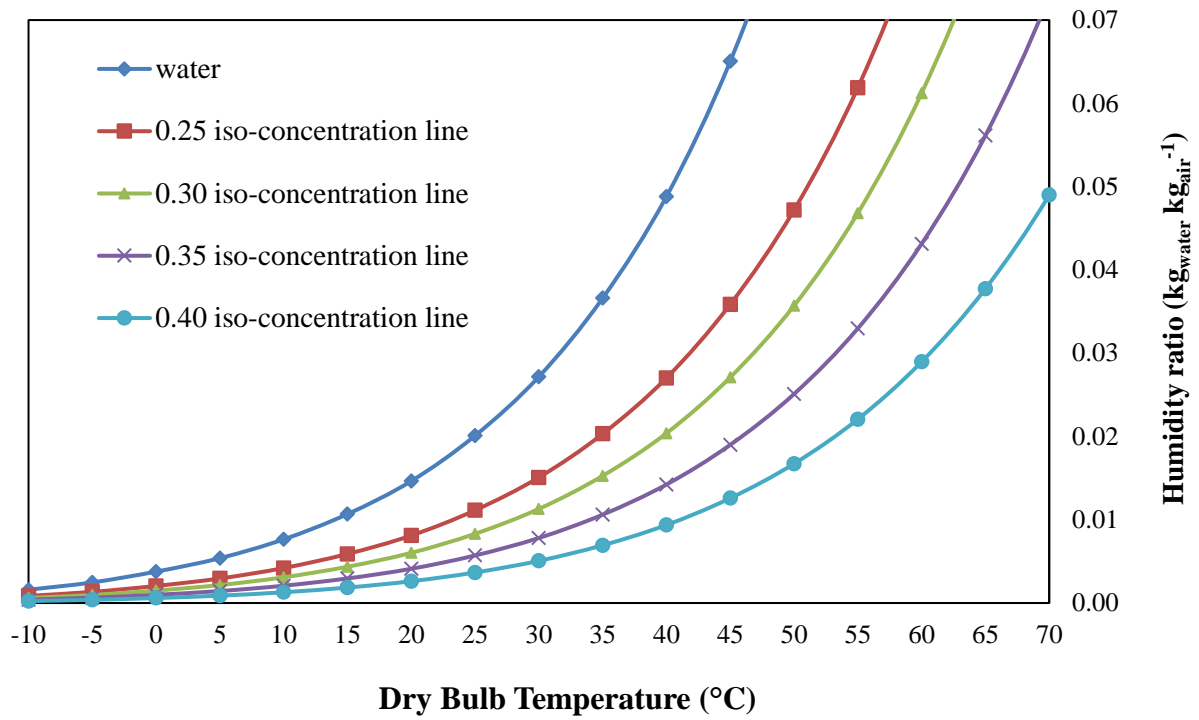


**Fig. 4.1.** LiCl solution Psychrometric chart

## 4.2. Results and discussions

Air and solution parameters at outlets of dehumidifier and regenerator (single pair air-solution channel LAMEE) are found at each solution inlet condition and indicated in psychrometric charts as shown in Figs. 4.2 and 4.5 respectively.

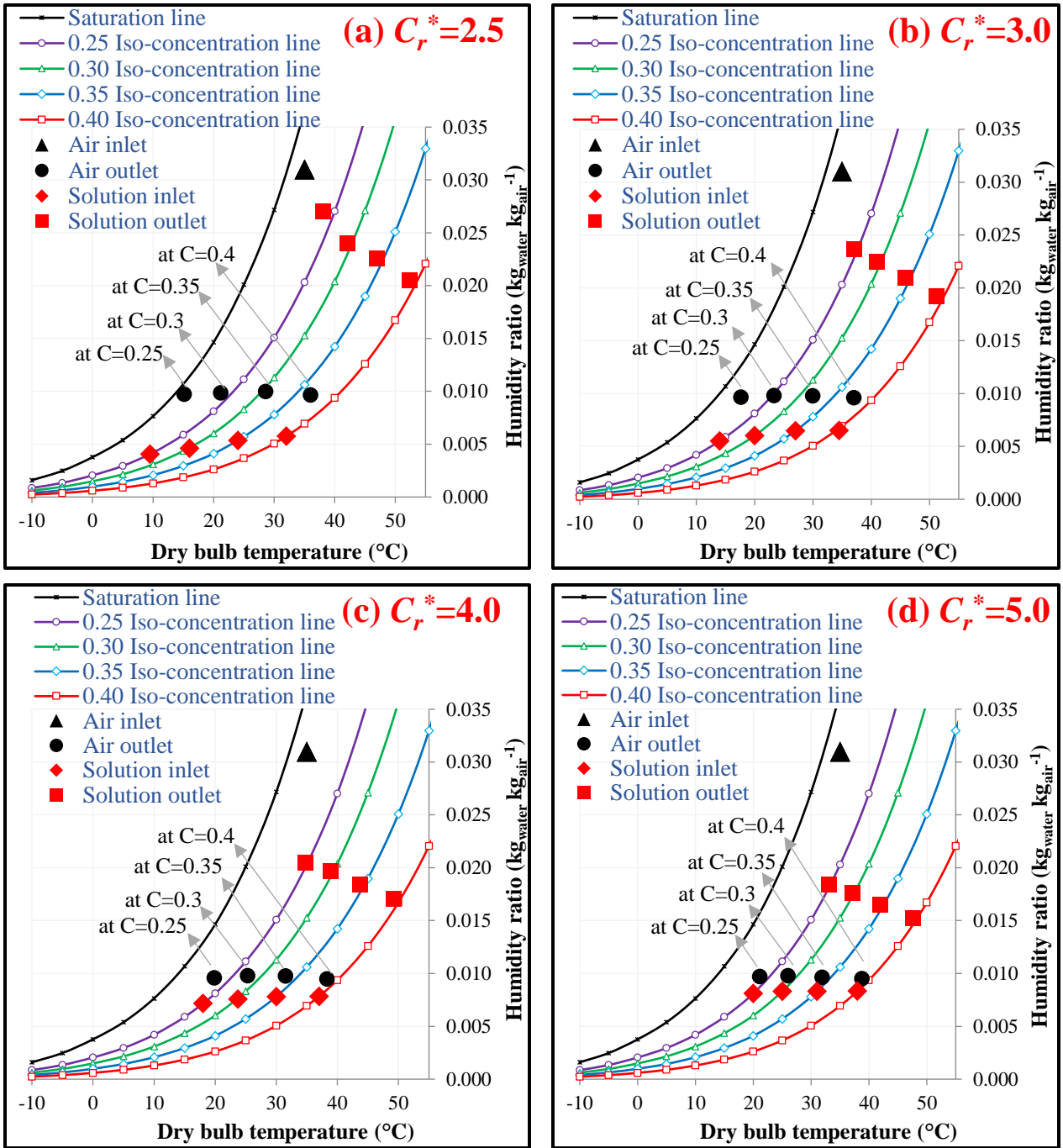


Fig. 4.2. Psychrometric chart indicates dehumidifier air and solution conditions at (a)  $C_r^* = 2.5$ , (b)  $C_r^* = 3.0$ , (c)  $C_r^* = 4.0$  & (d)  $C_r^* = 5.0$  and different concentrations

## 4.2.1. Variation in dehumidifier parameters and dehumidifier related performance indices

### 4.2.1.1. Variation in required dehumidifier solution inlet temperature ( $T_{d,s,i}$ )

Fig. 4.2 shows, at  $C_r^*=2.5$ , required dehumidifier solution inlet temperature ( $T_{d,s,i}$ ) increases from 10°C to 32°C as concentration increases from 0.25 to 0.4. This is because, to achieve the required dehumidification rate at same heat capacity ratio, solution equilibrium humidity ratio (vapor pressure) has to be same even solution concentration increases which can be achieved by rising  $T_{d,s,i}$ . As  $C_r^*$  increases from 2.5 to 5 at concentration,  $C_s=0.25$ , required  $T_{d,s,i}$  gradually increases from 10°C to 20°C. This is due to raise in mass solution mass flow rate which itself promotes the moisture absorption potential. Accordingly, solution equilibrium humidity ratio needs to be raised with increase in solution mass flow rate to achieve the required dehumidification rate. And also it is observed from Fig. 5 that as the slope of  $C_s=0.25$  iso-concentration slope line is more (due to more evaporation rate) than the slope of  $C_s=0.4$  iso-concentration line at same humidity ratio (vapor pressure), it requires less temperature raise at high concentration ( $C_s=0.4$ ) than at low concentration ( $C_s=0.25$ ) to get same humidity ratio (vapor pressure) raise. Thus  $T_{d,s,i}$  raise is only 5°C (from 32°C to 37°C) as  $C_r^*$  increases from 2.5 to 5 at concentration  $C_s=0.4$  whereas  $T_{d,s,i}$  raise is 10°C (from 10°C to 20°C) as  $C_r^*$  increases from 2.5 to 5 at concentration  $C_s=0.25$ .

### 4.2.1.2. Variation in dehumidifier solution outlet temperature ( $T_{d,s,o}$ )

It is to be noted that, in this study, phase change heat has no significance on variation in solution outlet temperature ( $T_{d,s,o}$ ) at different solution conditions since same phase change heat gets released to solution irrespective of solution inlet condition as dehumidification rate is fixed. Therefore  $T_{d,s,o}$  predominantly affected by solution heat capacity and its temperature. From Fig. 5, it is observed that solution temperature raise is 28°C (solution inlet and outlets are 10°C and 38°C) at  $C_r^*=2.5$  and  $C_s=0.25$ , whereas it is 12°C (solution inlet and outlets are 20°C and 32°C) at  $C_r^*=5$  and  $C_s=0.25$  in the dehumidification process. The same trend follows as concentration

increases from  $C_s = 0.25$  to 0.4. The decrease in solution temperature raise with the raise in  $C_r^*$  at any fixed concentration is because of increase in solution heat capacity with the raise in  $C_r^*$ . And also as observed from Fig. 3(a), at  $C_r^* = 2.5$ , solution temperature raise in the dehumidifier is decreasing with increase in concentration which means solution temperature raise are 28°C, 26°C, 23°C and 21°C at concentrations 0.25, 0.3, 0.35 and 0.4 respectively. This drop in solution temperature raise is due to the reduction in heat transfer potential because of reduction in the temperature difference between solution inlet and air inlet as concentration raises.

#### 4.2.1.3. Variation in dehumidifier air outlet temperature ( $T_{d,a,o}$ )

In this study, it is assumed that latent heat of condensation due to phase change in dehumidification process will be considered on solution side only. It means that phase change heat does not affect air temperature in the dehumidifier. It implies that dehumidifier air outlet temperature ( $T_{d,a,o}$ ) depends only on solution heat capacity and its temperature. It is observed from Fig. 4.2(a) that, as the solution inlet temperature ( $T_{d,s,i}$ ) is lower (10°C) at  $C_r^* = 2.5$  and  $C_s = 0.25$ ,  $T_{d,a,o}$  also becomes low (15°C), i.e., air temperature reduces from 35°C (ambient) to 15°C. As  $T_{d,s,i}$  increases from 10°C to 20°C with the increase in  $C_r^*$  from 2.5 to 5 at  $C_s = 0.25$ ,  $T_{d,a,o}$  also increases from 15°C to 21°C. Increases in  $T_{d,a,o}$  with the increase in  $C_r^*$  at 0.25 concentration is because of the raise in  $T_{d,s,i}$  with the raise in  $C_r^*$ . And also it is observed that  $T_{d,a,o}$  raises from 15°C to 36°C with the raise in concentration from 0.25 to 0.4 at  $C_r^* = 2.5$ . This is because of increase in  $T_{d,s,i}$  with the raise in concentration at any fixed  $C_r^*$ . One more observation found that  $T_{d,a,o}$  exceeds  $T_{d,a,i}$  at  $C = 0.4$  and at any  $C_r^*$  which means air gets heated at  $C_s = 0.4$ . This is because, required  $T_{d,s,i}$  is higher at higher solution concentration to attain required dehumidification rate. The same trend follows at different heat capacity ratios also ( $C_r^* = 3, 4$  and 5) as solution concentration increases from 0.25 to 0.4.

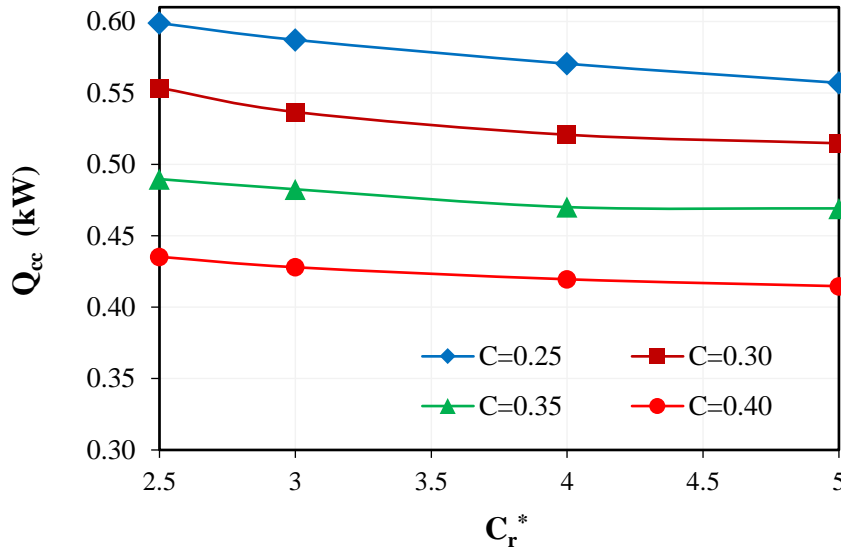
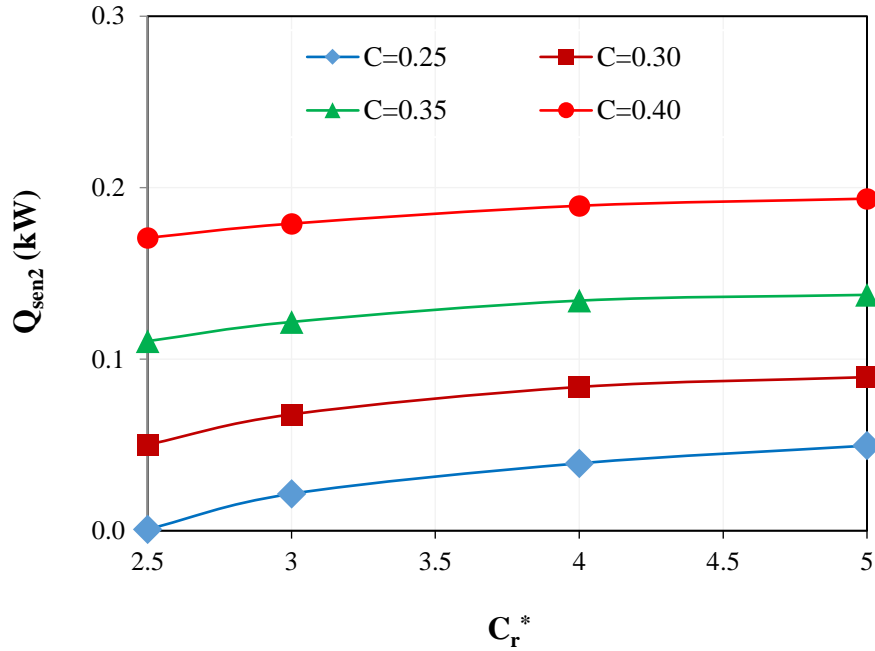


Fig. 4.3. Heat capacity ratio ( $C_r^*$ ) vs. air total cooling (sensible + latent cooling) achieved in the dehumidifier ( $Q_{cc}$ ) at different concentrations

#### 4.2.1.4. Variation in air cooling capacity achieved in the dehumidifier ( $Q_{cc}$ )

In this study, as the latent cooling (moisture absorption) is considered to be fixed, achieved air cooling capacity ( $Q_{cc}$ ) varies only with the sensible cooling load. Air Sensible cooling again depends only on the dehumidifier air outlet temperature. It is observed from Fig. 4.1 that, as dehumidifier solution inlet temperature ( $T_{d,s,i}$ ) increases from 10°C to 20°C with increase in  $C_r^*$  from 2.5 to 5 at  $C_s=0.25$ , dehumidifier air outlet temperature ( $T_{d,a,o}$ ) increases from 15°C to 21°C which results in decrease of air total cooling load from 0.60W to 0.56 kW. And also it is observed from Fig. 4.3 that air total cooling load ( $Q_{cc}$ ) decreases from 0.60 kW to 0.44 kW as  $T_{d,s,i}$  increases from 10°C to 32°C with the increase in concentration from 0.25 to 0.4 at  $C_r^*=2.5$ . This is due to raise in  $T_{d,a,o}$  from 15°C to 35°C. The same trend follows at different heat capacity ratios also ( $C_r^*=3, 4$  and 5) as solution concentration increases from 0.25 to 0.4.



**Fig. 4.4.** Heat capacity ratio ( $C_r^*$ ) Vs. required air sensible cooling after dehumidification ( $Q_{sen2}$ ) at different concentrations

#### 4.2.6. Variation in required air sensible cooling after dehumidification ( $Q_{sen2}$ )

Raise in dehumidifier solution inlet temperatures ( $T_{d,s,i}$ ) with the increase in  $C_r^*$  leads to increase in dehumidifier air outlet temperature ( $T_{d,a,o}$ ) (Fig.4.2). Subsequently required air sensible cooling ( $Q_{sen2}$ ) to reach supply point ( $T_{sup}=15^\circ\text{C}$ ) slightly increases as  $C_r^*$  increases (Fig.4.4). In addition to this, it is observed that  $Q_{sen2}$  significantly increases as concentration increases at given  $C_r^*$  which is also because of the decrease in the temperature difference between dehumidifier solution and air inlets.

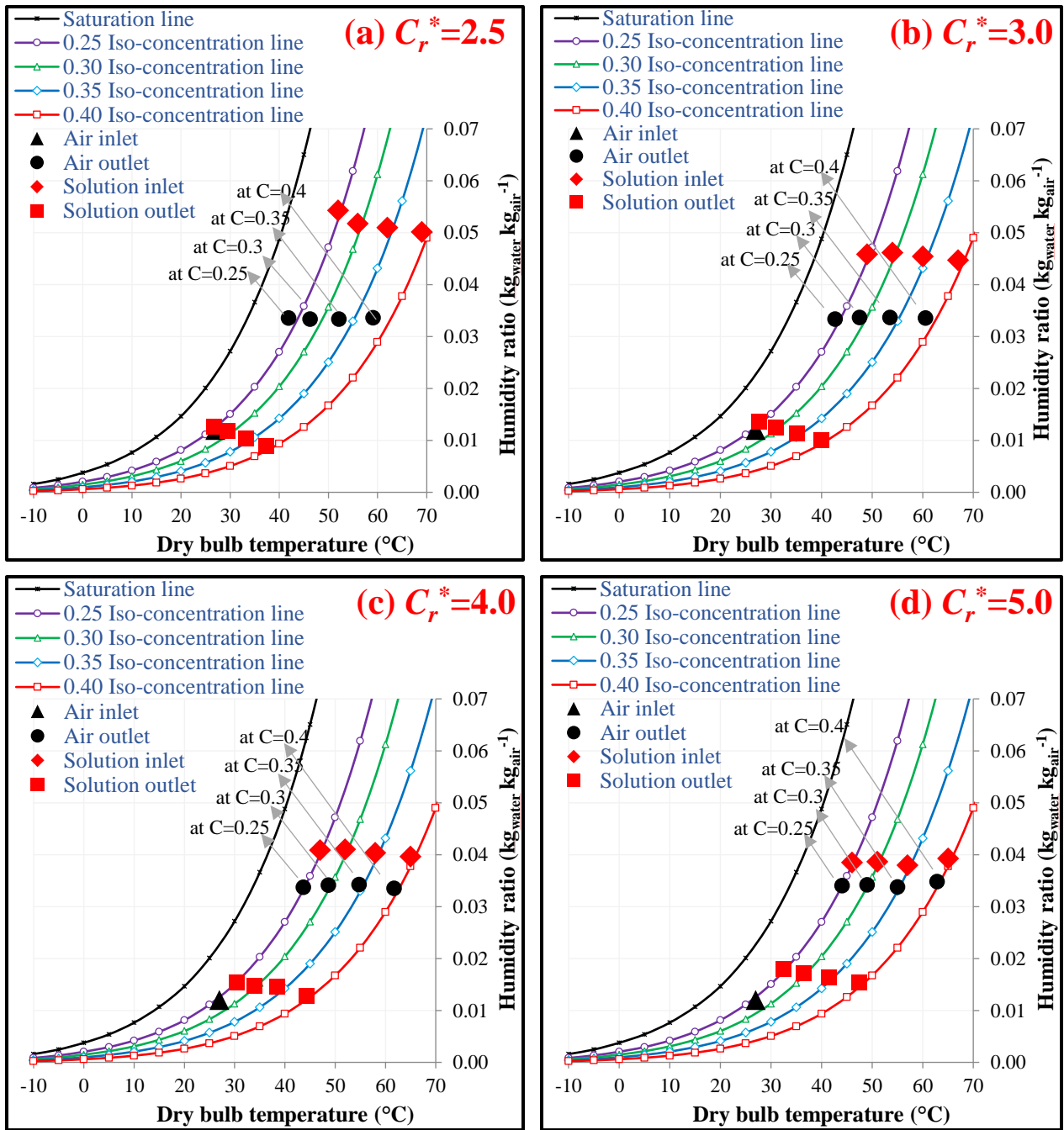


**Fig. 4.5.** Psychrometric chart indicates regenerator air and solution conditions at (a)  $C_r^* = 2.5$ , (b)  $C_r^* = 3.0$ , (c)  $C_r^* = 4.0$  & (d)  $C_r^* = 5.0$  and different concentrations

## 4.2.2. Variation in regenerator parameters and regenerator related performance indices

### 4.2.2.1. Variation in required regenerator solution inlet temperature ( $T_{r,s,i}$ )

Fig. 4.5 shows that required regenerator solution inlet temperature ( $T_{r,s,i}$ ) increases from 52°C to 69°C as concentration increases from 0.25 to 0.4 at  $C_r^* = 2.5$ . The reason for this is as explained above that, to re-concentrate the solution to initial condition ( $C_{d,s,i}$ ) in regenerator, required solution equilibrium humidity ratio (vapor pressure) has to be same even its solution concentration increases for a fixed solution flow rate. So to attain the same solution humidity ratio ( $w_{r,s,i}$ ), required  $T_{r,s,i}$  has to be increased as concentration increases. As  $C_r^*$  increases from 2.5 to 5 at concentration 0.25, required  $T_{r,s,i}$  gradually decreases from 52°C to 46°C since high mass solution mass flow rate itself promotes the moisture desorption potential which implies that  $w_{r,s,i}$  has to be lowered by decreasing  $T_{r,s,i}$  for getting the solution re-concentrated to required condition ( $C_{r,s,i} = 0.25$ ).

### 4.2.2.2. Variation in regenerator air outlet temperature ( $T_{r,a,o}$ )

It is assumed that latent heat of evaporation due to phase change in regeneration process will be considered on solution side only. It means that phase change heat does not affect air temperature in regenerator which implies that air temperature depends only on solution temperature. As regenerator solution inlet temperature ( $T_{r,s,i}$ ) decreases from 52°C to 46°C with increase in  $C_r^*$  from 2.5 to 5 at  $C_s = 0.25$ , regenerator air outlet temperature ( $T_{r,a,o}$ ) slightly increases from 41°C to 44°C ((Fig. 4.5). This is because, as heat capacity ratio ( $C_r^*$ ) increases, solution temperature drop decreases. And also it is observed that  $T_{r,a,o}$  increases from 41°C to 58°C as  $T_{r,s,i}$  increases from 52°C to 69°C with the increase in concentration from 0.25 to 0.4 at  $C_r^* = 2.5$ . The same trend follows at  $C_r^* = 3, 4$  and 5 also as solution concentration increases from 0.25 to 0.4.

#### 4.2.2.3. Variation in regenerator solution outlet temperature ( $T_{r,s,o}$ )

Fig. 4.5 indicates that outlet solution temperature drop is  $25^{\circ}\text{C}$  (temperatures at solution inlet and outlets are  $52^{\circ}\text{C}$  and  $27^{\circ}\text{C}$ ) at  $C_r^*=2.5$  and  $C_s=0.25$ , whereas it is only  $14^{\circ}\text{C}$  (temperatures at solution inlet and outlets are  $46^{\circ}\text{C}$  and  $32^{\circ}\text{C}$ ) at  $C_r^*=5$  and  $C_s=0.25$  in the regeneration process. The reason for this is, since the required moisture desorption rate is fixed, same phase change heat gets released from solution irrespective of solution inlet condition. Therefore more temperature drop occurs at less solution mass flow rates ( $C_r^*=2.5$ ) than at the higher solution mass flow rates ( $C_r^*=5$ ). Since regenerator solution inlet temperature ( $T_{r,s,i}$ ) increases with increase in concentration at any given fixed  $C_r^*$ , regenerator solution outlet temperature ( $T_{r,s,o}$ ) also increases accordingly.

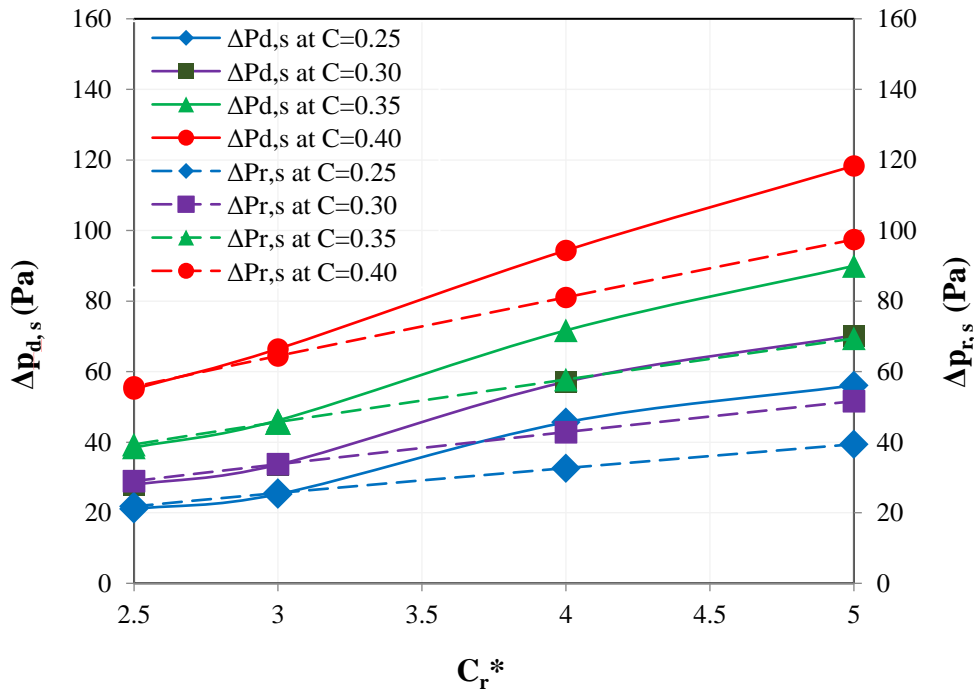


**Fig. 4.6.** Heat capacity ratio ( $C_r^*$ ) vs. Solution pressure drop in the dehumidifier ( $\Delta P_{d,s}$ ) and in regenerators ( $\Delta P_{r,s}$ ) at different concentrations

### 4.2.3. Variation in solution pressure drop in dehumidifier and regenerator channels ( $\Delta P_{d,s}$ and $\Delta P_{r,s}$ )

Fig. 4.6 shows the pressure drop in dehumidifier and regenerator solution channels ( $\Delta P_{d,s}$  and  $\Delta P_{r,s}$ ) increases as  $C_r^*$  raises at given fixed concentration in dehumidifier solution channel. This is due to decrease in channel solution velocity due to raise in solution mass flow rate. And also it is noticed that pressure drop ( $\Delta P_{d,s}$  and  $\Delta P_{r,s}$ ) raises as  $C_r^*$  raises as concentration raises at given fixed  $C_r^*$ . Because, as solution concentration increases, its viscosity also increases which raises the pressure drop in solution channel. And also Solution pressure in regenerator channel is less than in dehumidifier channel at any solution condition. Even solution mass flow rate slightly increased in regenerator due to moisture absorption, but because of reduction in solution viscosity due to solution hot condition in the regenerator, the pressure drop in regenerator channel becomes lesser than in dehumidifier channel.

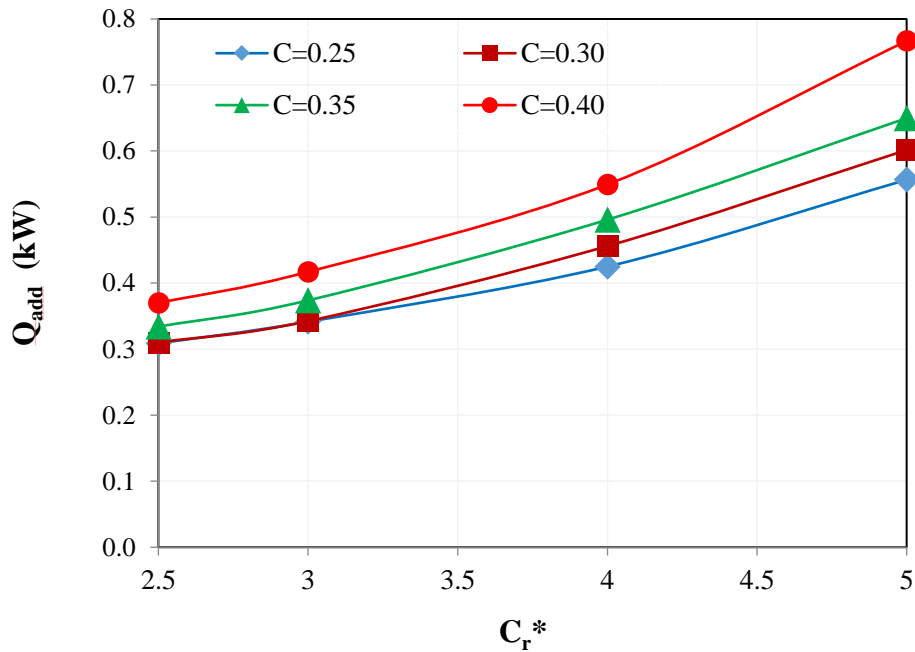


**Fig. 4.7.** Heat capacity ratio ( $C_r^*$ ) Vs. Solution heat addition rate ( $Q_{add}$ ) required for solution sensible heating at different concentrations

#### 4.2.4. Variation in required solution heat addition rate ( $Q_{add}$ )

It can be observed from Figs. 4.2 and 4.5 that slope of iso-concentration lines gradually increases with increase in humidity ratio which is predominantly due to increase in evaporation rate with raise in temperature. This implies that, as solution humidity ratio (vapor pressure) keep increases at a given concentration, required solution temperature rising rate gradually decreases to attain particular humidity ratio raise. Thus it is observed from Fig.4.7 that at 0.25 concentrated solution, required solution heat addition rate ( $Q_{add}$ ) for solution heating is 68.3% lesser at  $C_r^*=2.5$  than at  $C_r^*=5$ . It is also noticed that  $Q_{add}$  increases as  $C_r^*$  increases at given concentration. This is because of increasing in required solution temperature raise with the increase in concentration at given fixed  $C_r^*$ . At given vapor pressure, slight decrease in iso-concentration line slope with increase in concentration (decrease in specific heat causes to increase the required solution temperature raise to attain the same vapor pressure raise) leads to raise  $Q_{add}$  increasing rate with raise in concentration. Thus, slightly more  $Q_{add}$  rising rate can be observed at 0.4 concentration than at 0.25 concentration as  $C_r^*$  increases.

Since LDAS requires high amount of thermal energy (low grade) for solution regeneration, either of the following freely available heat sources can be accomodated to avoid electricity cost. As the required temperature at regenerator solution inlet ( $T_{r,s,i}$ ) is not exceeding 70°C (at peak summer), solar heat (renewable energy) can be tapped for solution regeneration by installing solar thermal collectors/solar electro dialysis/ solar photo voltaic cells. If LDAS coupled to VCR system, condensation heat can be utilized for regeneration. Alternatively, waste heat supply is also the one of the best options if it freely available in the industries.

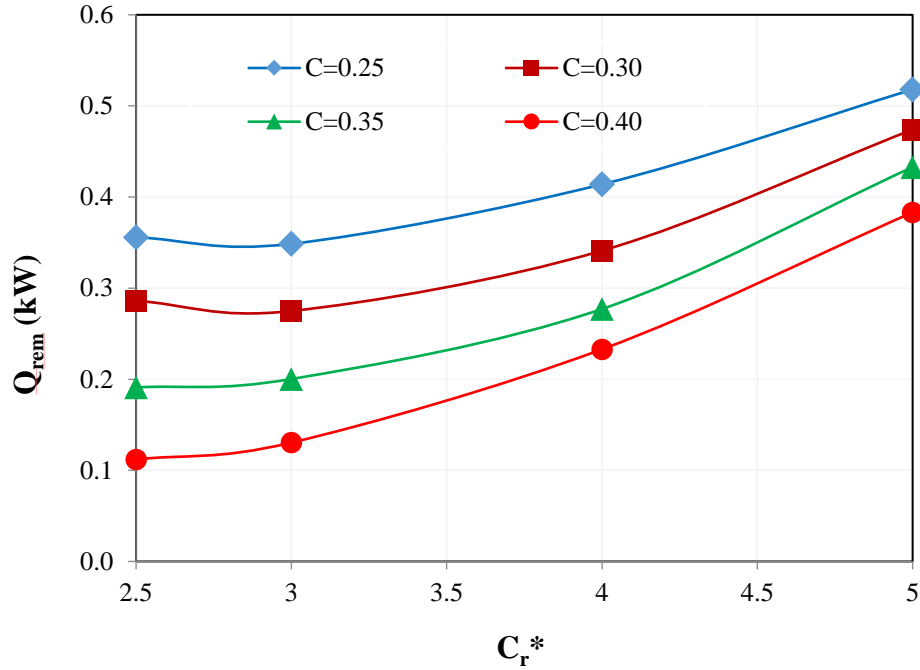


**Fig. 4.8.** Heat capacity ratio ( $C_r^*$ ) Vs. Solution heat removal rate ( $Q_{rem}$ ) required for solution sensible cooling at different concentrations

#### 4.2.5. Variation in required solution heat removal rate ( $Q_{rem}$ )

As explained earlier, required solution temperature raise to attain certain vapor pressure raise is slight decreases as solution humidity ratio (vapor pressure) increases because of increase in iso-concentration slope. Due to this, required heat removal rate for solution cooling ( $Q_{rem}$ ) has also increased considerably with the increase in  $C_r^*$  as observed for  $Q_{add}$ . Thus at concentration  $C_s = 0.25$ , required  $Q_{rem}$  raises from 0.36 kW to 0.52 kW as  $C_r^*$  increases from 2.5 to 5 as indicated in Fig. 4.8. Nearly same variations in required  $Q_{rem}$  with the raise in  $C_r^*$  are observed at other concentrations ( $C_s = 0.3, 0.35$  and  $0.4$ ) also. At given fixed  $C_r^*$ , as concentration increases, due to increase in the difference between regenerator solution and air inlet temperatures ( $T_{r,s,i}$  and  $T_{r,a,i}$ ), solution temperature drop in regeneration process increases which in turn reduces  $Q_{rem}$ . Therefore

at  $C_r^*=2.5$ ,  $Q_{rem}$  significantly decreases from 0.57 kW to 0.11 kW as concentration increases from 0.25 to 0.4. Due to slight decrease in iso-concentration line slope with increase in concentration, slightly more  $Q_{rem}$  rising rate can be observed at 0.4 concentration than at 0.25 concentration as  $C_r^*$  increases.

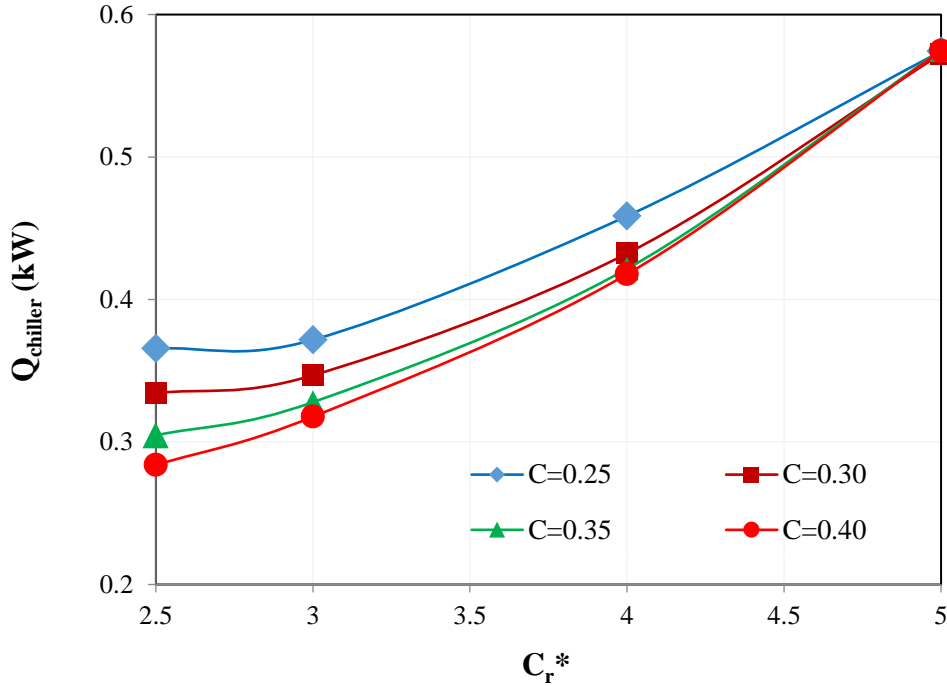


**Fig. 4.9.** Heat capacity ratio ( $C_r^*$ ) vs. required chiller load ( $Q_{chiller}$ ) at different concentrations

#### 4.2.6. Variation in chiller load ( $Q_{chiller}$ )

It is found from Fig.4.9 that chiller load ( $Q_{chiller} = Q_{rem} + Q_{sen2}$ ) decreases with increase in concentration and as well as with decrease in  $C_r^*$ . This is due to considerable drop in  $Q_{rem}$ . Thus LDAS at low solution heat capacity ratio and high concentration ( $C_r^*=2.5$  and  $C_s=0.40$ ) requires lesser  $Q_{chiller}$  (0.29 kW). This is 88% higher than the  $Q_{chiller}$  at high solution heat capacity and high concentration ( $C_r^*=5$  and  $C_s=0.4$ ) and 27% more than the  $Q_{chiller}$  at low solution heat capacity and low concentration ( $C_r^*=2.5$  and  $C_s=0.25$ ).

### 4.3. Major observations

In this study, at fixed ambient condition and dehumidification rate, performance study on 100% fresh air based LDAS at the different combination of solution parameters ( $C_r^*$  and  $C_s$ ) has been carried out. Single pair air-solution channel LAMEE (control volume in full scale LAMEE) has been considered to anatomize the LDAS performance at each solution inlet condition. Below are the few notable observations found from the present objective.

- Solution pressure drop ( $\Delta P_{d,s}$  and  $\Delta P_{r,s}$ ) reduces with the reduction in heat capacity ratio ( $C_r^*$ ) as well as with the reduction in concentration ( $C_s$ ). Consequently, required solution pumping power reduces with decrease in heat capacity ratio as well as with reduction in concentration due to low solution mass flow rate and low viscosity.
- Solution heat addition rate ( $Q_{add}$ ) is found to drop with drop in solution heat capacity ( $C_r^*$ ) as well as with drop in concentration ( $C_s$ ).
- It is also clear that, at given fixed concentration, as heat capacity ratio ( $C_r^*$ ) increases, cooling capacity ( $Q_{cc}$ ) slightly decreases whereas chiller load ( $Q_{chiller}=Q_{rem}+Q_{sen2}$ ) significantly increases.
- At low heat capacity ratio ( $C_r^*=2.5$ ),  $Q_{cc}$  and  $Q_{rem}$  significantly raise whereas  $Q_{add}$  slightly drops as concentration decreases from 0.4 to 0.25. This is due to drop in solution temperature at dehumidifier outlet ( $T_{d,s,o}$ ) with the decrease in concentration.
- At low heat capacity ratio ( $C_r^*=2.5$ ), due to considerable drop in  $Q_{rem}$  with the raise in concentration, required chiller load ( $Q_{chiller}$ ) noticeably drops with the raise in concentration.
- Thus,  $Q_{chiller}$  at low heat capacity ratio ( $C_r^*=2.5$ ) decreases from 0.37kW to 0.29kW as concentration increases from 0.25 to 0.4. This is at the cost of considerable raise (20% more) in solution heat addition rate ( $Q_{add}$ ) and extensive raise in solution pumping power (due to high pressure drop at higher concentration) with increase in concentration from 0.25 to 0.4 at

$C_r^*=2.5$ . Solution heat addition rate ( $Q_{add}$ ) per kW cooling capacity ( $Q_{cc}$ ) at this solution condition is found as 0.85kW.

If 100% fresh air based LDAS with low heat capacity and high concentrated solution ( $C_r^*=2.5$  and  $C_s=0.40$ ) is coupled to chiller, a chiller which has cooling capacity equal to 48% of required total cooling load is adequate to achieve required air supply point ( $T_{sup} = 15^\circ\text{C}$  (DBT) and  $w_{sup} = 0.010 \text{ kg}_{\text{water}} \text{ kg}_{\text{air}}^{-1}$ ). This is since, required total air cooling load ( $Q_{cc}+Q_{sen2}$ ) is 0.61 kW whereas  $Q_{chiller}$  ( $Q_{rem}+Q_{sen2}$ ) is only 0.29 kW at  $C_r^*=2.5$  and  $C_s=0.40$  (Fig.10). Therefore, it is recommendable to employ low heat capacity and high concentrated solution for 100% fresh air based LDAS coupled to chiller to achieve required cooling in summer condition. Solution Saturation concentration at given solution temperature is the maximum concentration for the corresponding solution beyond which crystallization occurs. Thus for a given solution, optimum operating concentration should be maximum safe concentration which means just below saturation concentration. On the other hand, solution optimum heat capacity ratio can be determined by analyzing the performance indices with decreasing the heat capacity ratio further.

## **Chapter 5**

### **Choosing the energy efficient liquid desiccant control strategy for system control performance**

#### **5.1. Methodology**

It is known for a specific air conditioning application that proper control of the desiccant solution parameters to suit the variations in space load due to frequent variation in ambient conditions leads to energy savings and thermal comfort. Even though considerable work has been addressed in literature survey on the control performance of the dehumidification system, no work has been addressed on the approach to choose efficient solution control strategies which is a vital part in designing energy efficient system. In proposed hybrid system (LDAS coupled to chiller), two different desiccant solution control strategies are followed namely dehumidifier solution inlet temperature (DSIT) control strategy and dehumidifier solution inlet mass flow rate (DSIM) control strategy. For each control strategy, solution heat addition rate, solution heat removal rate, required air sensible cooling to be achieved by the chiller, variation in chiller load, solution pressure drops will be analyzed at different ambient conditions. Based on these significant performance indices, energy efficient control strategy will be chosen for the system.

In building air conditioning applications, heat load will be estimated with consideration of the peak summer condition. However, room load varies frequently corresponding to variation in the

ambient condition which in turn causes to change in air conditioning system load. In conventional air conditioning systems, corresponding cooling load to the variation in ambient condition can be attained by controlling either chilled water flow rate or supply air flow rate or heating/humidifying the supply air to meet the room supply point. In proposed 100% fresh air supply hybrid system, LDAS and chiller are individual systems where LDAS primary function to attain the required latent load. Solution parameters will be selected to suit peak ambient condition. However, when ambient condition varies, room load also changes which necessitates a control strategy for the system to attain accurate thermal comfort as well as energy savings. Corresponding supply air humidity ratio ( $w_{d,a,o}$ ) can be attained by means of LDAS through controlling desiccant solution parameters.

Later dehumidified air will be sensibly cooled from preset point ( $T_{sup}$ ) by the chiller. Two different desiccant solution control strategies can be followed for this which are dehumidifier solution inlet temperature (DSIT) control strategy and dehumidifier solution inlet mass flow rate (DSIM) control strategy. This implies ambient air humidity ratio can be dropped to required supply humidity ratio either by controlling DSIT with designed DSIM as fixed or by controlling DSIM with DSIT as fixed. DSIT can be controlled by regulating the chilled water flow rate to solution cooler and DSIM can be altered by control valve after solution storage tank. In this chapter, the effect of this strategies on solution heat addition rate, solution heat removal rate, required air sensible cooling to be achieved by the chiller, variation in chiller load, solution pressure drops have been analyzed at different ambient conditions.

For a given air conditioning application, design solution parameters need to be selected before examining the effect of control strategies. It is found from chapter 4 that solution optimum concentration is maximum safe concentration this means just below saturation concentration. As the considered solution is LiCl Solution, optimum concentration is 0.4. To choose solution optimum mass flow rate (heat capacity ratio), system performance will be analyzed at different heat capacity ratios. Required chiller load (for solution sensible cooling and dehumidified air

sensible cooling) and solution heating loads will be evaluated for the system at different heat capacity ratios (5.0, 4.0, 3.0, 2.5, 2.0, and 1.5).

Based on these outcomes, design solution parameters (0.4 concentration and resulted optimum mass flow rate) have been selected as dehumidifier solution inlet parameters at this design condition. Afterward, different ambient conditions will (by lessening air temperature/humidity ratio) be considered as dehumidifier air inlet condition to analyze the effect of control strategies on the system performance.

## 5.2. Results and discussions

### 5.2.1. Methodology to choose design solution parameters

As mentioned earlier that considering Mumbai peak ambient condition as dehumidifier supply air condition and  $0.010 \text{ kg}_{\text{water}} \text{ kg}_{\text{air}}^{-1}$  as fixed  $w_{d,a,o}$ , solution heater and chiller loads will be analyzed at different heat capacity ratios ( $C_r^* = 5.0, 4.0, 3.0, 2.5, 2.0,$  and  $1.5$ ) and at fixed concentration (0.4). Required  $T_{d,s,i}$  will be found at each  $C_r^*$  to attain required humidity ratio ( $w_{d,a,o} = 0.010 \text{ kg}_{\text{water}} \text{ kg}_{\text{air}}^{-1}$ ). Dehumidified air will be sensibly cooled from  $T_{d,a,o}$  to  $T_{sup} = 15^\circ\text{C}$  (dry bulb temperature) by exchanging heat ( $Q_{sen2}$ ) with the chilled water flowing in the cooling coil. Regenerator solution inlet temperature ( $T_{r,s,i}$ ) will be found by trial and error method such that it gets concentrated in the regenerator to dehumidifier inlet concentration (0.4). Correspondingly required solution heat addition rate ( $Q_{add}$ ) will be calculated for heating the diluted solution left from dehumidifier to  $T_{r,s,i}$ . After solution gets concentrated and heated in the regenerator, required solution heat removal rate ( $Q_{rem}$ ) to drop the regenerator solution outlet temperature ( $T_{r,s,o}$ ) to dehumidifier solution inlet temperature ( $T_{d,s,i}$ ) will be found. Chiller load ( $Q_{rem} + Q_{sen2}$ ) required for concentrated solution sensible cooling and dehumidified air sensible cooling is the one more significant performance index in addition to solution heat addition rate ( $Q_{add}$ ) to choose

the optimum solution mass flow rate ( $m_{d,s,i}$ ) which could achieve energy savings. All the dehumidifier and regenerator parameters are listed in Table 5.1.

Table 5.1 : Dehumidifier and regenerator parameters at different heat capacity ratios ( $C_r^*$ )

Operating parameters		Inlet conditions						Outlet conditions				
$C_{s,i}$	$C_r^*$	$m_{a,i}$ ( $kg\ s^{-1}$ )	$m_{s,i}$ ( $kg\ s^{-1}$ )	$T_{a,i}$ ( $^{\circ}C$ )	$w_{a,i}$ ( $kg_{water}/kg_{air}$ )	$T_{s,i}$ ( $^{\circ}C$ )	$w_{s,i}$ ( $kg_{water}/kg_{air}$ )	$T_{a,o}$ ( $^{\circ}C$ )	$w_{a,o}$ ( $kg_{water}/kg_{air}$ )	$T_{s,o}$ ( $^{\circ}C$ )	$w_{s,o}$ ( $kg_{water}/kg_{air}$ )	$C_{s,o}$
<b>Dehumidification parameters</b>												
0.400	5.0	0.0081	0.0150	35	0.031	38	0.0083	38.8	0.0095	47.7	0.0147	0.395
0.400	4.0	0.0081	0.0120	35	0.031	37	0.0078	38.3	0.0095	49.2	0.0160	0.394
0.400	3.0	0.0081	0.0090	35	0.031	35	0.0065	37.0	0.0096	51.2	0.0178	0.392
0.400	2.5	0.0081	0.0076	35	0.031	32	0.0058	36.0	0.0097	52.3	0.0190	0.391
0.400	2.0	0.0081	0.0060	35	0.031	26	0.0039	33.0	0.0097	53.2	0.0200	0.389
0.400	1.5	0.0081	0.0046	35	0.031	14	0.0017	26.8	0.0099	53.6	0.0208	0.386
<b>Regeneration parameters</b>												
0.395	5.0	0.0081	0.0150	27	0.012	64	0.0372	61.8	0.0329	47.1	0.0148	0.400
0.394	4.0	0.0081	0.0121	27	0.012	65	0.0396	61.4	0.0330	43.9	0.0124	0.400
0.392	3.0	0.0081	0.0091	27	0.012	67	0.0447	59.9	0.0326	39.7	0.0096	0.400
0.391	2.5	0.0081	0.0076	27	0.012	69	0.0501	58.2	0.0322	37.3	0.0085	0.400
0.392	2.0	0.0081	0.0061	27	0.012	74	0.0661	56.4	0.0338	35.8	0.0078	0.400
0.386	1.5	0.0081	0.0048	27	0.012	80	0.0921	52.0	0.0335	34.4	0.0081	0.400

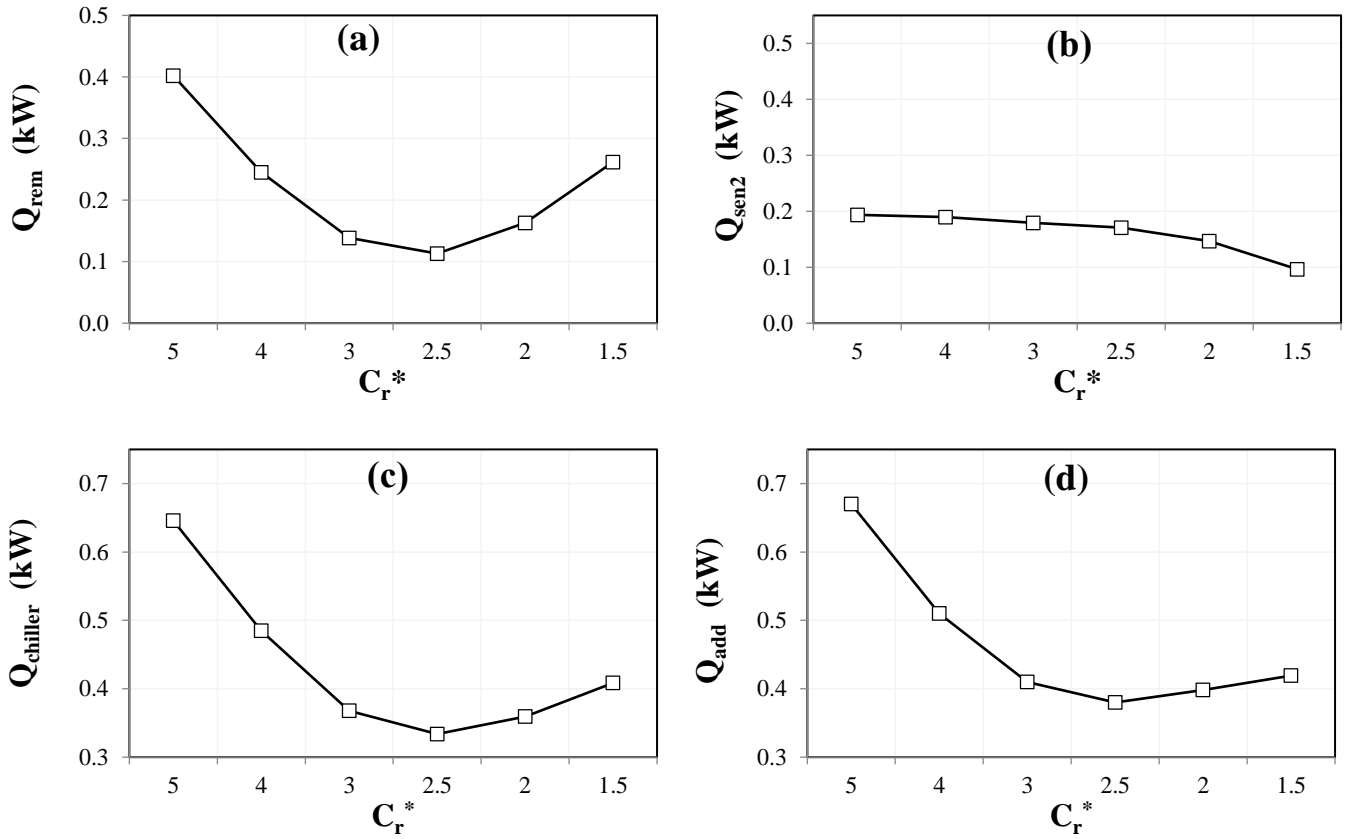


**Figure 5.1.** Variation in (a) solution heat removal rate ( $Q_{rem}$ ), (b) Required dehumidified air sensible cooling ( $Q_{sen2}$ ), (c) Chiller load ( $Q_{chiller}$ ) and (d) Solution heat addition rate ( $Q_{add}$ ) with heat capacity ratio ( $C_r^*$ )

It was observed from the Fig. 5.1a that  $Q_{rem}$  considerably reduces with reduction  $C_r^*$  up to a certain point ( $C_r^*=2.5$ ) and then raises. The explanation for the drop in  $Q_{rem}$  is as follows. It can be observed from LiCl psychrometric chart (Fig. 4.1), the slope of iso-concentration lines gradually decreases with the decrease in humidity ratio due to decline in evaporation rate as temperature drops. This implies that the temperature drop required to attain specific humidity ratio (vapor pressure) drop gradually increases as the humidity ratio decreases. For example, to drop 0.25 concentrated solution equilibrium humidity ratio from 0.07 to 0.05  $\text{kg}_{\text{water}} \text{kg}_{\text{air}}^{-1}$

( $\Delta w=0.02 \text{ kg}_{\text{water}} \text{ kg}_{\text{air}}^{-1}$ ), required solution temperature drop is  $6^\circ\text{C}$  (from  $57^\circ\text{C}$  to  $51^\circ\text{C}$ ) whereas to drop the same 0.25 concentrated solution humidity ratio from 0.11 to  $0.09 \text{ kg}_{\text{water}} \text{ kg}_{\text{air}}^{-1}$  ( $\Delta w=0.02 \text{ kg}_{\text{water}} \text{ kg}_{\text{air}}^{-1}$ ) required solution temperature drop is only  $4^\circ\text{C}$ . This means that as the solution humidity ratio (vapor pressure) keeps decreasing at a given concentration, required solution temperature drop gradually increases to attain a particular humidity ratio drop. Thus, as  $C_r^*$  decreases from 5 to 2.5,  $T_{d,s,i}$  decreases which causes to lessen the required solution heat removal rate ( $Q_{rem}$ ) and also considerably lowers the required air sensible cooling after dehumidification ( $Q_{sen2}$ ) (Fig. 5.1b). But as  $C_r^*$  decreases further from 2.5 to 1.5,  $T_{d,s,i}$  rising rate becomes very high. This is due to the reduction in moisture transfer potential at low solution mass flow rate. Thus,  $Q_{rem}$  raises as  $C_r^*$  decreases up to a certain limit (here it is  $C_r^* = 2.5$ ). Subsequently, chiller load ( $Q_{chiller}$ ) also increases as  $C_r^*$  decreases from 2.5 to 1.5 (Figure 5.1c). For the same reason as explained, solution heat addition rate ( $Q_{add}$ ) also follows the same trend (Figure 5.1d). From this analysis, solution parameters (solution concentration, its dehumidifier inlet temperature, and its mass flow rate) selected are 0.4,  $32^\circ\text{C}$  and  $0.08117 \text{ kg s}^{-1}$  ( $C_r^* = 2.5$  due to less chiller load and solution heat addition rate) respectively as design parameters based on summer peak condition.

### **5.2.2. Solution control strategies to suit the conditioned space load at different ambient conditions**

Different ambient conditions considered (A1-A7) to study the effect of two control strategies and are indicated in the psychrometric chart (Figure 5.2). Initially, the required air supply temperature ( $T_{sup}$ ) calculated from heat load calculations which is  $15^\circ\text{C}$  when the ambient temperature is  $35^\circ\text{C}$  and  $16.5^\circ\text{C}$  when the ambient temperature is  $30^\circ\text{C}$ . However, air outlet humidity ratio considered fixed as  $0.010 \text{ kg}_{\text{water}} \text{ kg}_{\text{air}}^{-1}$  irrespective of ambient condition since room latent load does not change much compared to sensible load. Dehumidifier solution and air parameters for both control to study the control strategies is as follows.

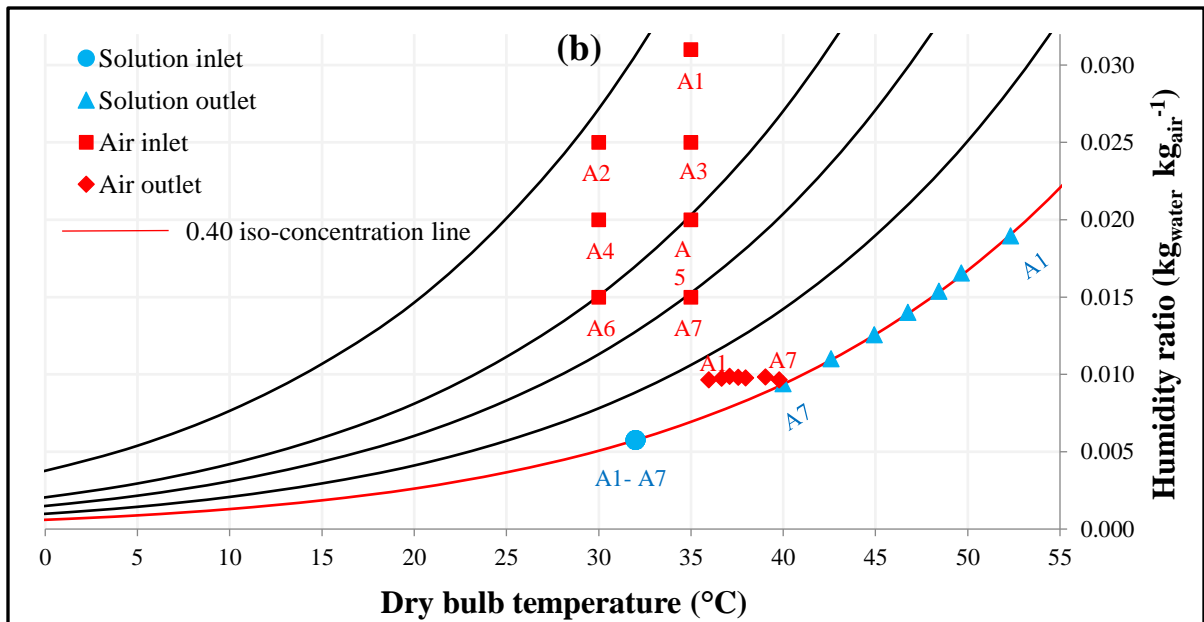
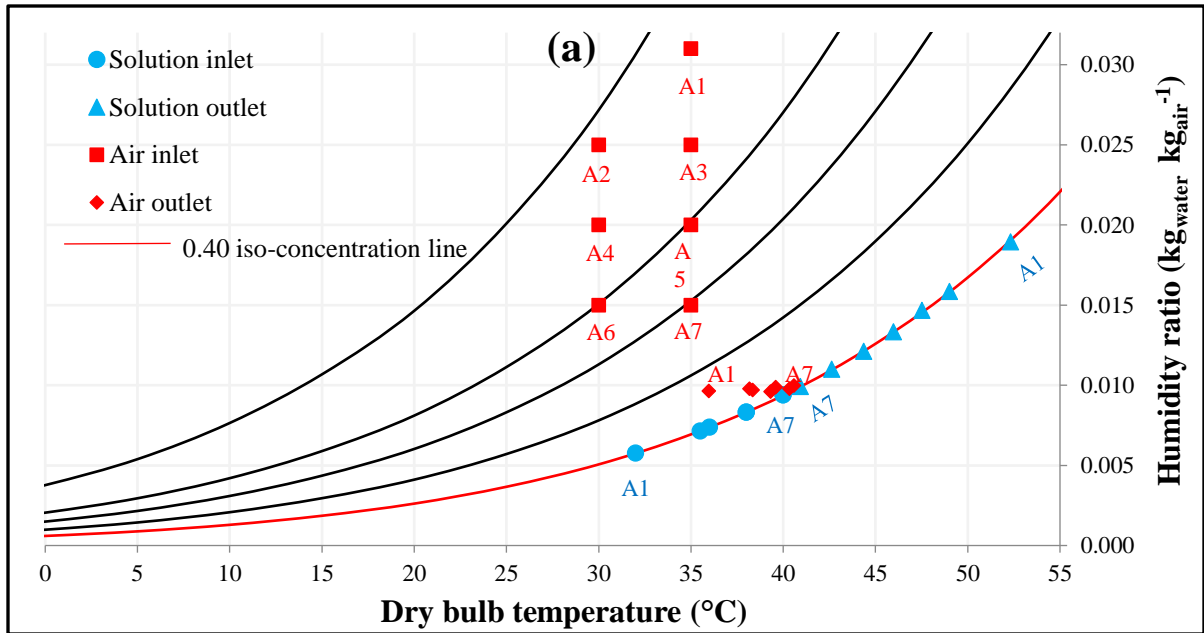


**Fig. 5.2.** The psychrometric chart indicates dehumidifier air and solution conditions at different ambient conditions when **a)** DSIT control strategy and **b)** DSIM control strategy adopted

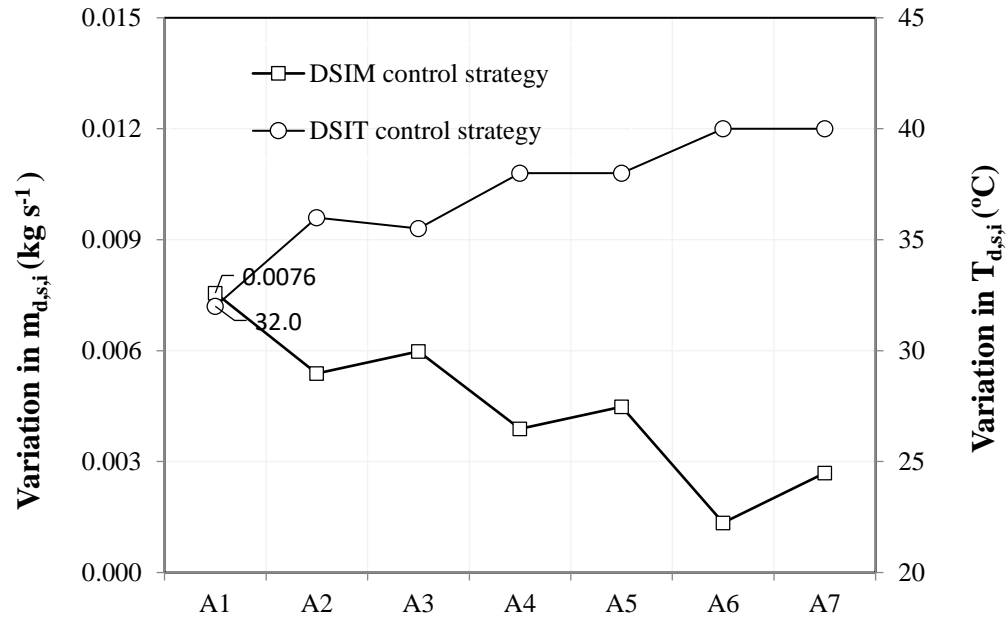


**Fig. 5.3.** Variation in solution inlet mass flow rate ( $m_{d,s,i}$ ) and dehumidifier solution inlet temperature ( $T_{d,s,i}$ ) at different ambient conditions

### 5.2.2.1 Variation in dehumidifier solution inlet temperature ( $T_{d,s,i}$ ) and its mass flow rate ( $m_{d,s,i}$ )

As ambient temperature/humidity reduces,  $T_{d,s,i}$  need to be increased when DSIT control strategy adopted whereas  $m_{d,s,i}$  need to be decreased when DSIM control strategy adopted (Fig. 5.3) to attain the required air outlet humidity ratio ( $w_{d,a,o}=0.010 \text{ kg}_{\text{water}} \text{ kg}_{\text{air}}^{-1}$ ). Air outlet temperature ( $T_{d,a,o}$ ) slightly raises for both control strategies as observed from Fig. 5.1. For the DSIT control strategy, as ambient temperature/humidity reduces,  $T_{d,s,i}$  need to be increased with fixed  $m_{d,s,i}$  to attain the required  $w_{d,a,o}$  which in turn causes to raise  $T_{d,a,o}$ . However, for the DSIM control strategy, even though  $m_{d,s,i}$  needs to be decreased, due to fixed  $T_{d,s,i}$  (32° C),  $T_{d,a,o}$  is always slightly less than for the DSIT control strategy. Thus,  $T_{d,a,o}$  rising rate with the reduction in

ambient temperature/humidity ratio is little more for DSIT control strategy than for DSIM control strategy.

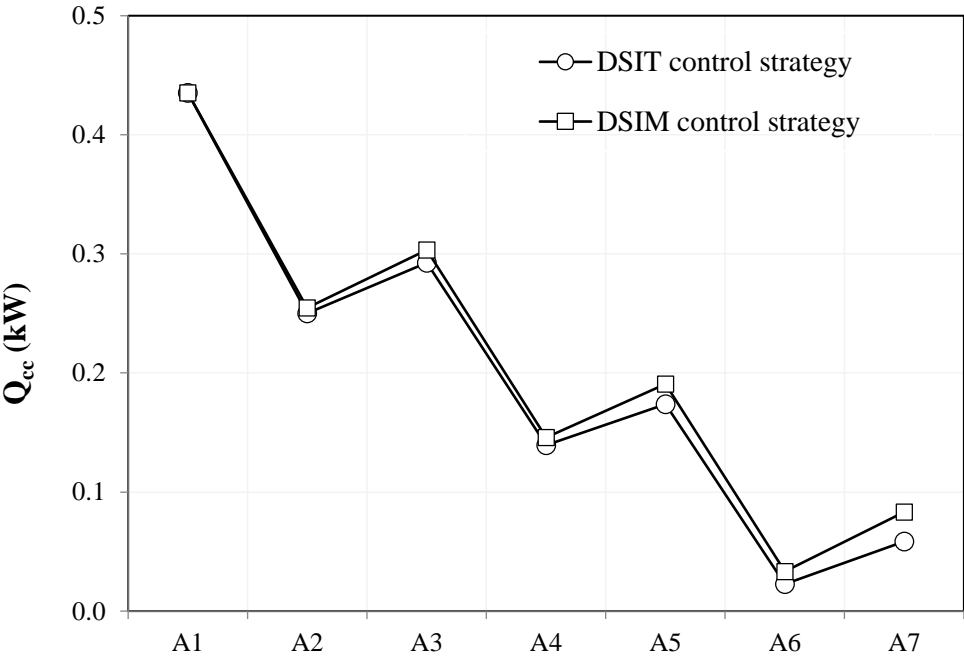


**Fig. 5.4.** Variation in air cooling capacity ( $Q_{cc}$ ) at different ambient conditions

**5.2.2.2. Variation in cooling capacity ( $Q_{cc}$ )**

As ambient temperature increases from 30°C to 35°C at given fixed humidity ratio, it is observed there is raise in cooling capacity ( $Q_{cc}$ ) for both control strategies (Fig. 5.4). The explanation for this phenomenon is as follows. For DSIT control strategy, as the temperature difference between air and solution inlets reduces due to raise in ambient temperature, heat transfer potential lessens which in turn causes to drop in air temperature increasing rate. Thus, even ambient temperature increases at given fixed humidity ratio, it is observed that there is raise in  $Q_{cc}$ . While for DSIM control strategy, with fixed  $T_{d,s,i}$ , its  $m_{d,s,i}$  need to be increased with increase in ambient

temperature at given fixed humidity ratio. This is since, as the temperature difference between air and solution inlets is increased due to raise in ambient temperature, heat transfer increases between the solution and air which in turn reduces the solution dehumidification potential. To overcome this,  $m_{d,s,i}$  need to be increased with raise in ambient temperature. For an instant, for air at 30°C and 0.015 kg<sub>water</sub> kg<sub>air</sub><sup>-1</sup>, required  $m_{d,s,i}$  is 0.013 kg s<sup>-1</sup> whereas for air at 35°C and 0.015 kg<sub>water</sub> kg<sub>air</sub><sup>-1</sup>, required  $m_{d,s,i}$  is nearly doubled which is 0.027 kg s<sup>-1</sup>. Solution temperature raise is supposed to be much higher when air at 30°C compared to air at 35°C due to less  $m_{d,s,i}$ . However, because of increase in heat transfer potential between air and solution due to increase in temperature difference with increase in ambient temperature, air gets heated much at lesser ambient temperature. Thus,  $Q_{cc}$  lessens when ambient air temperature increases at given fixed humidity ratio.

Latent load reduces due to the reduction in ambient humidity ratio which in turn reduces cooling capacity ( $Q_{cc}$ ). Slight higher  $T_{d,a,o}$  observed for DSIM control strategy than for DSIT control strategy observed from Fig. 5.1. This implies that a smaller raise in  $Q_{cc}$  is observed for the DSIM control strategy than for the DSIT control strategy.

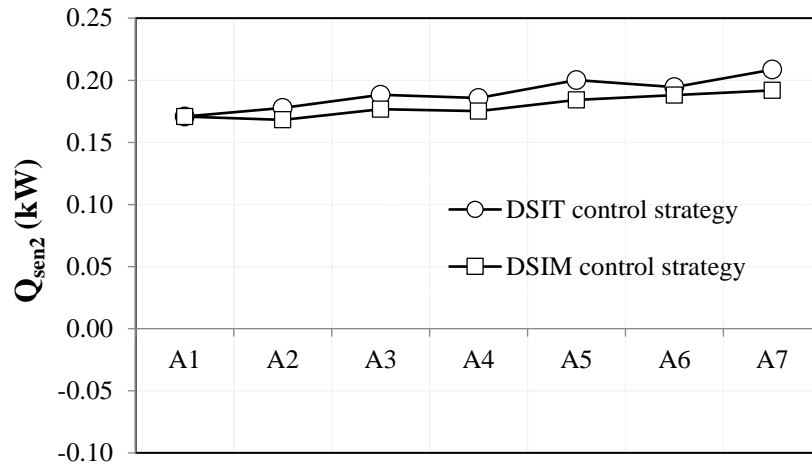


**Fig. 5.5.** Variation in required dehumidified air sensible cooling ( $Q_{sen2}$ ) at different ambient conditions

### 5.2.2.3 Variation in required dehumidified air sensible cooling ( $Q_{sen2}$ )

Air outlet temperatures are slightly lesser for DSIT control strategy than for DSIT control strategy at any ambient condition (Fig. 5.1). Thus, required dehumidified air sensible cooling ( $Q_{sen2}$ ) to meet supply temperature ( $T_{sup}$ ) is slightly higher for DSIT control strategy than for DSIT control strategy (Fig. 5.5).

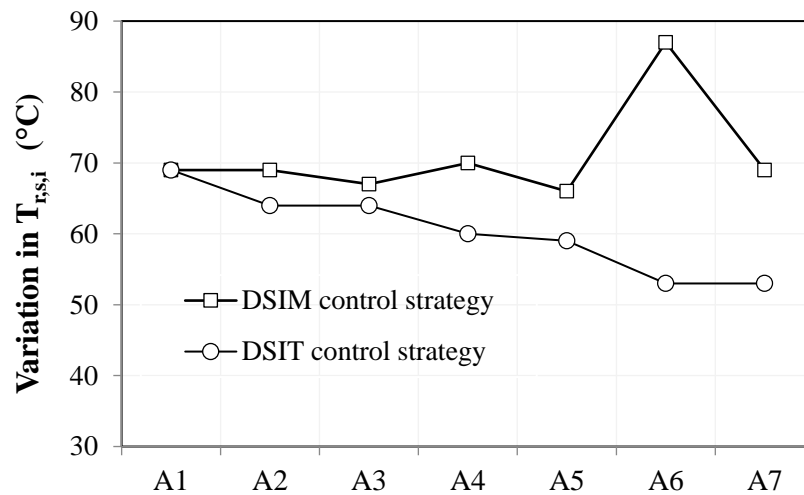


**Fig. 5.6.** Variation in regenerator solution inlet temperature at different ambient conditions

#### 5.2.2.4 Variation in regenerator solution inlet temperature ( $T_{r,s,i}$ )

Room return air at 27°C and 0.012 kg<sub>water</sub> kg<sub>air</sub><sup>-1</sup> (fixed mass flow rate) utilized as regenerator inlet air in this study. This means regenerator solution inlet condition depends only on desorption rate at respective ambient conditions. At DSIT control strategy,  $T_{r,s,i}$  decreases as ambient air temperature/humidity ratio decreases since desorption rate of moisture from solution decreases as indicated in Fig. 5.6. While for DSIM control strategy, it is known that  $m_{r,s,i}$  is nearly same (tiny variation due to moisture absorption during dehumidification) as  $m_{d,s,i}$  at the respective ambient condition. Therefore,  $T_{r,s,i}$  initially slightly increases and significantly raises as ambient air humidity ratio decreases further. At the same humidity ratio, as ambient temperature increases (for example A6-A7),  $T_{r,s,i}$  decreases for DSIM control strategy. This is due to increase in  $m_{r,s,i}$  with the increase in ambient condition.

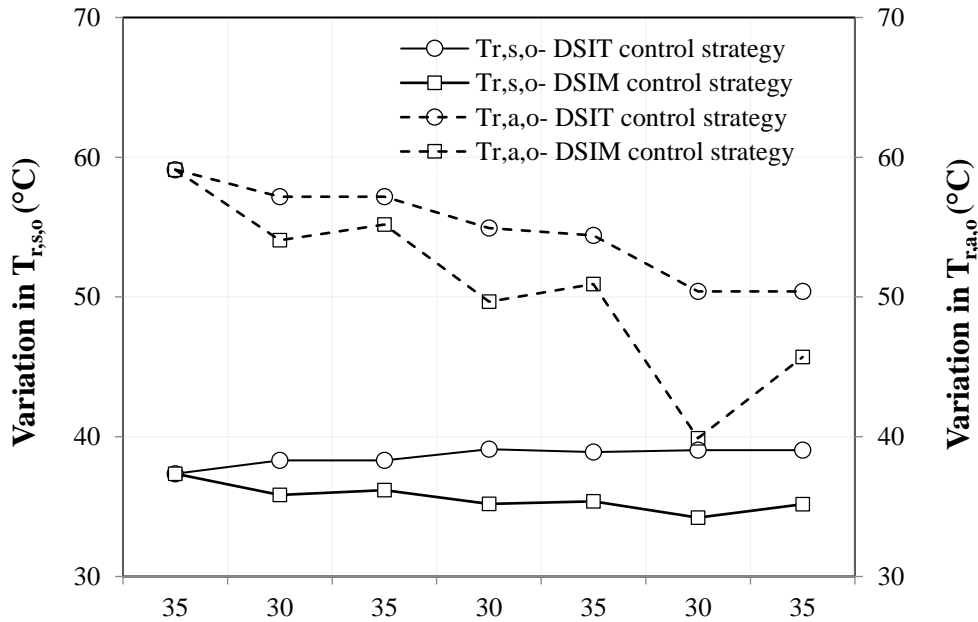


**Fig. 5.7.** Variation in regenerator solution outlet temperature and air outlet temperatures at different ambient conditions

### 5.2.2.5 Variation in regenerator solution and air outlet temperatures ( $T_{r,s,o}$ and $T_{r,a,o}$ )

As regenerator air inlet condition is fixed at any ambient condition,  $T_{r,s,o}$  and  $T_{r,a,o}$  depends on  $T_{r,s,i}$ ,  $m_{r,s,i}$  and moisture desorption rate. At any ambient condition, air gets heated in regenerator due to high  $T_{r,s,i}$  and also due to moisture absorption from solution. When DSIT control strategy adopted, air temperature rising rate decreases since  $T_{r,s,i}$  and moisture desorption rate decrease with the decrease in ambient humidity ratio (Fig. 5.7). At any ambient condition (A1-A7), solution temperature decreases in regenerator due to heat and mass transfer to air. As ambient temperature/humidity ratio decreases (from A1 to A7),  $T_{r,s,o}$  slightly increases with reduction in  $T_{r,s,i}$ . This is because of reduction in heat transfer potential between air and solution due to decrease in temperature difference with increase in regenerator solution inlet temperature. When DSIM control strategy adopted,  $T_{r,a,o}$  significantly decreases as ambient temperature/humidity ratio decreases. This is due to great reduction rate in  $m_{r,s,i}$  than rising rate in its  $T_{r,s,i}$  with decline in ambient humidity temperature/humidity ratio (Fig. 5.6). For the same reason,  $T_{r,s,o}$  slightly decreases as ambient temperature/humidity ratio decreases (from A1 to A7).

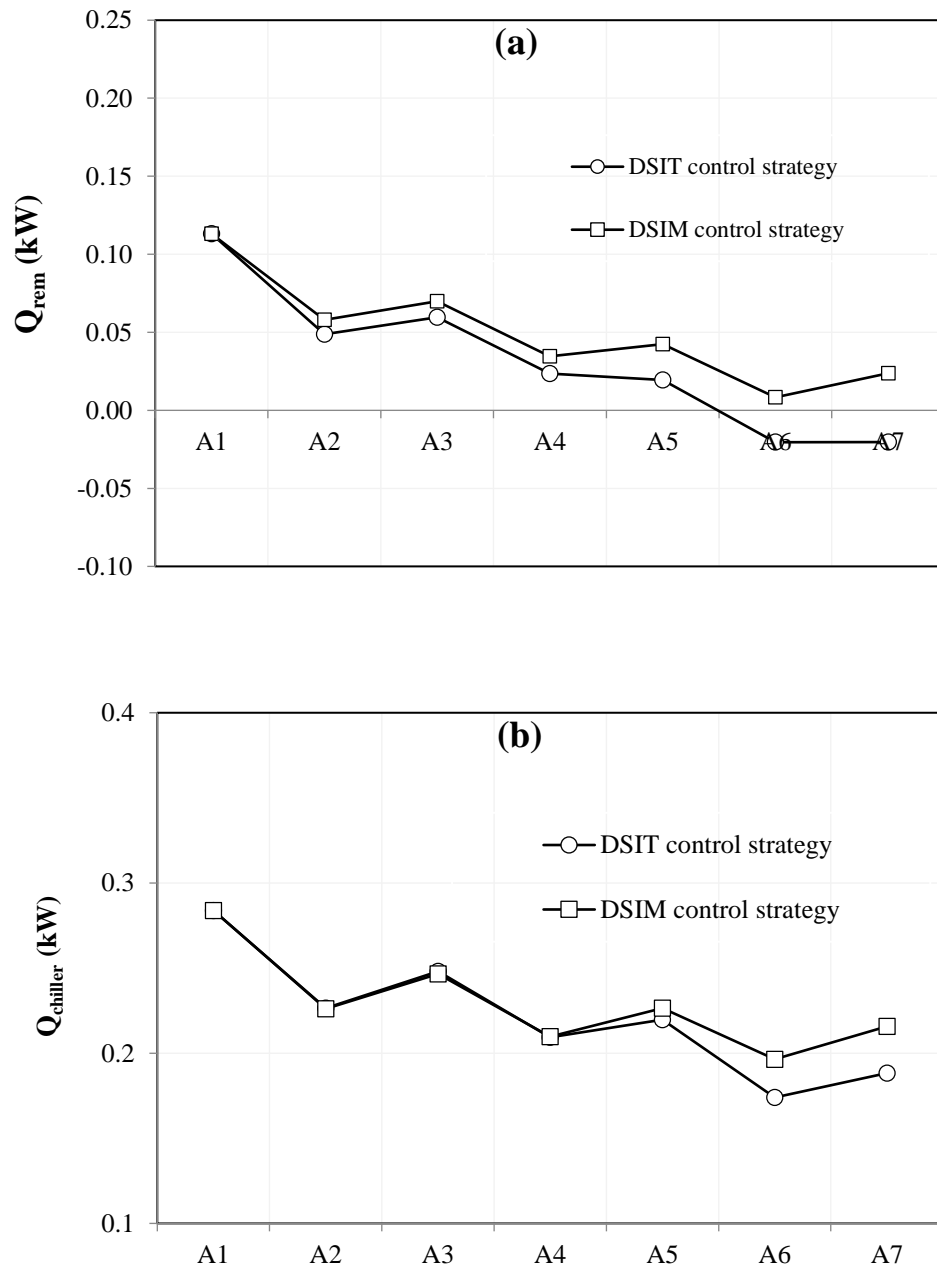


**Figure 5.8.** Variation in (a) required solution heat removal rate ( $Q_{rem}$ ) and (b) Chiller load ( $Q_{chiller}$ ) at different ambient conditions

### 5.2.2.6 Variation in chiller load ( $Q_{chiller}$ )

As explained in the earlier section (4.2.4), solution temperature decreases in the regenerator at any ambient condition due to both heat mass transfer to air. As ambient condition drops (from A1 to A7), this solution temperature drop rate slightly increases for DSIT control strategy whereas it slightly decreases for DSIM control strategy. This leads to drop in solution heat removal rate ( $Q_{rem}$ ) with drop in ambient condition (A1 to A7) slightly increases for DSIT control strategy than for DSIM control strategy (Figure 5.8a).

Required dehumidified air sensible cooling ( $Q_{sen2}$ ) to meet supply temperature ( $T_{sup}$ ) is slightly higher for DSIT control strategy than for DSIT control strategy (Figure 5.5). Thus, it is observed from Figure 5.8(b), even though no variation in chiller load ( $Q_{chiller} = Q_{rem} + Q_{sen2}$ ) at both control strategies found when the ambient conditions in the range (A1-A4), but its dropping rate is higher for DSIT control strategy than for DSIM control strategy as ambient condition changes from A4 to A7.

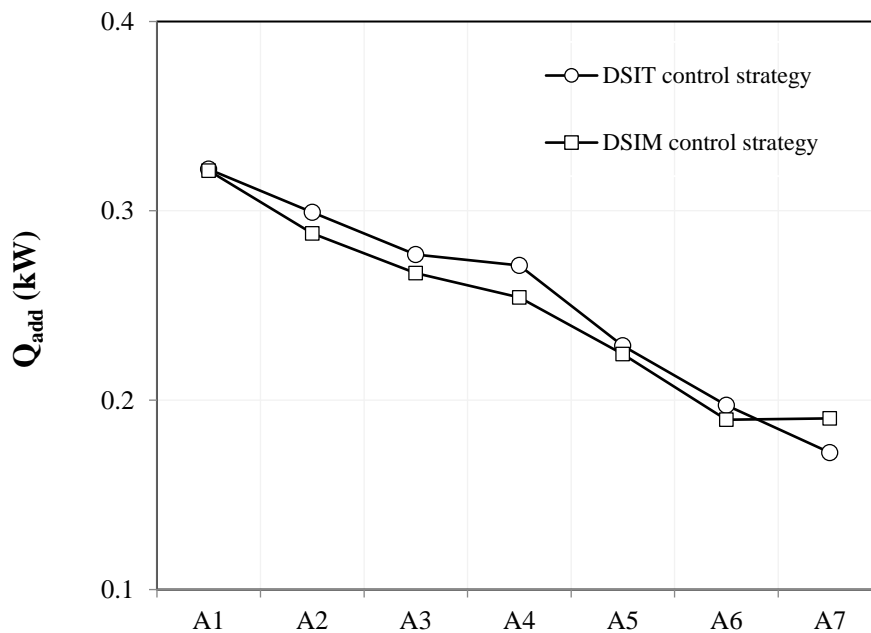


**Figure 5.9.** Variation in solution heat addition rate ( $Q_{add}$ )

### 5.2.2.7 Variation in Solution heat addition rate ( $Q_{add}$ )

Figure 5.9 indicates that the solution heat addition rate ( $Q_{add}$ ) steadily decreases as ambient condition varies from A1 to A7 for both control strategies. This is due to decrease in  $T_{d,s,o}$  and  $T_{r,s,i}$  with the change in ambient conditions from A1 to A7.

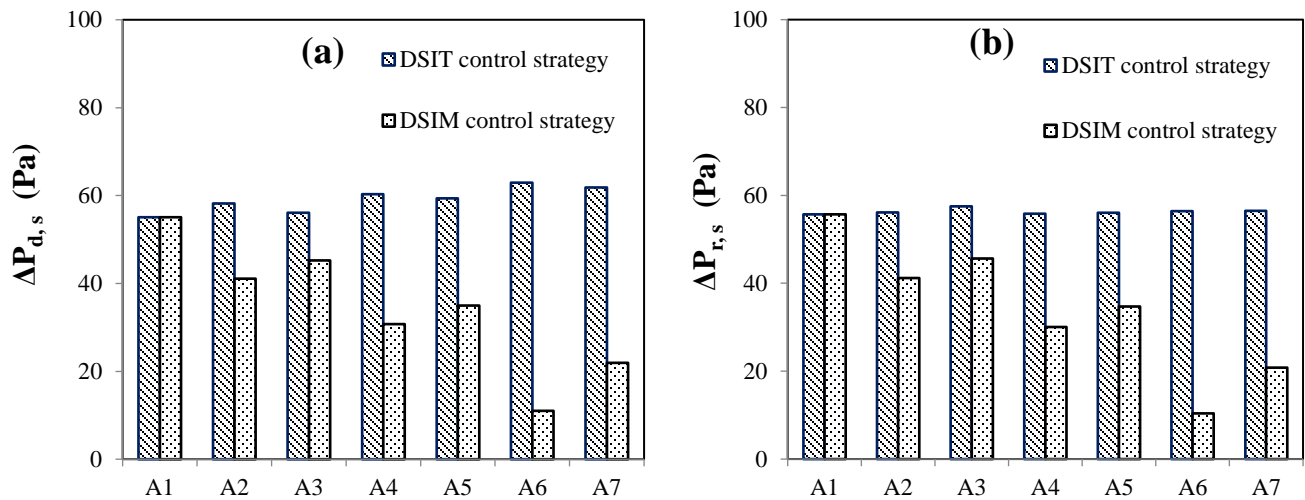


**Figure 5.10.** Variation in solution pressure drops in (a) dehumidifier ( $\Delta P_{d,s}$ ) (b) regenerator ( $\Delta P_{r,s}$ ) at different ambient conditions

### 5.2.2.8 Variation in pressure drops in dehumidifier and regenerator solution channels ( $\Delta P_{d,s}$ and $\Delta P_{r,s}$ )

Fig 5.10a indicates that pressure drop in dehumidifier solution channels ( $\Delta P_{d,s}$ ) is same for DSIT control strategy and reduces for DSIM control strategy with variation in ambient condition (from A1 to A7). This is due to the fixed mass flow rate for DSIT control strategy and reduction in mass flow rate for DSIM control strategy with the reduction in ambient condition

(temperature/humidity ratio). Pressure drop in regenerator solution channels ( $\Delta P_{r,s}$ ) also follows the same trend as  $\Delta P_{d,s}$  for both control strategies but with reduced magnitude (Fig 5.10b)). This is due to heat added to the solution in the regenerator.

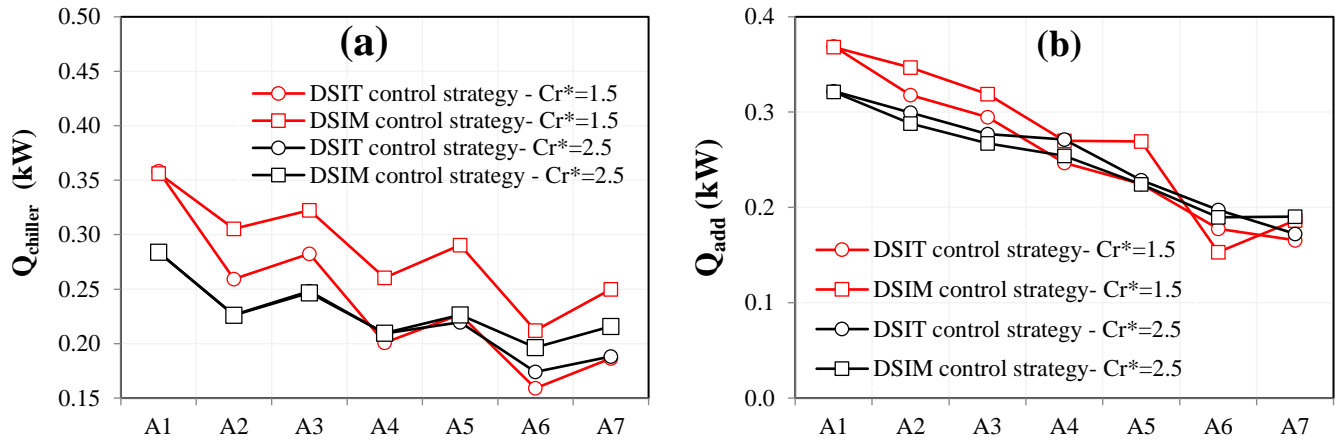


**Figure 5.11.** Variation in (a) chiller load ( $Q_{chiller}$ ) (b) solution heat addition rate ( $Q_{add}$ ) at different ambient conditions when  $C_r^*=1.5$  and 2.5

### 5.2.3 Impact of design solution parameters on performance at both control strategies

Even though  $C=0.4$  and  $C_r^*=2.5$  considered as design solution parameters for this specific application, same analysis performed at other heat capacity ratio ( $C_r^*=1.5$ ) to examine the impact of design solution parameter on the significant performance indices like chiller load ( $Q_{chiller}$ ) and solution heat addition rate ( $Q_{add}$ ). Figure 5.11a and 5.11b shows variation in  $Q_{chiller}$  and  $Q_{add}$  with ambient conditions when  $C_r^*=1.5$  for both control strategies (results at  $C_r^*=2.5$  also shown for comparison). It is observed that both  $Q_{chiller}$  and  $Q_{add}$  are higher (more for DSIT control strategy) at  $C_r^*=1.5$  than at  $C_r^*=2.5$ . In addition to this, it is also witnessed that, as ambient condition varies, significant difference in chiller load ( $Q_{chiller}$ ) between both control strategies found at  $C_r^*=1.5$ . This is contrast to the negligible difference in chiller load between both control strategies at  $C_r^*=2.5$ . Difference in the required solution heat addition rate ( $Q_{add}$ ) between both control strategies at  $C_r^*=1.5$  is also found little more than at  $C_r^*=2.5$ . The results at  $C_r^*=1.5$  may

suggest that DSIT control strategy is energy efficient one whereas DSIM control strategy is found as energy efficient one at  $C_r^*=2.5$  to attain the energy savings and thermal comfort. This can be concluded that design solution parameters have a significant influence on the selection of energy efficient control strategy.

### 5.3 Major observations

In this study, approach methodology for energy efficient control strategy selection has been studied for 100% fresh air based LDAS at different ambient conditions. Two solution control strategies followed are dehumidifier solution inlet temperature control strategy (DSIT control strategy) and dehumidifier solution inlet mass flow rate control strategy (DSIM control strategy). Energy transfer analysis between air and solution is studied by considering single pair air-solution channel LAMEE (control volume in full scale LAMEE).

It is clear from the results that, as ambient condition varies from A1 to A7,  $Q_{cc}$  as well as  $Q_{rem}$  reduces at both control strategies. But solution heat removal rate ( $Q_{rem}$ ) reduces at slight higher rate for DSIT control strategy. As required dehumidified air sensible cooling ( $Q_{sen2}$ ) varies (slightly increases) at the same rate for both control strategies, chiller load ( $Q_{chiller}$ ) reduces at slight higher rate with variation in ambient condition (from A1 to A7) for DSIT control strategy than for DSIM control strategy.  $Q_{add}$  at both control strategies is found to be nearly the same at any ambient condition.

Even though chiller load ( $Q_{chiller}$ ) is slightly high (3-14%) for DSIM control strategy at low ambient conditions, but due to the significant reduction in solution mass flow rate and its pressure drop, system solution pumping power remarkably reduces. Thus, it was found that DSIM control strategy as energy-efficient to control supply air condition according to variation in the ambient conditions.

It is also examined the system performance by varying design mass flow rate ( $C_r^*=1.5$  instead of 2.5) and found DSIT control strategy as efficient. Thus, control strategies selection is sensitive to the design parameter and therefore it is suggested to find the optimum design parameters initially and to follow the approach mentioned in this study.

## **Chapter 6**

### **Identification of the energy efficient liquid desiccant among potential liquid desiccants at optimum operating parameters**

#### **6.1. Methodology**

It is observed from chapter 4 that a given liquid desiccant with maximum safe concentration (just below saturation concentration to avoid crystallization risk) and optimum heat capacity ratio as design operating parameters requires lesser energy consumption for a LDAS application. Design operating parameters (solution concentration and heat capacity ratio) varies from liquid desiccant to liquid desiccant for any LDAS application. Different liquid desiccants at their corresponding design operating parameters can attain different magnitudes of energy savings. This implies that appropriate potential liquid desiccant at corresponding design parameters can only attain best possible energy savings.

From the literature, it is observed that research is mainly attentive to the influence of desiccant solution on dehumidifier/regenerator performance but not on other primary components of LDAS. In all their studies, operating conditions were considered as different solutions having same concentration and same temperature or same surface vapour pressure and same temperature. Lazzarin et.al and Longo et.al [49], [59] studied the packed type dehumidifier/regenerator performance using different desiccant solutions which have operating concentrations at the same crystallization temperature. However, influence of different desiccant solutions at their maximum safe concentrations (observed as optimum concentration from chapter 4) on solution pumping power, solution heat addition rate and solution heat removal rates has to be addressed which plays vital role in deciding to choose energy efficient desiccant solution for a given air conditioning application. It is observed that the most potential liquid desiccants for HVAC application are LiBr and LiCl for their higher dehumidification performance, CaCl<sub>2</sub> and MgCl<sub>2</sub> for its lower cost, and KCOOH for its lower corrosion to metals and crystallization[60]. However, at saturation condition, dehumidification performance is poor for MgCl<sub>2</sub> solution than other solutions while LiBr solution is strongest in dehumidification. Also, it is reported that, for a specific indoor and outdoor operating condition the risk of crystallization is greatest for MgCl<sub>2</sub>, followed by CaCl<sub>2</sub>, LiCl and LiBr. This made us to exclude the MgCl<sub>2</sub> solution from the current study[50].

Thus in this chapter, using analytical model, effect of commonly used potential desiccant solutions such as LiCl, CaCl<sub>2</sub>, LiBr and KCOOH solutions on the other primary components of membrane based LDAS such as solution cooler, solution heater and chiller has been addressed. Power consumption required to pump solution through energy exchanger channels for each solution also has been addressed. This analysis will be beneficial in choosing the appropriate desiccant solution at optimum heat capacity for an energy efficient membrane based LDAS.

Selection of desiccant material plays a key role in the design of an energy efficient LDAS for the required load (primarily latent load). In this study, LiCl, CaCl<sub>2</sub>, LiBr and KCOOH are considered as different desiccant materials. To supply cool and dry air to the conditioned room, initially, the

ambient air (100% fresh air) has to be dehumidified by LDAS to required humidity content and then it has to be sensibly cooled to supply air condition by another method (VCRS system/ indirect evaporation cooling system). It is observed from the literature that dehumidification performance increases with the raise in concentration. And also to avoid crystallization risk in exchanger or piping due to low ambient temperatures (winter), operating concentrations for the respective desiccant solutions considered to be just lesser than their corresponding saturation concentrations. This means working concentrations should be considered for the specified solutions in such a way that the solutions will not get crystallized even at 0°C in winter conditions. Therefore desiccant solutions have been considered at their respective maximum safe concentrations which are just below their saturated concentration to avoid crystallization. In addition to this, desiccant solutions employed in LDAS needs to dehumidify the ambient air to same required humidity point (but at different air temperatures). Thus in this study, LDAS performance with each desiccant has been investigated at different heat capacity ratios ( $C_r^*$ =4.0, 3.0, 2.5, 2.0 and 1.5) and respective concentrations (0.4 for LiCl, 0.35 for CaCl<sub>2</sub>, 0.55 for LiBr and 0.75 for KCOOH solution) by fixing the air outlet humidity ratio at dehumidifier LAMEE exit as 0.010 kg<sub>water</sub> kg<sub>air</sub><sup>-1</sup> [47], [61]–[63]. At their corresponding concentrations performance indices like solution pressure drop in the channels, power required to pump the solution through energy exchanger channels ( $P_{d,s}$  and  $P_{r,s}$ ), required solution cooling and heating loads and chiller load (dehumidified air sensible cooling and concentrated solution sensible cooling) have been analyzed for LiCl, CaCl<sub>2</sub>, LiBr and KCOOH based systems. Optimum  $C_r^*$  for each desiccant solution will be find out. However, this analysis has been done at fixed ambient condition (Mumbai summer peak condition). This study has been extended at different ambient conditions also (by reducing ambient humidity ratio and temperature) considering optimum  $C_r^*$  for the corresponding solution. As concluded from chapter 5 that dehumidifier solution inlet mass flow rate (DSIM) control strategy is adopted for the four desiccant solution based systems to suit the required load which varies according to the ambient condition.

As explained earlier that 100% fresh air supply has been considered as supply air condition in this study. Mumbai summer peak parameters are chosen as inlet air condition for dehumidifier LAMEE as the air is high humid and hot. Room return air at 27°C dry bulb temperature (DBT) which is 2°C higher than room condition and  $w_{room} = 0.012 \text{ kg}_{\text{water}} \text{ kg}_{\text{air}}^{-1}$  is employed as supply air for regenerator LAMEE since it is comparatively drier and cooler than ambient air. Initially to attain fixed air outlet humidity ratio at dehumidifier LAMEE exit ( $0.010 \text{ kg}_{\text{water}} \text{ kg}_{\text{air}}^{-1}$ ), required dehumidifier solution inlet temperature will be found out for each desiccant at different heat capacity ratios ( $C_r^*$ ). Accordingly, variations in solution outlet concentration, solution mass flow rate, solution outlet temperature and air temperature at LAMEE outlet will be established. To achieve the solution outlet concentration at regenerator LAMEE outlet equal to the solution inlet concentration at dehumidifier LAMEE inlet, required regenerator solution inlet temperature will be determined. Subsequently, variations in solution exit temperature, air exit temperature and air exit humidity at regenerator exit will be found out.

LiCl and  $\text{CaCl}_2$  solution properties are considered from the correlations developed by [47] and LiBr properties are estimated from the correlation developed by [64] whereas KCOOH properties are assessed from the correlation established by [63], [65]. Equilibrium humidity ratios at different concentrations and temperatures for each desiccant solution are determined and indicated in Fig.6.1.

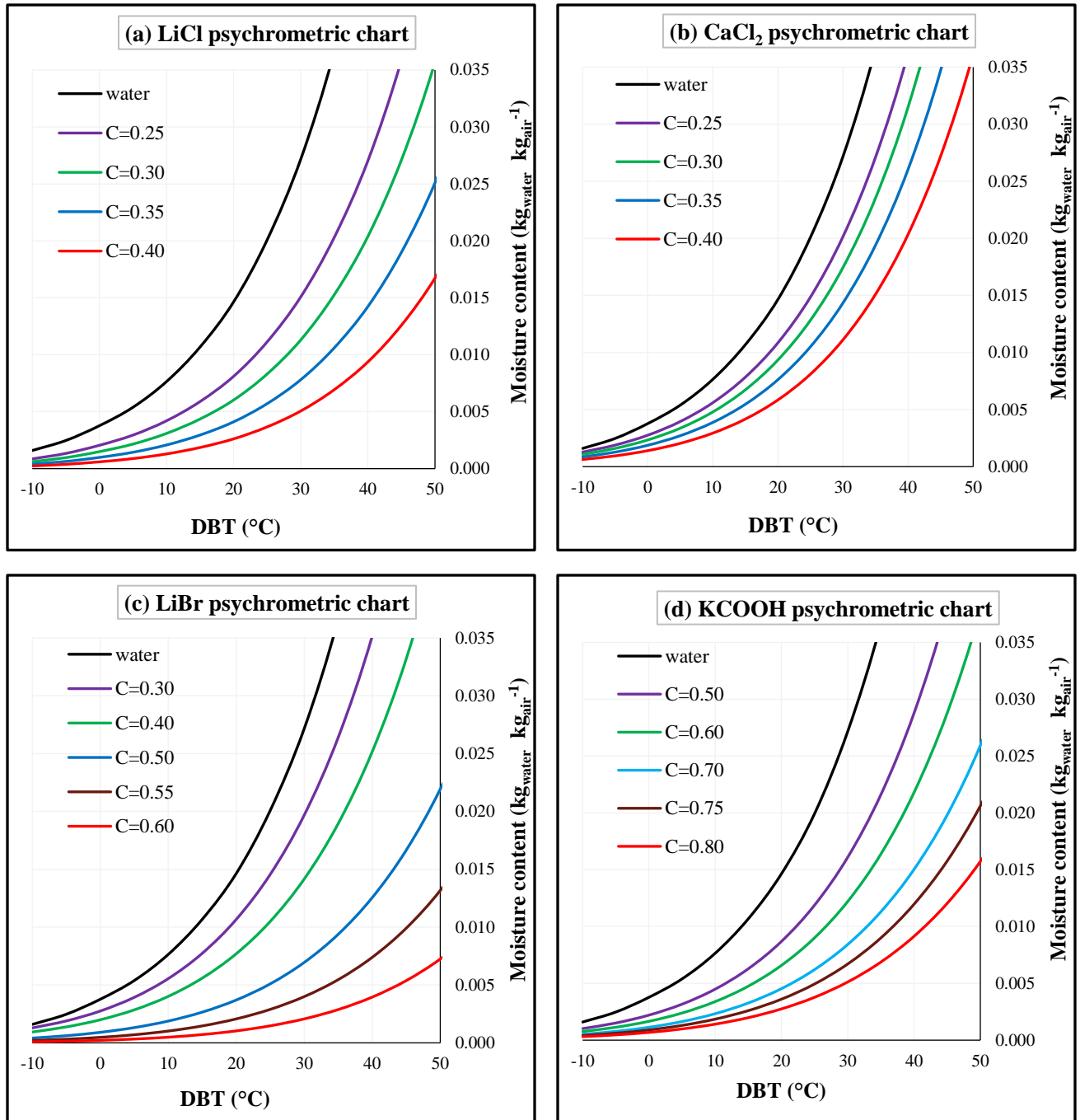


**Fig. 6.1.** Psychrometric charts of LiCl, CaCl<sub>2</sub>, LiBr and KCOOH solutions at different concentrations

## 6.2. Results and discussions

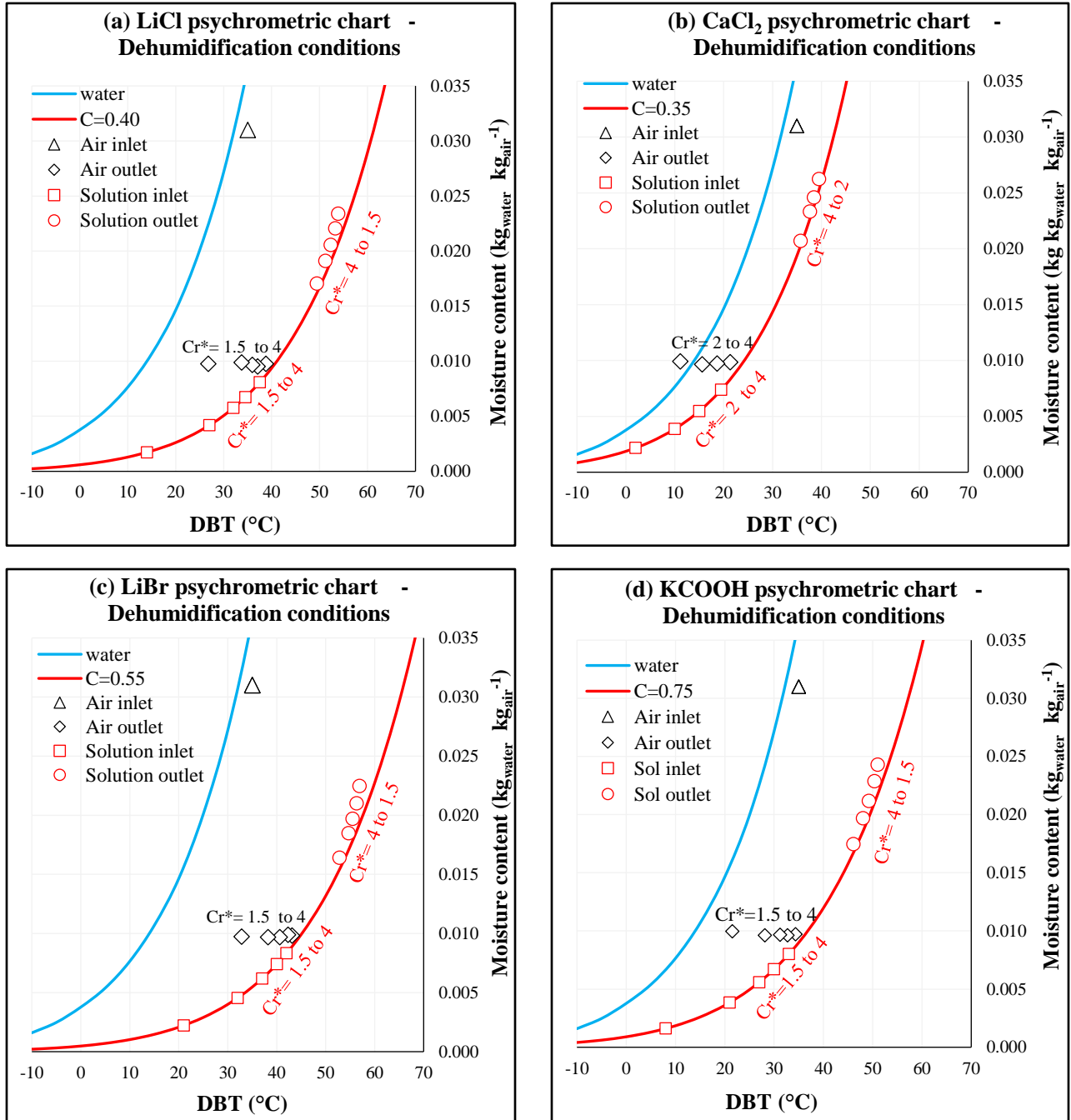


**Fig. 6.2.** Psychrometric chart specifies dehumidifier air and solution conditions at  $C_r^*=4, 3, 2.5, 2, 1.5$  & 1 and operating concentrations for (a) LiCl, (b)  $CaCl_2$ , (c) LiBr and (d) KCOOH desiccant solutions

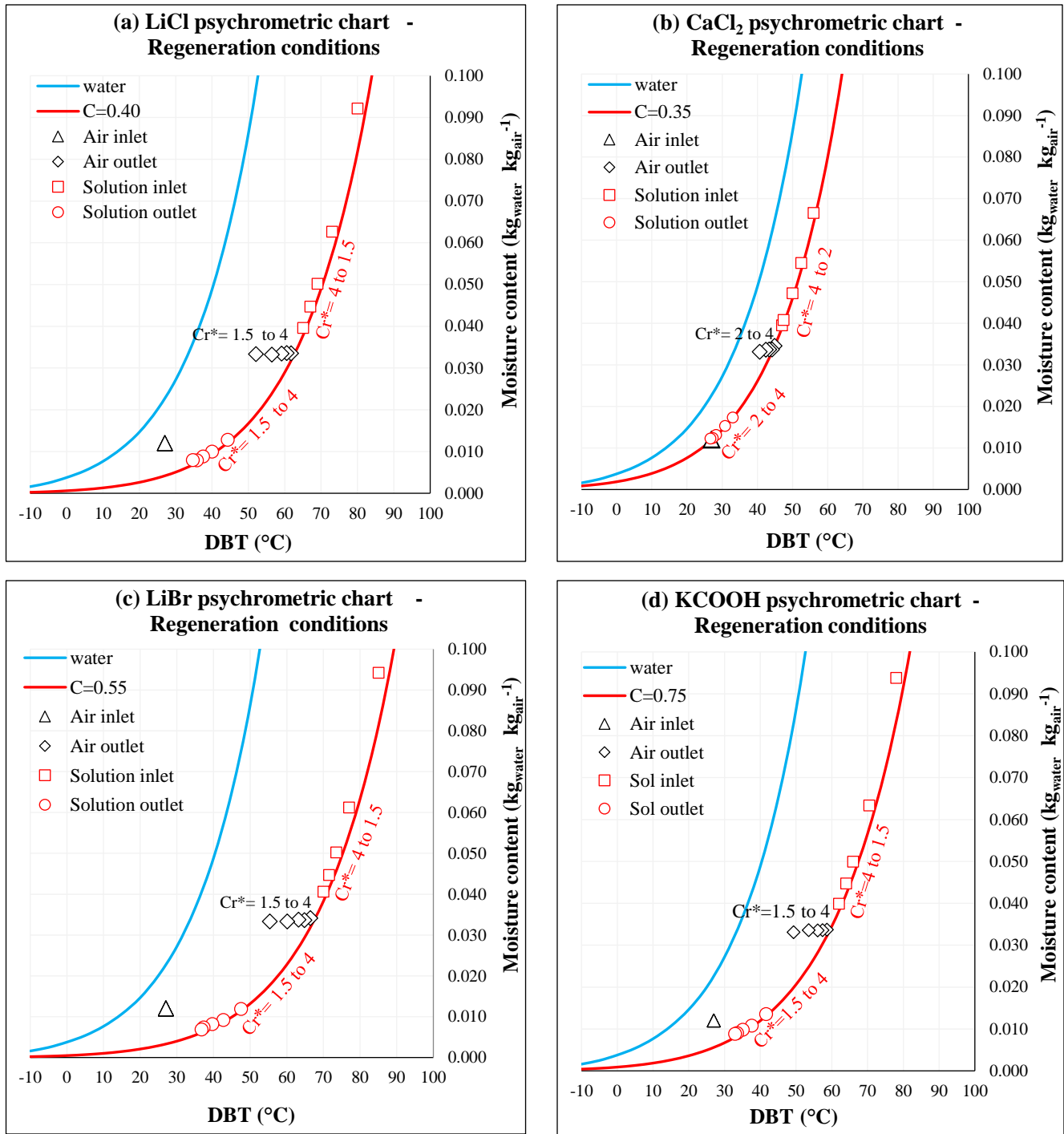


**Fig. 6.3.** Psychrometric chart specifies regenerator air and solution conditions at  $C_r^*=4, 3, 2.5, 2$  &  $1.5$  and operating concentration for (a) LiCl, (b) CaCl<sub>2</sub>, (c) LiBr and (d) KCOOH desiccant solutions

With validated analytical model, air and solution parameters at outlets of dehumidifier and regenerator are established at each solution inlet condition and indicated in psychrometric charts as indicated in Figs. 6.2 & 6.3 respectively.

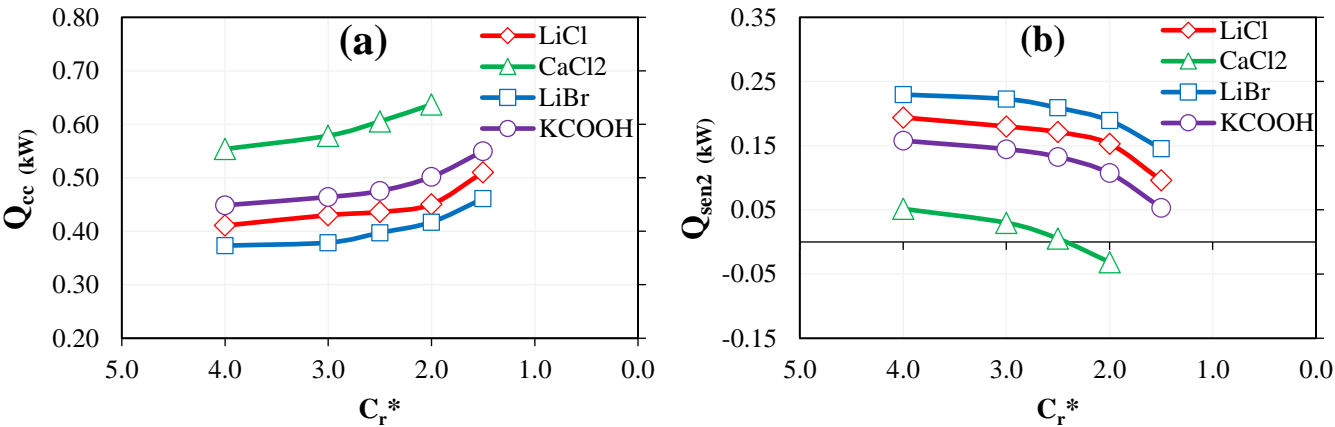


**Fig. 6.4.** Heat capacity ratio ( $C_r^*$ ) vs. (a) air total cooling (sensible + latent cooling) achieved in the dehumidifier ( $Q_{cc}$ ) and (b) Required dehumidified air sensible cooling for each solution ( $Q_{sen2}$ )

### 6.2.1. Variation in air cooling capacity ( $Q_{cc}$ ) and required dehumidified air sensible cooling ( $Q_{sen2}$ )

To achieve the required dehumidification rate at their respective concentrations, solution equilibrium humidity ratio (vapour pressure) has to be the same at given heat capacity. At any given temperature and their considered respective concentrations, solution vapour pressure is always lower for LiBr than remaining. This implies that LiBr solution requires little higher solution temperature than other to attain required dehumidification rate (Fig. 6.2c). Since it is assumed that latent heat of condensation due to phase change in heat and mass transfer process will be considered on solution side only, phase change heat does not affect air temperature in the dehumidifier. It implies that dehumidifier air outlet temperature ( $T_{d,a,o}$ ) depends only on solution heat capacity and its temperature. Accordingly, dehumidifier air outlet temperature ( $T_{d,a,o}$ ) for

LiBr is also higher which leads to lesser sensible cooling. Consequently, cooling capacity ( $Q_{cc}$ ) also turn out to be lower as shown in Fig. 6.4a.

Required dehumidifier solution inlet temperature ( $T_{d,s,i}$ ) for  $C_r^* < 2$  will be lesser than  $0^\circ\text{C}$  (sub-zero temperatures). Such low temperatures for  $\text{CaCl}_2$  solution are not possible to achieve with chilled water. This made us to limit  $C_r^*$  up to 2 for  $\text{CaCl}_2$ . As  $\text{CaCl}_2$  solution vapour pressure at a given temperature is higher than other solutions, it requires a low solution temperature which causes to have high  $Q_{cc}$  and low  $Q_{sen2}$ . In addition to this, as  $C_r^*$  decreases, solution mass flow rate decreases which necessitates the lessening in  $T_{d,s,i}$ . As a result,  $Q_{cc}$  increases with the decrease in  $C_r^*$  for any solution. Accordingly, required dehumidified air sensible cooling ( $Q_{sen2}$ ) to attain supply condition ( $T_{sup}=15^\circ\text{C}$ ) follows reverse trends as shown in fig.6.4b. This means  $Q_{sen2}$  is low for LiBr solution at given  $C_r^*$  and  $Q_{sen2}$  decreases with the decrease in  $C_r^*$ .

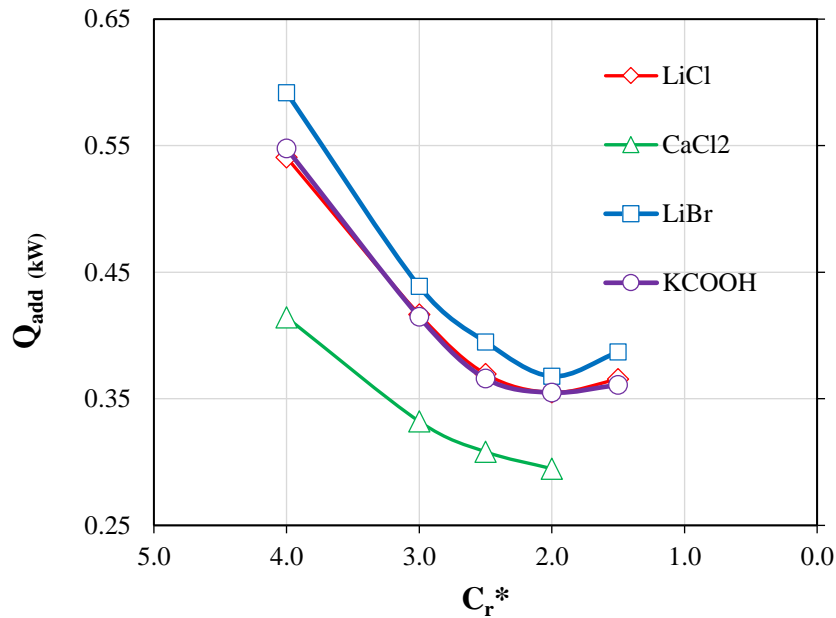


**Fig. 6.5.** Variation in required  $Q_{add}$  at different  $C_r^*$  for different solutions

### 6.2.2. Variation in the required solution heat addition rate ( $Q_{add}$ )

Fig.6.3 shows that required regenerator solution inlet temperature ( $T_{r,s,i}$ ) increases as  $C_r^*$  decreases from 4 to 1.5. This is due to the fact that reduction in solution mass flow rate deteriorates the moisture desorption potential which implies that  $w_{r,s,i}$  has to be increased by increasing  $T_{r,s,i}$  for getting the solution re-concentrated to the required condition. Also it can be observed that, with slight increase in slope of iso-concentration curve as a result of increasing vapour pressure (increase in specific heat also causes to decrease the required solution temperature raise to attain the same vapour pressure raise), there is a drop in  $Q_{add}$  with the decrease in  $C_r^*$  (Fig. 6.5). Accordingly,  $Q_{add}$  decreases. But as  $C_r^*$  decreases beyond certain limit, the increasing rate in  $T_{r,s,i}$  is drastic which is due to the extreme drop in mass transfer potential. Consequently,  $Q_{add}$  starts rising after certain  $C_r^*$ . At given concentration, LiBr solution requires slightly higher  $Q_{add}$  due to higher solution inlet temperature ( $T_{r,s,i}$ ) which is due to its lesser vapour pressure at a given temperature than others. It is obvious that  $Q_{add}$  for  $\text{CaCl}_2$  solution is lesser due to its high vapour pressure at a given temperature than other solutions.

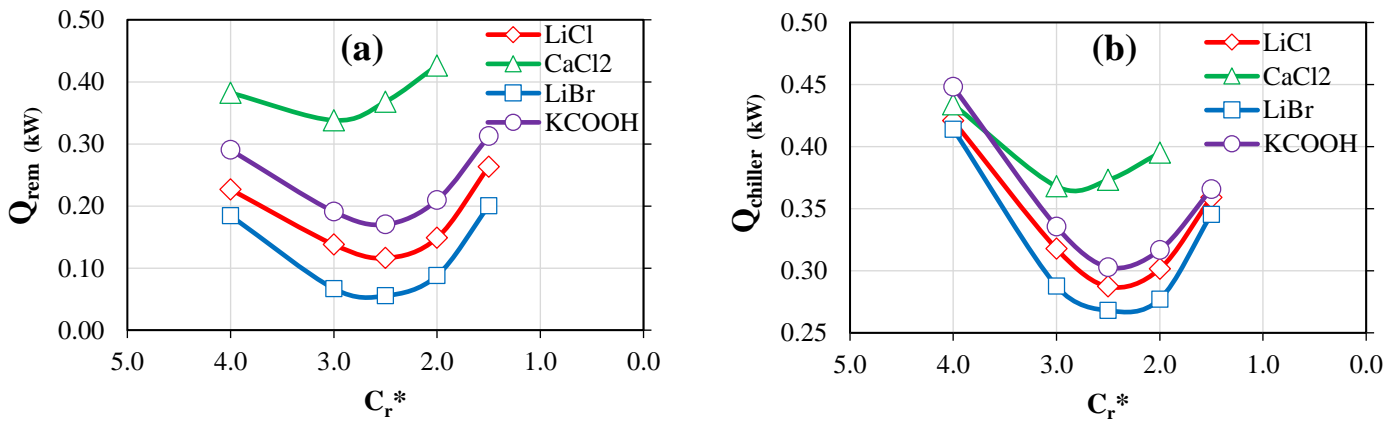


**Fig. 6.6.** Variation in (a) required solution heat removal rate ( $Q_{rem}$ ) and (b) Chiller load ( $Q_{chiller}$ ) at different  $C_r^*$  and for different solutions

### 6.2.3. Variation in chiller load ( $Q_{chiller}$ )

As Fig. 6.6 indicates that solution temperature drop during in regeneration process increases as  $C_r^*$  decreases. The cause for this is explained as follows. Since the required moisture desorption rate is fixed, same phase change heat gets released from solution irrespective of solution inlet condition which causes to increase in solution temperature drop as solution mass flow rate decreases ( $C_r^*$ ). Thus  $Q_{rem}$  decreases up to certain limit (Fig. 6.6a). But as  $C_r^*$  decreases beyond certain limit (3.0 for  $CaCl_2$  and 2.5 for remaining),  $Q_{rem}$  starts inclining. This is because of the excessive drop in  $T_{d,s,i}$  as solution mass flow rate becomes low. In addition to this, it is obvious that  $Q_{rem}$  for LiBr solution is very low because of its high vapour pressure at a given temperature than other solutions.  $Q_{rem}$  for  $CaCl_2$  solution is very high as a result of its high vapour pressure at a given temperature than other solutions. Subsequently chiller load ( $Q_{chiller} = Q_{rem} + Q_{sen2}$ ) is high for  $CaCl_2$  solution and lesser for LiBr solution (Fig. 6.6b). It is observed from Fig. 6.4b that  $Q_{sen2}$  decreases with reduction in  $C_r^*$  and also higher for LiBr solution than for other solutions. However which is less amount compared to  $Q_{rem}$ . Consequently, chiller load ( $Q_{chiller} = Q_{rem} + Q_{sen2}$ ) is lesser for LiBr solution than for other solutions.

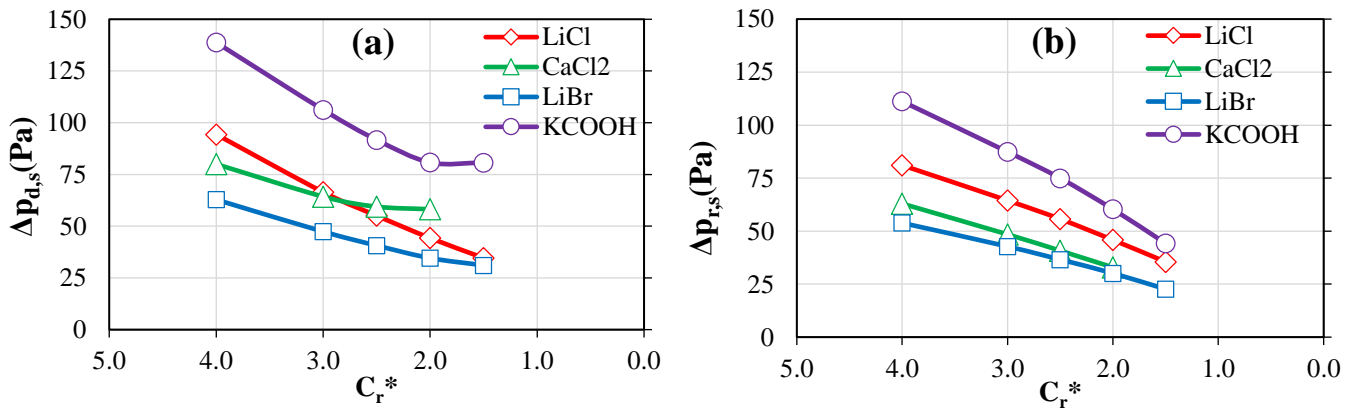


**Fig. 6.7.** Heat capacity ratio ( $C_r^*$ ) vs. (a) solution pressure drop in dehumidifier and (b) solution pressure drop in regenerator for different solutions

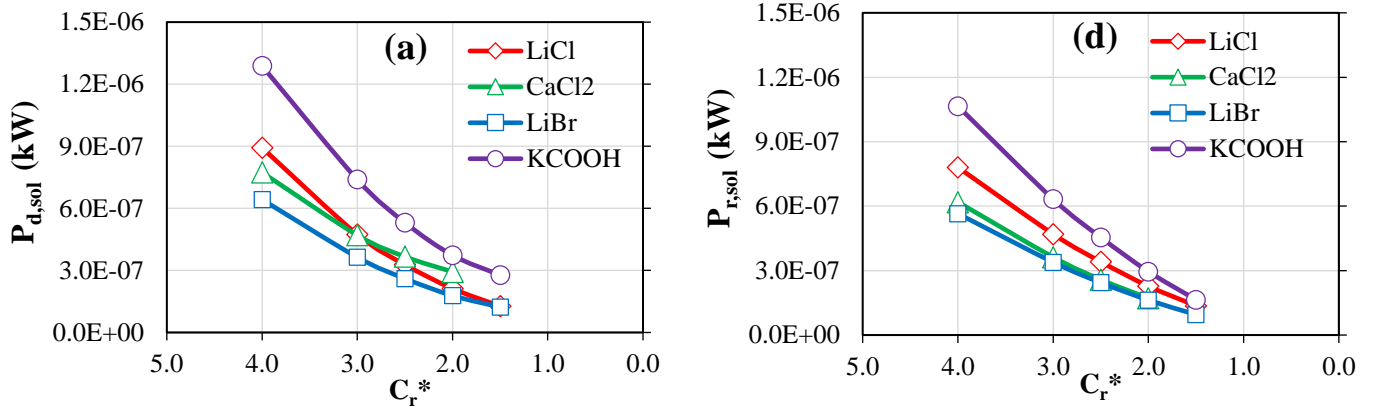


**Fig. 6.8.** Heat capacity ratio ( $C_r^*$ ) vs. (a) power consumption for solution pumping in dehumidifier channel and (b) power consumption for solution pumping in regenerator channel for different solutions

#### 6.2.4. Variation in solution pressure drop ( $\Delta p_{d,s}$ and $\Delta p_{r,s}$ ) and its pumping power ( $P_{d,s}$ and $P_{r,s}$ )

Fig. 6.7a and 6.7b shows that the pressure drop in dehumidifier and regenerator solution channels ( $\Delta p_{d,s}$  and  $\Delta p_{r,s}$ ) decreases as  $C_r^*$  decreases which is due to the decrease in solution mass flow rate. Consequently, solution pumping power ( $P_{d,s}$  and  $P_{r,s}$ ) also drops as indicated in Fig. 6.8a and 6.8b.  $\Delta p_{d,s}$  and  $P_{d,s}$  for KCOOH solution is higher than others since its viscosity is high. Even though the density of LiBr solution is higher than other solutions but because of its low viscosity,  $\Delta p_{d,s}$  and  $P_{d,s}$  for LiBr solution is found to be lower than others. Solution pressure drop and pumping power for regeneration channels ( $\Delta p_{r,s}$  and  $P_{r,s}$ ) is always less than in dehumidifier channel at any solution condition because of reduction in solution viscosity due to solution hot condition in the regenerator.

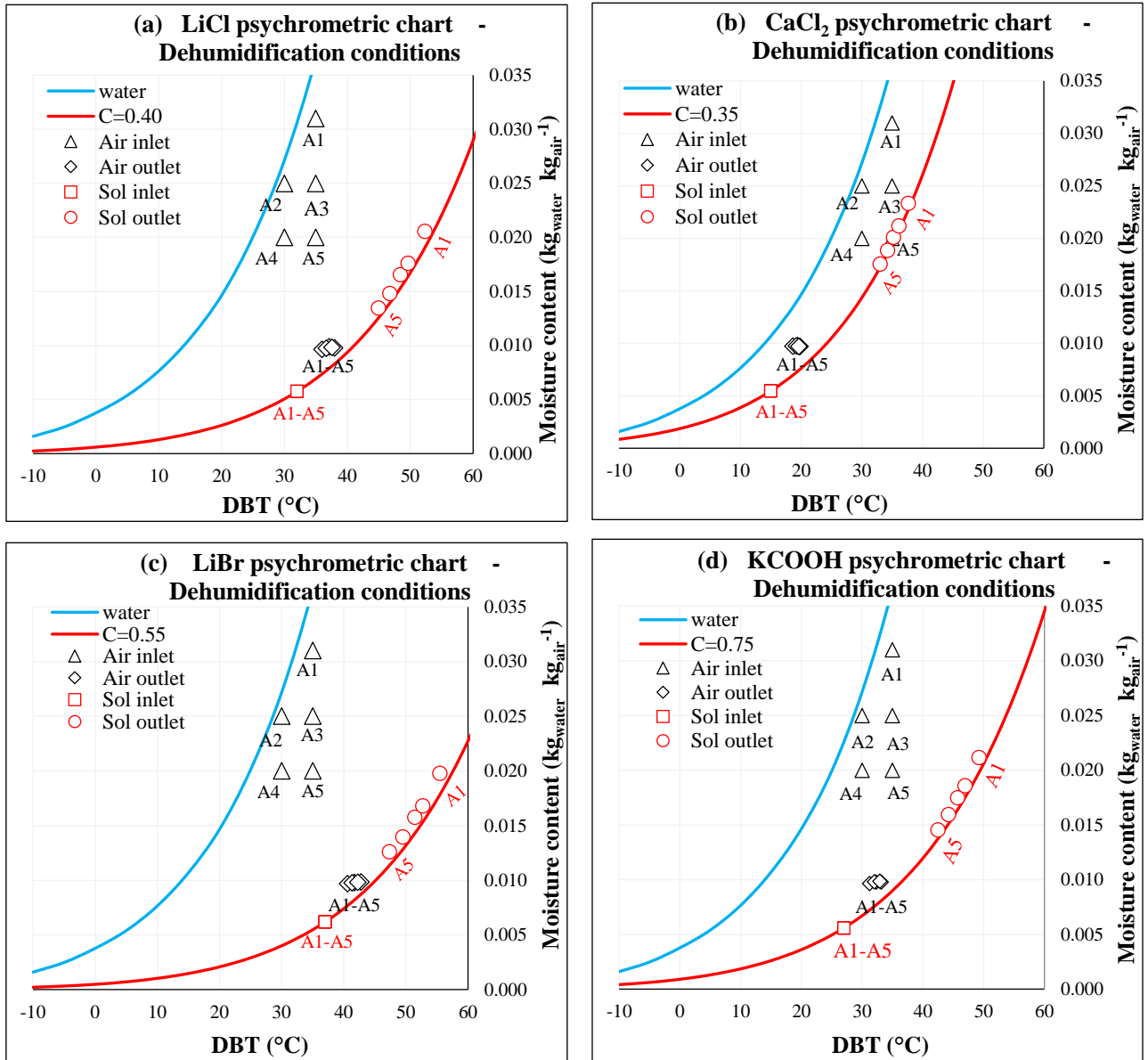


**Fig. 6.9.** Psychrometric chart specifies dehumidifier solution and air conditions for (a) LiCl at  $C_r^*=2.5$ , (b) CaCl<sub>2</sub> at  $C_r^*=3.0$ , (c) LiBr at  $C_r^*=2.5$  and (d) KCOOH at  $C_r^*=2.5$  at different ambient conditions

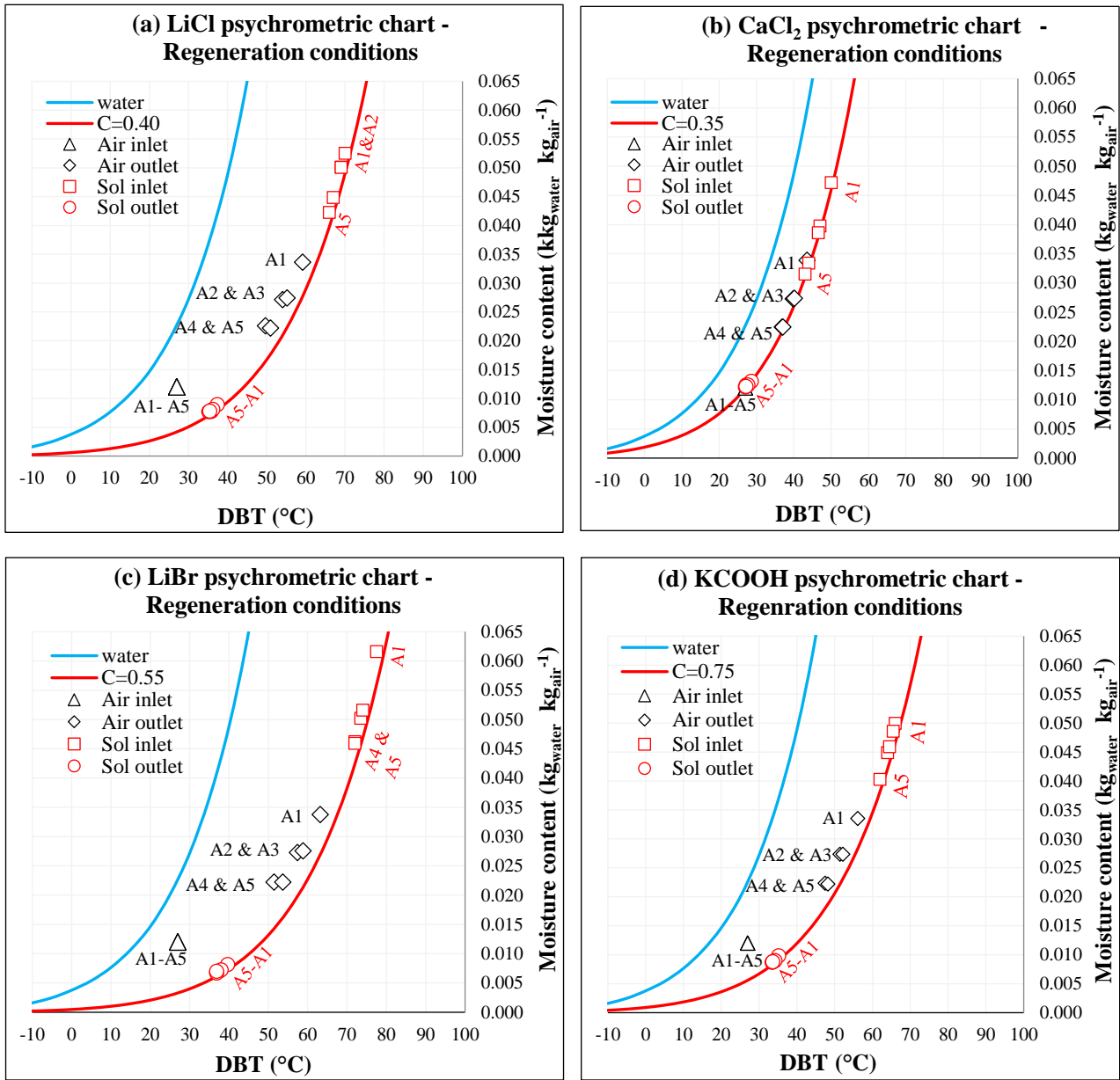


**Fig. 6.10.** Psychrometric chart specifies regenerator solution and air conditions for (a) LiCl at  $C_r^*=2.5$ , (b) CaCl<sub>2</sub> at  $C_r^*=3.0$ , (c) LiBr at  $C_r^*=2.5$  and (d) KCOOH at  $C_r^*=2.5$  at different ambient conditions

### 6.2.5. Solution and air conditions at different ambient conditions

Optimum heat capacity ratio (design parameter) for each solution has been found out at fixed peak ambient condition and fixed dehumidification rate which are 3.0 for CaCl<sub>2</sub> and 2.5 for other solutions. It is observed that LiBr solution requires least chiller load ( $Q_{chiller}$ ) and least solution pumping power ( $P_{d,s}$  and  $P_{r,s}$ ) at  $C_r^*=2.5$  (optimum heat capacity ratio) than other solutions. However, it requires higher solution heat addition rate ( $Q_{add}$ ) which is inevitable. But the frequent change in ambient condition necessitates further analysis to confirm the appropriate solution. Thus, at optimum  $C_r^*$  for each solution, performance indices have been analyzed by varying ambient condition. Dehumidifier and regenerator solution & air conditions for four solutions were indicated at different ambient conditions (A1-A5) as shown in Figs. 6.9 and 6.10. Dehumidifier solution inlet mass flow rate (DSIM) control strategy has been adapted to suit the conditioned load which varies as according to change in ambient condition.

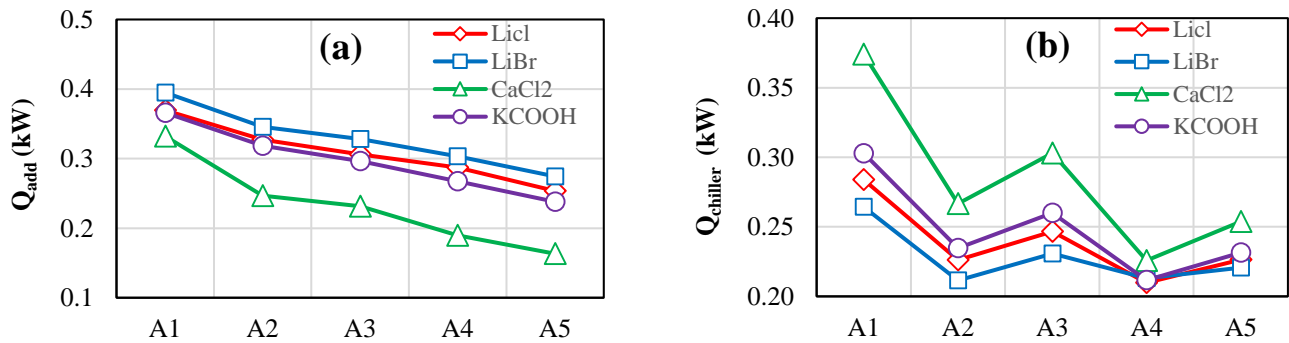


**Fig. 6.11.** Variation in (a) required solution heat addition rate ( $Q_{add}$ ) and (b) Chiller load ( $Q_{chiller}$ ) at different ambient conditions

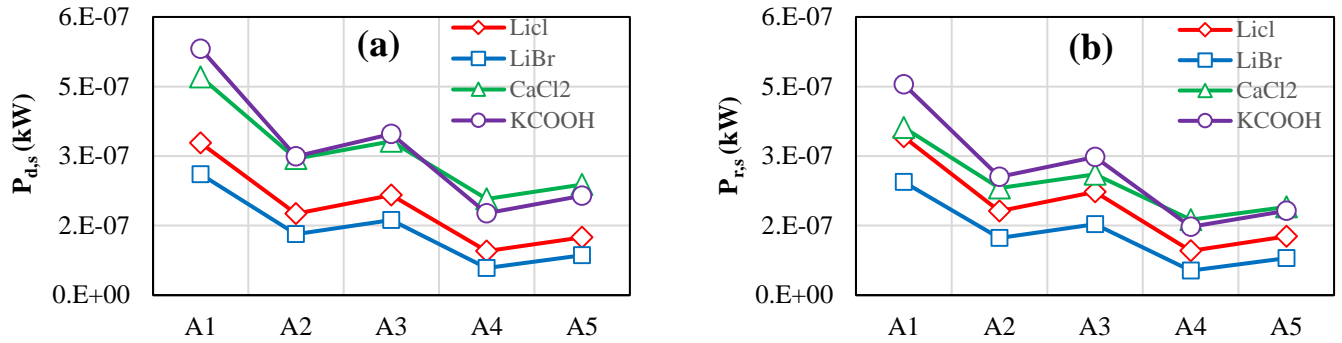


**Fig. 6.12.** Variation in (a) solution pumping power for dehumidifier channel ( $P_{d,s}$ ) and (b) solution pumping power for regenerator channel ( $P_{r,s}$ ) at different ambient conditions

### 6.2.6. Variation in solution heat addition rate ( $Q_{add}$ ), chiller load ( $Q_{chiller}$ ) and solution pumping power ( $P_{d,s}$ & $P_{r,s}$ ) at different ambient conditions

As ambient condition varies (humidity ratio or temperature decreases), solution mass flow rate (optimum mass flow rate) to be controlled to suit the required conditioned load. Respective solution and air conditions are shown in Figs. 6.9 and 6.10. It is observed from Figs. 6.11 and 6.12 that solution heat addition rate ( $Q_{add}$ ), chiller load ( $Q_{chiller}$ ) and solution pumping power ( $P_{d,s}$  &  $P_{r,s}$ ) trends declines as ambient condition varies from A1-A5 for any solution due to the drop in solution mass flow rate. Even though ambient condition varies, LiBr solution is found to be an efficient solution ignoring  $Q_{add}$ . LiCl solution requires less energy ( $Q_{chiller}$ ,  $P_{d,s}$  &  $P_{r,s}$ ) next to LiBr solution..

### 6.3. Major observations

Selection of energy efficient desiccant at optimum heat capacity for LDAS leads to energy savings. Thus this study is intended to analyze the performance parameters such as required

solution heat addition rate ( $Q_{add}$ ), solution heat removal rate ( $Q_{rem}$ ), solution pumping power ( $P_{d,s}$  and  $P_{r,s}$ ) and chiller load ( $Q_{chiller}$ ) for LiCl, CaCl<sub>2</sub>, LiBr and KCOOH solutions (commonly used potential desiccant solutions) based LDAS at different operating conditions. Initially, at fixed ambient condition and dehumidification rate, performance indices were analyzed for each solution at different heat capacity ratios ( $C_r^*=4.0, 3.0, 2.5, 2.0$  and  $1.5$ ) and at their respective maximum safe concentrations ( $0.40, 0.35, 0.55$  and  $0.75$  respectively). Later, at observed optimum heat capacity ratio for each solution, same considered performance indices were estimated at different ambient conditions by adopting DSIM control strategy to suit the required conditioned load which frequently varies according to change in ambient condition.

- It is clear that cooling capacity ( $Q_{cc}$ ) for CaCl<sub>2</sub> is higher and for LiBr is lower than remaining solutions at given  $C_r^*$ . Accordingly required dehumidified air sensible cooling ( $Q_{sen2}$ ) to attain required supply temperature ( $T_{sup}=15^\circ\text{C}$ ) is lesser for CaCl<sub>2</sub> and higher for LiBr solution than remaining solutions at given  $C_r^*$ . This is because dehumidifier solution inlet temperature ( $T_{d,s,i}$ ) is lesser for CaCl<sub>2</sub> solution and higher for LiBr solution.
- solution heat addition rate ( $Q_{add}$ ) is found to be dropping with the reduction in  $C_r^*$  upto optimum  $C_r^*$  and then starts incline. At their respective optimum  $C_r^*$ ,  $Q_{add}$  is found to be little higher for LiBr solution and lesser for CaCl<sub>2</sub> solution. Higher  $Q_{add}$  for LiBr solution is due to low vapour pressure than other solutions at a given temperature which requires high solution temperature to attain the required vapour pressure for desorbing the moisture in the regenerator.
- solution heat removal rate ( $Q_{rem}$ ) is also found to be dropping with the reduction in  $C_r^*$  upto optimum  $C_r^*$  and then starts incline. At their respective optimum  $C_r^*$ ,  $Q_{rem}$  is found to be lower for LiBr solution and higher for CaCl<sub>2</sub> solution. Low  $Q_{rem}$  for LiBr solution is due to low vapour pressure than other solutions at a given temperature.

- Subsequently, chiller load ( $Q_{chiller} = Q_{rem} + Q_{sen2}$ ) is observed lesser for LiBr solution and higher for  $CaCl_2$  solutions.  $Q_{chiller}$  for LiCl solution is next to LiBr solution. It is estimated that required  $Q_{chiller}$  to achieve 1 kW cooling capacity is 0.44 kW for LiBr solution whereas it is 0.47 kW for LiCl solution at their respective optimum  $C_r^*$ .
- Pressure drop in dehumidifier and regenerator solution channels ( $\Delta p_{d,s}$  and  $\Delta p_{r,s}$ ) and Solution pumping power ( $P_{d,s}$  &  $P_{r,s}$ ) are found to be drop with the drop in  $C_r^*$  which is due to the decrease in solution mass flow rate.  $P_{d,s}$  &  $P_{r,s}$  for KCOOH solution are higher because of its high viscosity. Even though the density of LiBr solution is higher than other solutions but because of its low viscosity  $P_{d,s}$  &  $P_{r,s}$  for LiBr solution are found to be lower than others. For an instant, it is witnessed that  $P_{d,s}$  for LiBr solution 103% lesser than *KCOOH* solution.
- The investment cost for LiBr solution at design parameter ( $C_r^*=2.5$  and  $0.55C$ ) is 30% higher than for LiCl solution at design parameter ( $C_r^*=2.5$  and  $0.40C$ ) as per the Indian market prices. But operating cost ( $P_{d,s}$  &  $P_{r,s}$ ) for LiBr solution is significantly lesser (26% & 57%) than for LiCl solution.
- Even though ambient condition varies, performance parameters for all solutions follow the same trends as they followed at fixed peak ambient condition.

The analysis done in this study therefore suggests that LiBr solution is an appropriate solution to achieve energy savings due to its low chiller load requirement and its low operating cost. The drawback of the LiBr solution is high investment cost and requires little high  $Q_{add}$  than LiCl solution.  $CaCl_2$  solution requires lesser  $Q_{add}$  but its operating cost and  $Q_{chiller}$  are very high. LiCl solution followed by KCOOH solution is next to LiBr solution in attaining energy savings.

## Chapter 7

### Conclusions and Recommendations for future work

#### 7.1. Conclusions

It is known that a given liquid desiccant at different combinations of operating parameters (heat capacity ratio, concentration and temperature) can achieve required dehumidification rate for a given ambient condition. But suitable liquid desiccant at corresponding optimum operating parameters only can attain energy savings. Therefore this study is intended to present the methodology to find the appropriate potential liquid desiccant at its corresponding optimum operating parameters to design energy efficient LDAS. The following conclusions were drawn from the present study.

- Desiccant solution with maximum safe concentration (just lesser than saturation concentration for a given liquid desiccant) and optimum heat capacity ratio (varies from liquid desiccant to liquid desiccant) is found to have lesser chiller load requirement. This is at the expense of considerable raise in solution heat addition rate ( $Q_{add}$ ) and extensive raise in solution pumping power (due to high pressure drop at higher concentration).
- Two solution control strategies followed are dehumidifier solution inlet temperature control strategy (DSIT control strategy) and dehumidifier solution inlet mass flow rate control strategy (DSIM control strategy).

- Even though chiller load ( $Q_{chiller}$ ) is slightly high (3-14%) for DSIM control strategy at low ambient conditions, but due to the significant reduction in solution mass flow rate and its pressure drop, system solution pumping power remarkably reduces. Thus, it was found that DSIM control strategy as energy-efficient to control supply air condition according to variation in the ambient conditions.
- Later, selection methodology of energy efficient liquid desiccant at optimum operating parameters for LDAS has been studied. This means influence of (commonly used potential desiccant solutions LiCl, CaCl<sub>2</sub>, LiBr and KCOOH solutions at different operating conditions on the performance parameters has been studied.
- It is found that LiBr at  $C_r^*=2.5$  and  $C_s=0.55$  (maximum safe concentration) is the appropriate solution to achieve energy savings due to its low chiller load requirement and its low operating cost.
- The drawback of the LiBr solution is high investment cost and requires little high  $Q_{add}$  than LiCl solution. CaCl<sub>2</sub> solution requires lesser  $Q_{add}$  but its operating cost and  $Q_{chiller}$  are very high. LiCl solution followed by KCOOH solution is next to LiBr solution in attaining energy savings.

It is to be noted that the results obtained in this study are applicable to this specific air conditioning application only (Table 3.2). Suitable liquid desiccant as well as its optimum operating parameters may vary as air conditioning application (peak ambient condition/room condition) varies. However the methodology followed in this study is beneficial for LDAS designers in choosing the suitable liquid desiccant at its corresponding operating parameters to design an energy efficient LDAS for any given air conditioning application.

## **7.2. Recommendations for future work**

- For a specific air conditioning application, performing the thermal energy analysis on the LDAS with addition of cooling tower to the system. With this analysis, energy savings from the chiller load can be estimated.
- For a specific air conditioning application, optimizing the LAMEE size for energy efficient LDAS design.
- Examining the feasibility of low grade potential heat usage for liquid desiccant regeneration for power plant Turbine Generator (TG) building which leads to significant reduction in power consumption.

### **List of research articles published in Journals**

1. **Siva Kumar Reddy, Y., Balasubramanian, K., & Chandramohan, V. (2019).** Thermal energy analysis on liquid desiccant air conditioning system at different desiccant solution parameters. *Proceedings of the Institution of Mechanical Engineers, Part E: Journal of Process Mechanical Engineering*. <https://doi.org/10.1177/0954408919825721>. (SCI)
2. **Siva Kumar Reddy Y, Karthik Balasubramanian & V. P. Chandramohan (2019)** Study on desiccant solution control strategies for efficient liquid desiccant air conditioning system control performance, *Science and Technology for the Built Environment*, 25:3, 322-335, DOI: 10.1080/23744731.2018.1526017. (SCI)
3. **Y. Siva Kumar Reddy, Karthik Balasubramanian & V.P. Chandramohan (2019)** Influence of potential liquid desiccants on solution cooling, heating, and pumping loads of membrane-based liquid desiccant air conditioning system: An analytical study, *Science and Technology for the Built Environment*, 25:6, 753-766, DOI: 10.1080/23744731.2019.1600332. (SCI)

## References

- [1] D. B. Jani, M. Mishra, and P. K. Sahoo, "Investigations on effect of operational conditions on performance of solid desiccant based hybrid cooling system in hot and humid climate," *Therm. Sci. Eng. Prog.*, vol. 7, pp. 76–86, Sep. 2018.
- [2] D. B. Jani and M. Mishra, "EXERGY ANALYSIS OF SOLID DESICCANT - VAPOR COMPRESSION HYBRID IHMTC2015-155," no. December, 2015.
- [3] D. B. Jani, M. Mishra, and P. K. Sahoo, "Solid desiccant air conditioning - A state of the art review," *Renew. Sustain. Energy Rev.*, vol. 60, pp. 1451–1469, 2016.
- [4] M. M. Rafique, P. Gandhidasan, and H. M. S. Bahaidarah, "Liquid desiccant materials and dehumidifiers - A review," *Renew. Sustain. Energy Rev.*, vol. 56, pp. 179–195, 2016.
- [5] G. Fekadu and S. Subudhi, "Renewable energy for liquid desiccants air conditioning system: A review," *Renew. Sustain. Energy Rev.*, vol. 93, no. March 2017, pp. 364–379, 2018.
- [6] T. S. Ge, Y. Li, R. Z. Wang, and Y. J. Dai, "A review of the mathematical models for predicting rotary desiccant wheel," *Renew. Sustain. Energy Rev.*, vol. 12, no. 6, pp. 1485–1528, Aug. 2008.
- [7] D. B. Jani, M. Mishra, and P. K. Sahoo, "A critical review on application of solar energy as renewable regeneration heat source in solid desiccant – vapor compression hybrid cooling system," *J. Build. Eng.*, vol. 18, no. March, pp. 107–124, 2018.
- [8] D. B. Jani, "A review on application of desiccant dehumidification – vapor compression hybrid cooling system in hot-humid climates," no. February, 2018.
- [9] D. B. Jani, M. Mishra, and P. K. Sahoo, "Performance analysis of hybrid solid desiccant-

vapor compression air conditioning system in hot and humid weather of India,” *Build. Serv. Eng. Res. Technol.*, vol. 37, no. 5, pp. 523–538, 2016.

- [10] E. Elsarrag, “HVAC&R Research Dehumidification of Air by Chemical Liquid Desiccant in a Packed Column and Its Heat and Mass Transfer Effectiveness Dehumidification of Air by Chemical Liquid Desiccant in a Packed Column and Its Heat and Mass Transfer Effectiveness,” 2011.
- [11] a Lowenstein, S. Slayzak, and E. Kozubal, “A zero carryover liquid-desiccant air conditioner for solar applications,” *ASME/Solar06, Denver, USA*, pp. 1–11, 2006.
- [12] V. Morillon *et al.*, “Water vapour pressure above saturated salt solutions at low temperatures,” *Fluid Phase Equilib.*, vol. 155, no. 2, pp. 297–309, Feb. 1999.
- [13] A. Ertas, E. E. Anderson, and I. Kiris, “Properties of a New Liquid Desiccant Solution-Lithium Chloride and Calcium Chloride Mixture,” *Sol. Energy*, vol. 49, no. 3, pp. 205–212, 1992.
- [14] G. C. and G. R. Yu.I. Aristov, M.M. Tokarev, “SELECTIVE WATER SORBENTS FOR MULTIPLE APPLICATIONS, 1. CaCl<sub>2</sub> CONFINED IN MESOPORES OF SILICA GEL: SORPTION PROPERTIES,” vol. 59, no. 2, pp. 325–333, 1996.
- [15] A. H. Abdel-Salam and C. J. Simonson, “State-of-the-art in liquid desiccant air conditioning equipment and systems,” *Renew. Sustain. Energy Rev.*, vol. 58, pp. 1152–1183, 2016.
- [16] P. Bansal, S. Jain, and C. Moon, “Performance comparison of an adiabatic and an internally cooled structured packed-bed dehumidifier,” *Appl. Therm. Eng.*, 2011.
- [17] T.-W. CHUNG and H. WU, “Mass Transfer Correlation for Dehumidification of Air in a Packed Absorber with an Inverse U-Shaped Tunnel,” *Sep. Sci. Technol.*, vol. 35, no. 10,

pp. 1503–1515, Jan. 2000.

- [18] A. K. Hueffed, L. M. Chamra, and P. J. Mago, “A Simplified Model of Heat and Mass Transfer Between Air and Falling-Film Desiccant in a Parallel-Plate Dehumidifier,” 2009.
- [19] X. H. Liu and Y. Jiang, “Handling zone dividing method in packed bed liquid desiccant dehumidification/regeneration process,” *Energy Convers. Manag.*, vol. 50, no. 12, pp. 3024–3034, Dec. 2009.
- [20] J. Woods, “Membrane processes for heating, ventilation, and air conditioning,” *Renew. Sustain. Energy Rev.*, vol. 33, pp. 290–304, May 2014.
- [21] C. Isetti, E. Nannei, and A. Magrini, “On the application of a membrane air-liquid contactor for air dehumidification,” *Energy Build.*, vol. 25, no. 3, pp. 185–193, 1997.
- [22] M. R. H. Abdel-Salam, M. Fauchoux, G. Ge, R. W. Besant, and C. J. Simonson, “Expected energy and economic benefits, and environmental impacts for liquid-to-air membrane energy exchangers (LAMEEs) in HVAC systems: A review,” *Appl. Energy*, vol. 127, pp. 202–218, 2014.
- [23] L.-Z. Zhang, S.-M. Huang, and W.-B. Zhang, “Turbulent heat and mass transfer across a hollow fiber membrane bundle considering interactions between neighboring fibers,” *Int. J. Heat Mass Transf.*, vol. 64, pp. 162–172, Sep. 2013.
- [24] M. R. H. Abdel-salam, R. W. Besant, and C. J. Simonson, “International Journal of Heat and Mass Transfer Design and testing of a novel 3-fluid liquid-to-air membrane energy exchanger ( 3-fluid LAMEE ),” *Int. J. Heat Mass Transf.*, vol. 92, pp. 312–329, 2016.
- [25] A. M. Radhwan, H. N. Gari, and M. M. Elsayed, “Parametric study of a packed bed dehumidifier/regenerator using CaCl<sub>2</sub> liquid desiccant,” *Renew. Energy*, vol. 3, no. 1, pp. 49–60, 1993.

- [26] A. Ertas, P. Gandhidasan, I. Kiris, and E. E. Anderson, "Experimental study on the performance of a regeneration tower for various climatic conditions," *Sol. Energy*, vol. 53, no. 1, pp. 125–130, 1994.
- [27] N. Fumo and D. Y. Goswami, "Study of an aqueous lithium chloride desiccant system: Air dehumidification and desiccant regeneration," *Sol. Energy*, vol. 72, no. 4, pp. 351–361, 2002.
- [28] Y. Yonggao, Z. Xiaosong, W. Geng, and L. Lei, "Experimental study on a new internally cooled/heated dehumidifier/regenerator of liquid desiccant systems," *Int. J. Refrig.*, vol. 31, pp. 857–866, 2008.
- [29] Y. Yin, X. Zhang, D. Peng, and X. Li, "Model validation and case study on internally cooled/heated dehumidifier/regenerator of liquid desiccant systems," *Int. J. Therm. Sci.*, vol. 48, no. 8, pp. 1664–1671, 2009.
- [30] K. Mahmud, G. I. Mahmood, C. J. Simonson, and R. W. Besant, "Performance testing of a counter-cross-flow run-around membrane energy exchanger (RAMEE) system for HVAC applications," *Energy Build.*, vol. 42, no. 7, pp. 1139–1147, 2010.
- [31] G. Q. Qiu and S. B. Riffat, "Experimental Investigation on a Novel Air Dehumidifier Using Liquid Desiccant," *Int. J. Green Energy*, vol. 7, no. 2, pp. 174–180, 2010.
- [32] L. Zhang, E. Hihara, F. Matsuoka, and C. Dang, "Experimental analysis of mass transfer in adiabatic structured packing dehumidifier/regenerator with liquid desiccant," *Int. J. Heat Mass Transf.*, vol. 53, no. 13–14, pp. 2856–2863, 2010.
- [33] H. B. Hemingson, C. J. Simonson, and R. W. Besant, "Steady-state performance of a run-around membrane energy exchanger (RAMEE) for a range of outdoor air conditions," *Int. J. Heat Mass Transf.*, vol. 54, no. 9–10, pp. 1814–1824, 2011.

- [34] L.-Z. Zhang, "An Analytical Solution to Heat and Mass Transfer in Hollow Fiber Membrane Contactors for Liquid Desiccant Air Dehumidification," *J. Heat Transfer*, vol. 133, no. 9, p. 092001, 2011.
- [35] H. Pahlavanzadeh, "Experimental and Theoretical Study of Liquid Desiccant Dehumidification System by Using the Effectiveness Model," *J. Therm. Sci. Eng. Appl.*, vol. 4, no. 1, p. 011008, 2012.
- [36] D. Ghadiri Moghaddam, P. LePoudre, R. W. Besant, and C. J. Simonson, "Steady-State Performance of a Small-Scale Liquid-to-Air Membrane Energy Exchanger for Different Heat and Mass Transfer Directions, and Liquid Desiccant Types and Concentrations: Experimental and Numerical Data," *J. Heat Transfer*, vol. 135, no. 12, p. 122002, 2013.
- [37] A. H. Abdel-Salam, G. Ge, and C. J. Simonson, "Performance analysis of a membrane liquid desiccant air-conditioning system," *Energy Build.*, vol. 62, pp. 559–569, 2013.
- [38] M. Kassai, G. Ge, and C. J. Simonson, "Dehumidification performance investigation of run-around membrane energy exchanger system," *Therm. Sci.*, vol. 2014, no. 6, pp. 1927–1938, 2014.
- [39] M. Kassai, "Effectiveness and humidification capacity investigation of liquid-to-air membrane energy exchanger under low heat capacity ratios at winter air conditions," *J. Therm. Sci.*, vol. 24, no. 4, pp. 391–397, 2015.
- [40] G. Ge, D. Ghadiri Moghaddam, A. H. Abdel-Salam, R. W. Besant, and C. J. Simonson, "Comparison of experimental data and a model for heat and mass transfer performance of a liquid-to-air membrane energy exchanger (LAMEE) when used for air dehumidification and salt solution regeneration," *Int. J. Heat Mass Transf.*, vol. 68, pp. 119–131, 2014.
- [41] B. S. Mohan, S. Tiwari, and M. P. Maiya, "Experimental investigations on performance of liquid desiccant-vapor compression hybrid air conditioner," *Appl. Therm. Eng.*, vol. 77, pp.

153–162, 2015.

- [42] J. Ahn, J. Kim, B. H. Kang, J. Ahn, J. Kim, and B. H. A. Kang, “Performance of a Hybrid Desiccant Cooling System in a Residential Environment Performance of a Hybrid Desiccant Cooling System in a Residential,” vol. 7632, 2016.
- [43] H. Bai, J. Zhu, Z. Chen, L. Ma, R. Wang, and T. Li, “Performance testing of a cross-flow membrane-based liquid desiccant dehumidification system,” *Appl. Therm. Eng.*, vol. 119, pp. 119–131, 2017.
- [44] S. Sabek, K. Ben Nasr, F. Tiss, R. Chouikh, and A. Guizani, “Performance investigation of desiccant liquid air membrane energy exchanger: Air and lithium chloride effects,” *Int. J. Refrig.*, vol. 80, pp. 145–157, 2017.
- [45] Z. Wang, X. Zhang, and Z. Li, “Investigation on the coupled heat and mass transfer process between extremely high humidity air and liquid desiccant in the counter-flow adiabatic packed tower,” *Int. J. Heat Mass Transf.*, vol. 110, pp. 898–907, 2017.
- [46] L. G. Harriman, *The dehumidification handbook*, no. 978. 2002.
- [47] M. R. Conde, “Properties of aqueous solutions of lithium and calcium chlorides: Formulations for use in air conditioning equipment design,” *Int. J. Therm. Sci.*, vol. 43, no. 4, pp. 367–382, 2004.
- [48] J. Pátek and J. Klomfar, “A computationally effective formulation of the thermodynamic properties of LiBr-H<sub>2</sub>O solutions from 273 to 500 K over full composition range,” *Int. J. Refrig.*, vol. 29, no. 4, pp. 566–578, 2006.
- [49] G. A. Longo and A. Gasparella, “Experimental and theoretical analysis of heat and mass transfer in a packed column dehumidifier/regenerator with liquid desiccant,” *Int. J. Heat Mass Transf.*, vol. 48, no. 25–26, pp. 5240–5254, 2005.

- [50] M. Afshin, "Selection of the Liquid Desiccant in a Run-Around Membrane Energy Exchanger," *J. Chem. Inf. Model.*, vol. 53, p. 160, 1989.
- [51] X. H. Liu, X. Q. Yi, and Y. Jiang, "Mass transfer performance comparison of two commonly used liquid desiccants: LiBr and LiCl aqueous solutions," *Energy Convers. Manag.*, vol. 52, no. 1, pp. 180–190, 2011.
- [52] I. P. Koronaki, R. I. Christodoulaki, V. D. Papaefthimiou, and E. D. Rogdakis, "Thermodynamic analysis of a counter flow adiabatic dehumidifier with different liquid desiccant materials," *Appl. Therm. Eng.*, vol. 50, no. 1, pp. 361–373, 2013.
- [53] A. Gurubalan, M. P. Maiya, and S. Tiwari, "Performance characterization of membrane dehumidifier with desiccants in flat-plate arrangement," *Energy Build.*, vol. 156, pp. 151–162, 2017.
- [54] M. R. H. Abdel-Salam, R. W. Besant, and C. J. Simonson, "Sensitivity of the performance of a flat-plate liquid-to-air membrane energy exchanger (LAMEE) to the air and solution channel widths and flow maldistribution," *Int. J. Heat Mass Transf.*, vol. 84, pp. 1082–1100, 2015.
- [55] D. G. Moghaddam, G. Mahmood, G. Ge, J. Bolster, R. W. Besant, and C. J. Simonson, "STEADY-STATE PERFORMANCE OF A PROTOTYPE (200 CFM) LIQUID-TO-AIR MEMBRANE ENERGY EXCHANGER (LAMEE) UNDER SUMMER AND WINTER TEST CONDITIONS," *Proc. ASME 2013 Heat Transf. Summer Conf.*, pp. 1–7, 2017.
- [56] G. Ge, D. Ghadiri Moghaddam, R. Namvar, C. J. Simonson, and R. W. Besant, "Analytical model based performance evaluation, sizing and coupling flow optimization of liquid desiccant run-around membrane energy exchanger systems," *Energy Build.*, vol. 62, pp. 248–257, 2013.
- [57] F. P. Incropera, T. L. Bergman, A. S. Lavine, and D. P. DeWitt, *Fundamentals of Heat and*

*Mass Transfer*. 2011.

- [58] D. Ghadiri Moghaddam, M. Fauchoux, R. W. Besant, and C. J. Simonson, "Investigating similarity between a small-scale liquid-to-air membrane energy exchanger (LAMEE) and a full-scale (100 L/s) LAMEE: Experimental and numerical results," *Int. J. Heat Mass Transf.*, vol. 77, pp. 464–474, 2014.
- [59] R. M. Lazzarin, A. Gasparella, and G. A. Longo, "Chemical dehumidification by liquid desiccants: Theory and experiment," *Int. J. Refrig.*, vol. 22, no. 4, pp. 334–347, 1999.
- [60] A. Giampieri, Z. Ma, A. Smallbone, and A. P. Roskilly, "Thermodynamics and economics of liquid desiccants for heating, ventilation and air-conditioning – An overview," *Appl. Energy*, vol. 220, pp. 455–479, Jun. 2018.
- [61] D. R. Lide, "CRC Handbook of Chemistry and Physics," *CRC Handb. Chem. Phys.*, pp. 1264–1266, 2003.
- [62] D. A. Boryta, "Solubility of lithium bromide in water between -50.deg. and +100.deg. (45 to 70% lithium bromide)," *J. Chem. Eng. Data*, vol. 15, no. 1, pp. 142–144, Jan. 1970.
- [63] G. A. Longo and A. Gasparella, "Experimental measurement of thermophysical properties of H<sub>2</sub>O/KCOOH (potassium formate) desiccant," *Int. J. Refrig.*, vol. 62, pp. 106–113, 2016.
- [64] D. I. Stevens, J. E. Braun, and S. A. Klein, "An effectiveness model of liquid-desiccant system heat/mass exchangers," *Sol. Energy*, vol. 42, no. 6, pp. 449–455, 1989.
- [65] G. A. Longo and L. Fedele, "Experimental measurement of equilibrium vapour pressure of H<sub>2</sub>O/KCOOH (potassium formate) solution at high concentration," *Int. J. Refrig.*, vol. 93, pp. 176–183, 2018.

